



## Deglaciation of the north American ice sheet complex in calendar years based on a comprehensive database of chronological data: NADI-1

April S. Dalton<sup>a,\*<sup>1</sup></sup>, Helen E. Dulfer<sup>a</sup>, Martin Margold<sup>a</sup>, Jakob Heyman<sup>b</sup>, John J. Clague<sup>c</sup>, Duane G. Froese<sup>d</sup>, Michelle S. Gauthier<sup>e</sup>, Anna L.C. Hughes<sup>f</sup>, Carrie E. Jennings<sup>g</sup>, Sophie L. Norris<sup>h</sup>, Benjamin J. Stoker<sup>a</sup>

<sup>a</sup> Department of Physical Geography and Geoecology, Charles University, Prague, Czech Republic

<sup>b</sup> Department of Earth Sciences, University of Gothenburg, Sweden

<sup>c</sup> Department of Earth Sciences, Simon Fraser University, Burnaby, British Columbia, Canada

<sup>d</sup> Department of Earth and Atmospheric Sciences, University of Alberta, Edmonton, Canada

<sup>e</sup> Manitoba Geological Survey, Winnipeg, Manitoba, Canada

<sup>f</sup> Department of Geography, University of Manchester, Manchester, United Kingdom

<sup>g</sup> Department of Earth and Environmental Sciences, University of Minnesota, Twin Cities, Minnesota, United States

<sup>h</sup> Department of Geography, University of Victoria, Victoria, British Columbia, Canada



### ARTICLE INFO

Handling Editor: C. O'Cofaigh

### ABSTRACT

The most recent deglaciation of the North American Ice Sheet Complex (NAISC: comprising the Innuitian, Cordilleran, and Laurentide ice sheets) offers a broad perspective from which to analyze the timing and rate of ice retreat, deglacial sea-level rise, and abrupt climate change events. Previous efforts to portray the retreat of the NAISC have been focused largely on minimum-limiting radiocarbon ages and ice margin location(s) tied to deglacial landforms that were not, for the most part, chronologically constrained. Here, we present the first version of North American Deglaciation Isochrones (NADI-1) spanning 25 to 1 ka in calendar years before present. Key new features of this work are (i) the incorporation of cosmogenic nuclide data, which offer a direct constraint on the timing of ice recession; (ii) presentation of all data and time-steps in calendar years; (iii) optimal, minimum, and maximum ice extents for each time-step that are designed to capture uncertainties in the ice margin position, and; (iv) extensive documentation and justification for the placement of each ice margin. Our data compilation includes 2229 measurements of  $^{10}\text{Be}$ , 459 measurements of  $^{26}\text{Al}$  and 35 measurements of  $^{36}\text{Cl}$  from a variety of settings, including boulders, bedrock surfaces, cobbles, pebbles, and sediments. We also updated a previous radiocarbon dataset ( $n = 4947$ ), assembled luminescence ages ( $n = 397$ ) and gathered uranium-series data ( $n = 2$ ). After scrutiny of the geochronological dataset, we consider >90% of data to be reliable or likely reliable. Key findings include (i) a highly asynchronous maximum glacial extent in North America, occurring as early as 27 ka to as late as 17 ka, within and between ice sheets. In most marine realms, extension of the ice margin to the continental shelf break at 25 ka is somewhat speculative because it is based on undated and spatially scattered ice stream and geomorphic evidence; (ii) detachment of the Laurentide and Cordilleran ice sheets took place gradually via southerly and northerly ‘unzipping’ of the ice masses, starting at 17.5 ka and ending around 14 ka; (iii) the final deglaciation of Hudson Bay began at 8.5 ka, with the collapse completed by 8 ka. The maximum extent of ice during the last glaciation occurred at 22 ka and covered 15,470,000 km<sup>2</sup>. All North American ice sheets merged at 22 ka for the first time in the Quaternary. The highly asynchronous Last Glacial Maximum in North America means that our isochrones (starting at 25 ka) capture ice advance across some areas, which is based on limited evidence and is therefore somewhat speculative. In the Supplementary Data, the complete NADI-1 chronology is available in PDF, GIF and shapefile format, together with additional visualizations and spreadsheets of geochronological data. The NADI-1 shapefiles are also available at <https://doi.org/10.5281/zenodo.8161764>.

\* Corresponding author.

E-mail address: [aprls.dalton@gmail.com](mailto:aprls.dalton@gmail.com) (A.S. Dalton).

<sup>1</sup> Present address: Department of Physics and Physical Oceanography, Memorial University of Newfoundland, St. John's, Newfoundland and Labrador, Canada.

## 1. Introduction

The North American Ice Sheet Complex (NAISC; comprising the Innuitian, Cordilleran, and Laurentide ice sheets; Fig. 1) was the largest body of ice in the Northern Hemisphere to grow and recede during the Quaternary, accounting for roughly ~80 m of global sea level change at the Last Glacial Maximum (LGM; Clark and Mix, 2002; Clark and Tarasov, 2014). Accordingly, the complete (and repeated) deglaciation of the NAISC offers a long-term perspective from which to analyze the response of large continental ice sheets to changes in the Earth System. Moreover, the NAISC contained various settings of glaciation (for example marine-terminating ice margins, alpine glaciation and regional ice-streaming), that are now studied, and are of future concern, in Antarctica and Greenland (Gilbert et al., 2017; Catania et al., 2020; Miles et al., 2021). A refined understanding of North American ice dynamics is important for a wide variety of research fields, such as constraining numerical models of ice sheets and global isostatic adjustment (Tarasov et al., 2012; Peltier et al., 2015; Gowan et al., 2021), understanding the timing of arrival and migration route(s) of humans and other species to the North American continent (Heintzman et al., 2016; Pedersen et al., 2016; Waters, 2019), constraining global climate dynamics such as the timing of meltwater pulses (Teller et al., 2005; Carlson and Clark, 2012), and determining future change to modern-day continental ice sheets (Antarctic and Greenland) and their impact on sea level (Gregoire et al., 2012; Shepherd et al., 2020; Slater et al., 2021).

There have been over 100 years of research tracing the deglacial history of the NAISC. Prior to the advent of radiocarbon dating in the 1950s, much of the work was based on broad inferences from the stratigraphic and geomorphic record (see deglacial landforms and eskers in Fig. 2). Notably, Dawson (1890) first used the name Laurentide glacier, and Flint (1943) proposed the term Laurentide Ice Sheet for what was then believed to be a single large dome centered over Hudson Bay. Several early workers also mapped terminal moraines around the Great Lakes (Wayne and Thornbury, 1951; Horberg and Anderson, 1956). Eventually, the onset of radiocarbon dating allowed the geomorphic record (and thus deglaciation) to be placed into a chronological perspective and correlated with other regional and global events. These radiocarbon ages, in combination with dedicated surficial mapping across the glaciated region (e.g. Stalker, 1962; Fyles, 1963; Karrow, 1963), were fundamental for tracing the rate and dynamics of ice recession, and underpinned several first-generation deglaciation maps for the NAISC (Bryson et al., 1969; Prest, 1969). These maps were subsequently updated to reflect an ever-increasing collection of radiocarbon dates and more detailed surficial mapping of the glaciated region (Dyke and Prest, 1987; Fulton, 1995; Dyke et al., 2003a; Dyke, 2004). The most recent depiction of North American deglaciation was that of Dalton et al. (2020), which was a series of updates to the work of Dyke (2004). All aforementioned studies were based on uncalibrated radiocarbon ages; this was the only option prior to the 1990s because radiocarbon calibration had not yet been formalized. The later works of

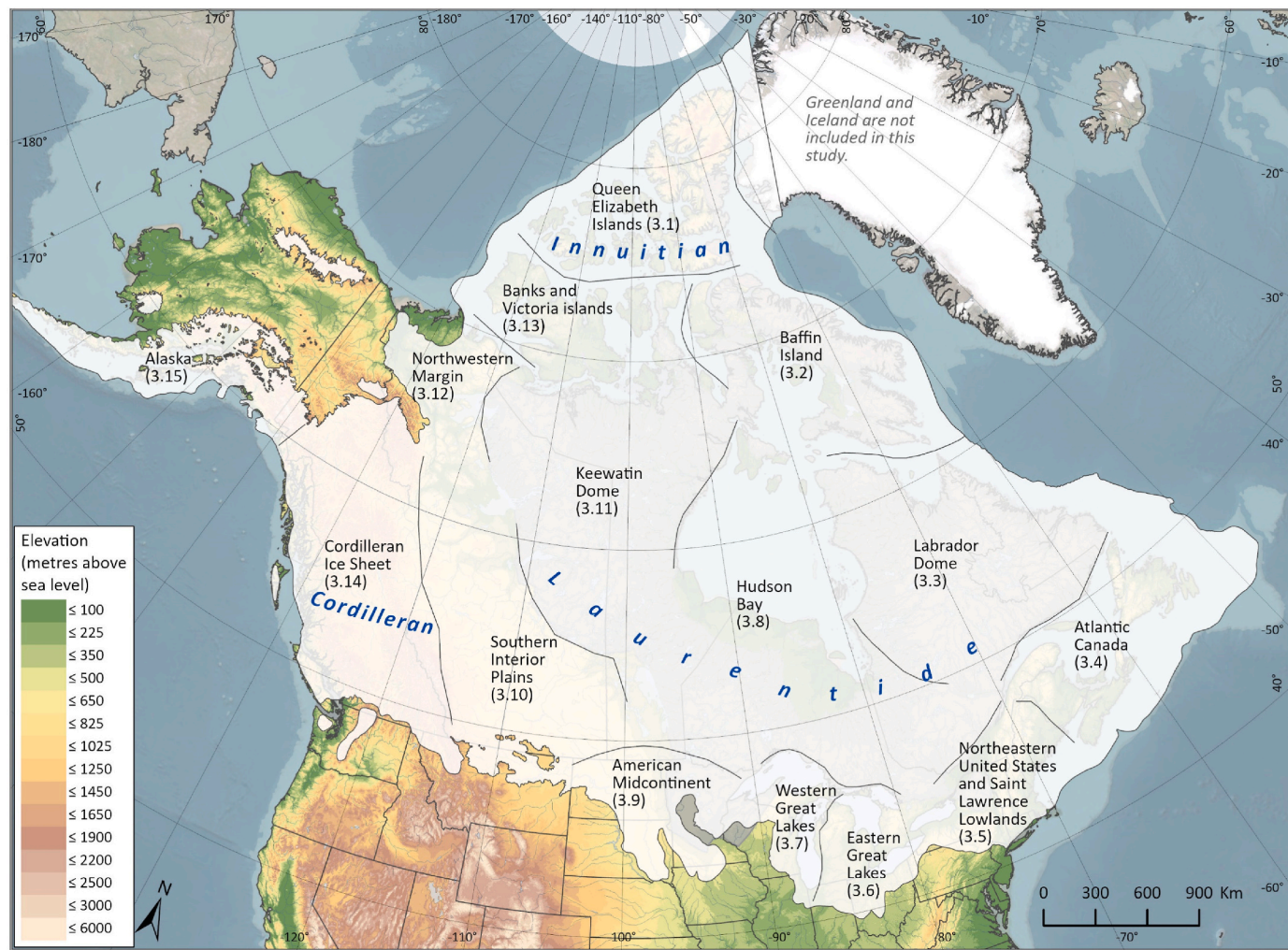


**Fig. 1.** The North American Ice Sheet Complex (NAISC; comprising the Innuitian, Cordilleran and Laurentide ice sheets), along with the 15 regions discussed in the text. The 22-ka optimal ice margin is shown here.

Dyke et al. (2003a); Dyke (2004) as well as Dalton et al. (2020) used this method, in part, to avoid the complications associated with calibration into calendar years (Reimer, 2021).

Although radiocarbon dating has played a fundamental role in placing North American deglaciation into a chronological perspective as well as bracketing intervals of ice advance, these data are not ideally suited for reconstructing ice-sheet retreat because they typically offer only minimum-limiting constraints on it. Cosmogenic nuclide dating, on the other hand, can directly date the emplacement of and retreat from ice-marginal features (e.g. moraines) as long as the assumptions regarding exposure to cosmic rays are fulfilled. This surface exposure technique was developed in the 1980s and 1990s and yields an age by measuring the cosmogenic nuclide concentration in rock surfaces exposed to cosmic radiation since deglaciation (e.g. Phillips et al., 1986; Bierman, 1994; Gosse and Phillips, 2001; Marrero et al., 2016). In recent years, several studies have integrated cosmogenic nuclide dating with other geochronological data to create robust deglacial chronologies for glaciated regions, including the major ice sheets in Eurasia and South America (Hughes et al., 2016; Clark et al., 2018, 2022a; Davies et al., 2020). These chronologies benefit from multiple lines of evidence for

constraining the ice margin, whereas previous efforts were focused largely on minimum-limiting radiocarbon ages with ice margin location(s) tied to deglacial landforms that were not, for the most part, chronologically constrained. To date, no such ‘complete’ deglacial chronology has been presented for the NAISC, despite an acceleration in the use of cosmogenic nuclides to directly date the timing of ice retreat of both the Cordilleran and Laurentide ice sheets (e.g. Balco et al., 2002; Balco and Schaefer, 2006; Briner et al., 2009a; Stroeven et al., 2010; Ullman et al., 2016; Corbett et al., 2017; Menounos et al., 2017; Thompson et al., 2017; Darvill et al., 2018; Lesnek et al., 2018; Margold et al., 2019; Lesnek et al., 2020a; Norris et al., 2022).

Here, we present the first version of North American Deglaciation Isochrones (NADI-1). We use the term “deglaciation isochrones” because it is well-suited to the overall trend of ice retreat through this interval. However, readers should bear in mind that some areas of the NAISC underwent advance during this interval, especially prior to 20 ka. Our work is based on a fully checked chronological database including: (i) cosmogenic nuclide exposure ages that have been re-calculated and standardized across the entire dataset; (ii) calibrated radiocarbon ages, and (iii) luminescence and uranium-thorium ages. Ice margins are

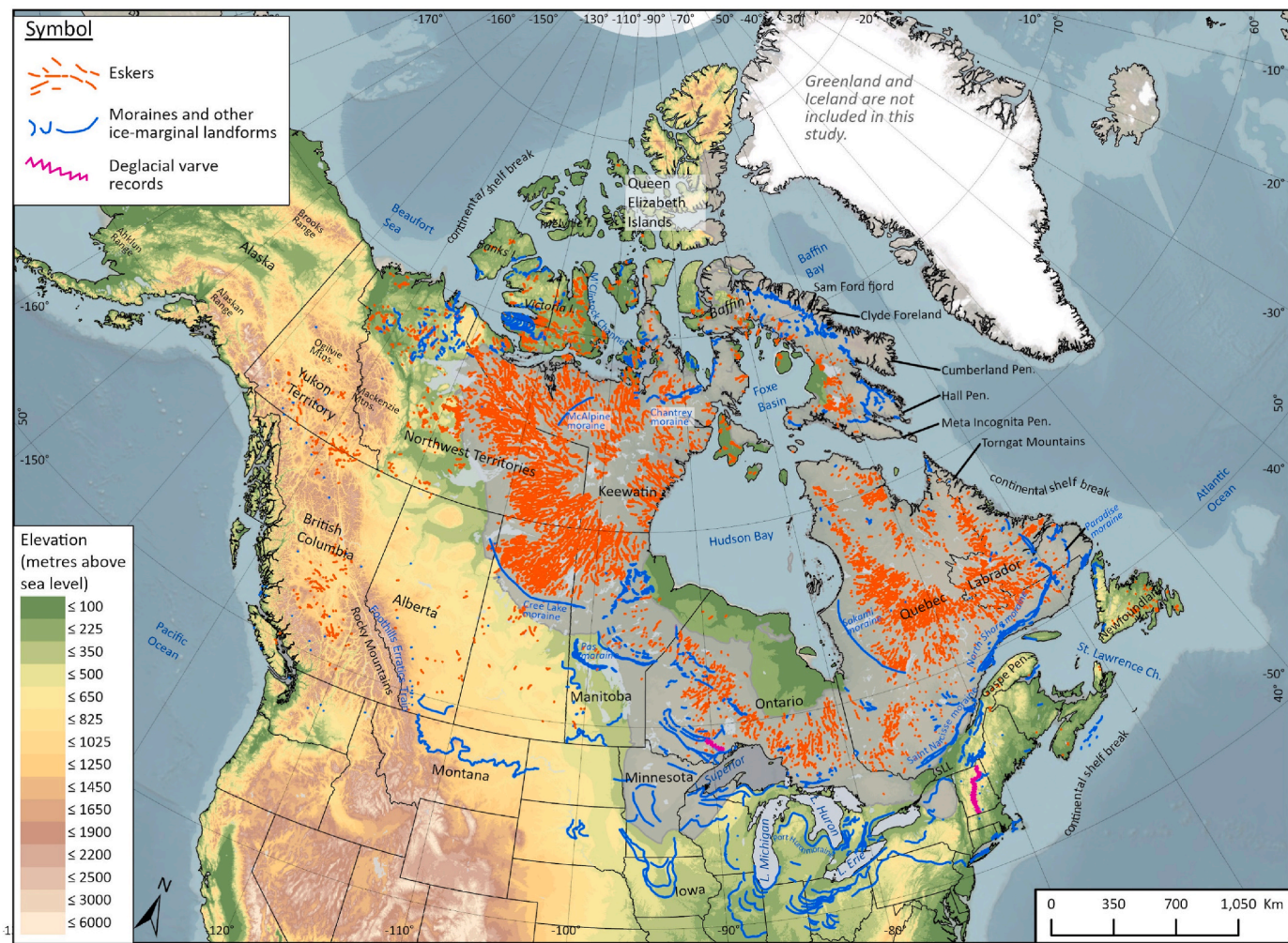


**Fig. 2.** Distribution of major deglacial landforms (eskers and moraines) associated with the North American Ice Sheet Complex, with locations/features mentioned in the text. Eskers are shown for Canada only after Storrar et al. (2013). Moraines are after Prest et al. (1968) and supplemented with major moraines in Manitoba (Gauthier, 2022a), as well as from the United States, as detailed in Supplemental Document 1. Deglacial varve records include the new North American Varve Chronology in the eastern United States (Ridge et al., 2012) and glacial Lake Agassiz in south-central Canada (Breckenridge et al., 2021). The broad grey region covering much of central/eastern Canada is the Canadian Shield. SLL= St. Lawrence Lowland. All moraine and esker outlines in this figure are drawn with the same line thickness. Accordingly, some may appear larger or more prominent in this figure than in real life (ie. several moraines in Manitoba, including the Brandon hills, Alexander, Darlingford and the Bowsman Lake moraines). The reader is encouraged to consult regional maps for more accurate depiction of major and minor moraines, some of which are available online (for example, <https://www.manitoba.ca/iem/info/libmin/geofile1.zip>).

informed by the glacial geomorphological record from the last deglaciation and surficial geology as displayed in the Glacial Map of Canada (Prest et al., 1968) and several local studies (e.g. Teller et al., 2005; McMartin et al., 2012; Barnett and Karrow, 2017; McMartin et al., 2021; Gauthier, 2022a). To facilitate both transparency and future re-interpretations, we have included extensive documentation of all decisions that guided the reconstruction of each of the presented ice margin positions at each time-slice (Supplementary Document 1). The result is a fully documented series of maps showing deglaciation of the NAISC from 25 to 1 ka in 0.5-kyr intervals (49 maps in total), with uncertainties quantified to include our optimal, minimum, and maximum ice extent estimates for each isochrone. All maps and data are presented in calendar years. Our isochrones capture ice advance across some areas, which is based only on limited evidence and is therefore somewhat speculative. In this study, we exclude small mountain ice masses in the western United States that did not coalesce with the NAISC (Marcott et al., 2019). The Greenland Ice Sheet, which was merged with the NAISC in earlier parts of the deglaciation sequence, is beyond the scope of this study. Readers interested in the Greenland Ice Sheet can consult the extensive relevant regional literature (e.g. Larsen et al., 2014; Sinclair et al., 2016; Young et al., 2020; Carlson et al., 2021; Leger et al., 2023).

## 2. Methods

Our assembly and treatment of geochronological data was similar to that of Hughes et al. (2016), who reconstructed the Eurasian ice sheets (40–1 ka) based on a comprehensive geochronological database. Thus, our first task was the compilation of a comprehensive geochronological database (detailed below in Sections 2.1 to 2.4). We then assessed these data in terms of utility for constraining the ice margin, and their reliability (Section 2.5). Finally, we reconstructed the ice margin based on integration of the geochronological database with geomorphic data from the local area (Section 2.6). Extensive justification on the placement of ice margins is available in Supplementary Document 1. The census date for most of our geochronological database is December 31, 2021. However, cosmogenic nuclide data from some 2022 studies were also included here because these data are critical for defining some ice margins. The distribution of geochronological data is plotted spatially in Fig. 3 and temporally in Fig. 4. As a final note, given the enormity of our work, certain data (including geochronological constraints and regional maps) are likely to have been missed. We request to be notified of these omissions so that these data may be integrated into evolving databases and considered in updated versions of the NADI. We herein use the term “LGM” to refer to the maximum ice extents that varied both in extent and timing across the NAISC.

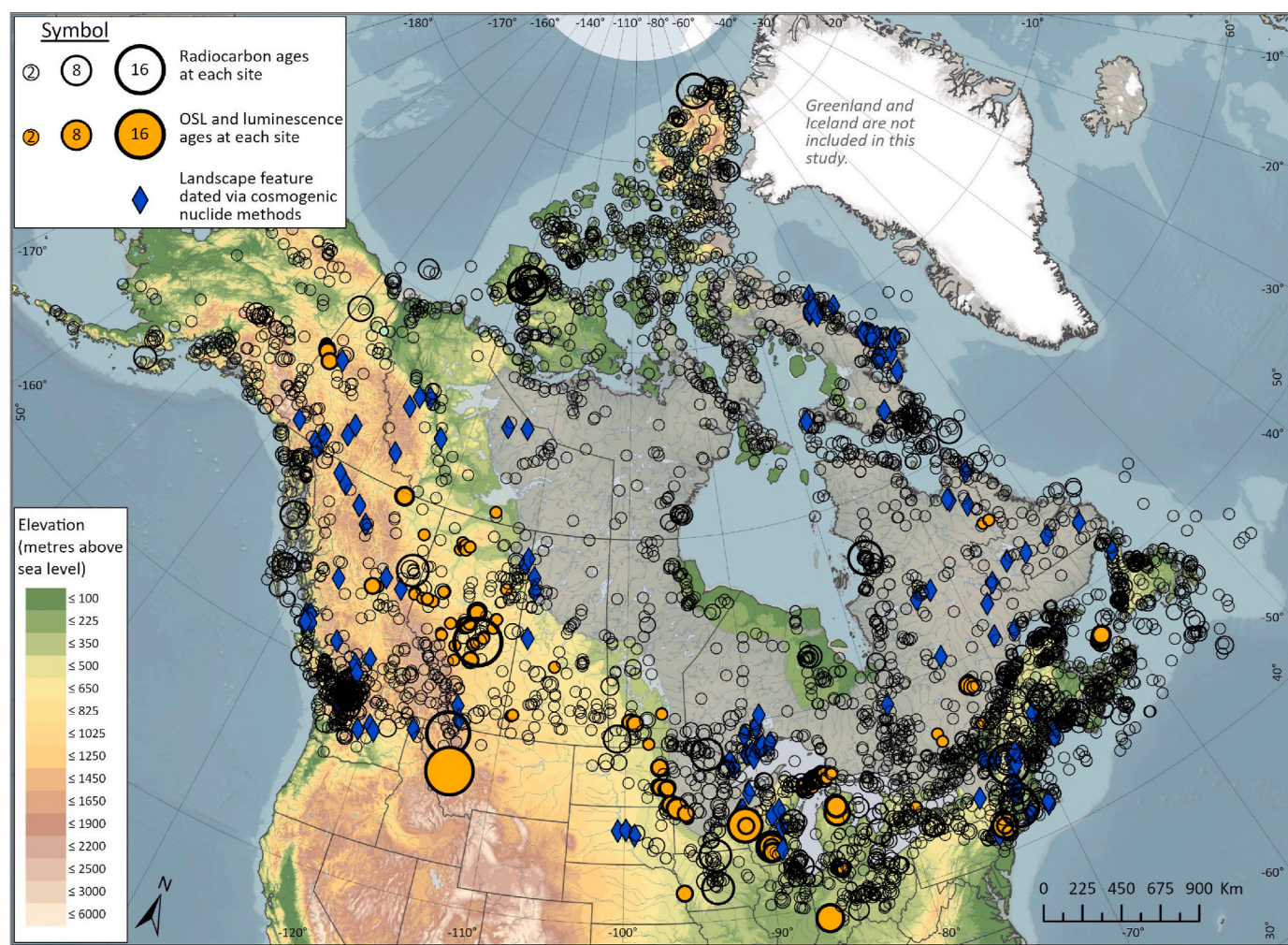


**Fig. 3.** Areal distribution of reliable and likely reliable geochronological data (ranks 1 and 2) that constrain the North American Ice Sheet Complex (NAISC; Laurentide, Cordilleran and Innuitian ice sheets) from 25 to 1 ka. The broad grey region covering much of central/eastern Canada is the Canadian Shield.

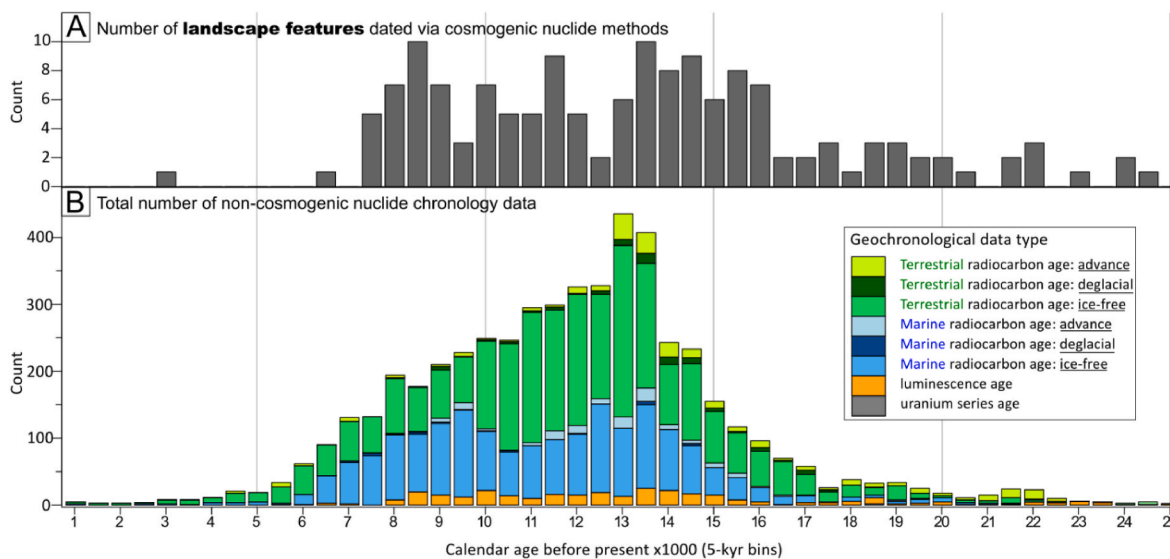


**Fig. 4.** Temporal distribution of reliable and likely reliable geochronological data (ranks 1 and 2) that constrain the North American Ice Sheet Complex (NAISC) from 25 ka to 1 ka. Data were rounded to the nearest 0.5 ka and binned. A) Numbers and temporal distribution of landscape features that we consider to be reliably dated using cosmogenic nuclide methods. In most cases, these directly anchor the ice margin in each time-slice. B) Numbers and temporal distribution of radiocarbon, U-Series and luminescence ages. In most cases, these data offer only minimum constraints on the ice margin in each time-slice.

### 2.1. Compilation of the cosmogenic nuclide database

Cosmogenic nuclide data are highly valuable for reconstructing the dynamics of past ice sheets because they offer a direct age constraint on the abandonment of ice-marginal features. This dating method employs cosmogenic nuclides such as  $^{10}\text{Be}$  and  $^{26}\text{Al}$  that are produced in rocks exposed to cosmic rays at the Earth's surface (Nishizumi et al., 1989; Lal, 1991; Gosse and Phillips, 2001). Assuming the previously un-exposed rock was sufficiently eroded by the last ice sheet and that it has been continuously exposed to cosmic rays since the ice disappeared, the concentration of cosmogenic nuclides in the rock sample can be converted into a deglacial age (Balco, 2011; Heyman et al., 2011). The theoretical upper time limit for cosmogenic nuclide dating using  $^{10}\text{Be}$  and  $^{26}\text{Al}$  extends far beyond the last glacial cycle, with nuclide half-lives of 1.4 and 0.7 million years, respectively (Nishizumi, 2004; Chmeleff et al., 2010; Korschinek et al., 2010), and the method has been successfully applied to date glacial deposits younger than 1000 kyr (Schaefer et al., 2009; Young et al., 2015). Over the last 30 years, cosmogenic nuclide dating has become a major geochronological tool for studies of past glaciations, including dating of glacial retreat and investigation of glacial erosion and burial under non-erosive ice (Briner et al., 2003, 2014; Staiger et al., 2005; Margreth et al., 2016).

Here, we used the *expage* compilation of cosmogenic  $^{10}\text{Be}$  and  $^{26}\text{Al}$  ages (<http://expage.github.io/>) to constrain the deglaciation of the NAISC. We started with all samples from the region covered by the Laurentide and Cordilleran ice sheets ( $n = 2688$ ) including all samples from Alaska. As detailed in Supplementary Table 1, this includes 2229 measurements of  $^{10}\text{Be}$  and 459 measurements of  $^{26}\text{Al}$  from a variety of settings, including boulders ( $n = 1854$ ), bedrock surfaces ( $n = 664$ ), cobbles ( $n = 115$ ), pebbles ( $n = 41$ ), and sediments ( $n = 14$ ). The samples were primarily derived from the eastern, western, and southern regions of the NAISC (Supplementary Document 2), with 58% of all samples located east of  $81^\circ\text{W}$ , and 37% of all samples located on Baffin Island. The cosmogenic nuclide data were derived from studies published from 1994 to August 2022, and include the data from Stoker et al. (2022) and Clark et al. (2022b).

We calculated  $^{10}\text{Be}$  and  $^{26}\text{Al}$  exposure ages using the *expage* calculator version 201912 (<http://expage.github.io/calculator>). This calculator is based on code from the CRONUS calculator v.2 (Balco et al., 2008) and the CRONUScalc calculator (Marrero et al., 2016), and uses

the nuclide-specific  $^{10}\text{Be}$  and  $^{26}\text{Al}$  LSD production rate scaling and the geomagnetic framework from Lifton et al. (2014). Since the region of the NAISC has been affected by different amounts of glacioisostatic uplift following deglaciation, both the calibrated production rates and the calculated exposure ages use time-dependent atmospheric pressure based on interpolated uplift histories (see Supplementary Document 2). As part of our calculations on the *expage* database, we used the ANU uplift reconstruction from Lambeck et al. (2017) for all samples within the uplift reconstruction domain, and the global ICE-6G\_C reconstruction (Argus et al., 2014; Peltier et al., 2015) for the samples outside the domain (samples west of  $140^\circ\text{W}$  and east of  $60^\circ\text{W}$ ). For further details of the exposure age calculations (including comparisons between databases with different uplift and erosion parameters), we refer the reader to Supplementary Document 2 and to the open-source code that is available at <http://expage.github.io/>.

All exposure ages were calculated with input from the *expage* database and assume no erosion. Because we present cosmogenic  $^{10}\text{Be}$  and  $^{26}\text{Al}$  ages assuming a rate of 0 mm/kyr of erosion, they provide a minimum age of deposition. While erosion rates can vary greatly depending on sample lithology, the vast majority of cosmogenic  $^{10}\text{Be}$  and  $^{26}\text{Al}$  ages collated in the NADI-1 database are derived from crystalline lithologies. These resistant lithologies typically exhibit low erosion rates of  $<0.5\text{--}2.0\text{ mm/kyr}$  (Zimmerman et al., 1994; Gosse and Phillips, 2001; Balco, 2011; Davies, 2022). While the impact of erosion on an exposure age will increase with the duration of exposure, an erosion rate between  $<0.5$  and  $2.0\text{ mm/kyr}$  would have a minimal effect on the age of a sample that is less than  $\sim 30\text{ kyr}$  (Gosse and Phillips, 2001; Balco, 2011; Davies, 2022). For example, assuming an average erosion rate of 1 mm/kyr, the exposure age of a sample would increase by 1.0% on average ( $\sim 0.3\%$  for 5 kyr years of exposure,  $\sim 1.2\%$  for 15 kyr of exposure).

To finalize the  $^{10}\text{Be}$  and  $^{26}\text{Al}$  cosmogenic nuclide database, we reduced it to include only those dates that were relevant to our new interpretation of North American deglaciation. This included removal of most ages from Alaska ( $n = 435$ ) because we adopt the ice margins from the Alaska PaleoGlacier Atlas (Kaufman et al., 2011), with the exception of those from Lesnek et al. (2018, 2020b) that are relevant for the central sector of the Cordilleran Ice Sheet region. Second, we removed data ( $n = 922$ ) focusing on glacial erosion and preservation of landscapes under non-erosive ice (Bierman et al., 1999; Briner et al., 2006; Margreth et al.,

2016) as well as data outside the 25 to 1 ka range (Crump et al., 2017; Ceperley et al., 2019). Third, we removed all landscape features that were dated only with a single age ( $n = 92$ ), including transects built using sites with single ages (i.e. McQuinn, 1996; Carlson et al., 2007; Rice et al., 2019). Lastly, we removed all data from ice bodies that are independent of the ice sheets (i.e. Menounos et al., 2017 dated advances of valley and cirque glaciers that were independent from the Cordilleran Ice Sheet). The result of this data screening was 1239 cosmogenic nuclide ages (1121  $^{10}\text{Be}$  ages; 118  $^{26}\text{Al}$  ages) that we then grouped into 164 landscape features (Fig. 4a).

Following the screening of the  $^{10}\text{Be}$  and  $^{26}\text{Al}$  cosmogenic nuclide database, we obtained the average age for each dated landscape feature (e.g. moraine), removing any outliers identified in the original publication. We then rounded this number to the nearest 0.5-ka interval and considered this as the ‘optimal’ position for the ice margin (e.g. 9.8 ka = 10 ka). Next, we averaged the errors for each dated landscape feature and the oldest and youngest possible ages are incorporated into the minimum and maximum uncertainties. In cases where the cosmogenic nuclide errors were less than 1 kyr, we applied a 1-kyr error. We also considered  $^{36}\text{Cl}$  cosmogenic nuclide data, however, following Hughes et al. (2016) we made no recalculation of the ages (see Supplementary Table 1). Age recalculations on  $^{36}\text{Cl}$  cosmogenic nuclide data sometimes result in a 10–15% reduction in age, with a further 1–5% reduction when erosion is taken into account (Margold et al., 2019).

Boulders and bedrock were the most common sample types for cosmogenic nuclide dating, having been used to date ~144 and ~30 sites across the NAISC, respectively. Bedrock samples were combined with samples collected from erratics to date one landscape feature in some locations (Darvill et al., 2018; Clark et al., 2022b). A large number of cosmogenic nuclide ages from bedrock samples were excluded from NADI-1 because they are from studies aimed at determining exhumation and erosion rates, rather than ice retreat (e.g. Fame et al., 2019). Similarly, most of the samples taken from cobbles and pebbles were removed from our database, with only five samples remaining after the database was screened. Of the boulder samples, samples collected from moraine boulders were used to date ~43 sites, while the remaining boulder samples came from erratics.

## 2.2. Compilation of radiocarbon database

Radiocarbon dates offer a minimum constraint on the retreating ice margin because they date the establishment of organic material, which occurred with or at some point after ice withdrawal. Our radiocarbon database ( $n = 4947$  dates; Supplementary Table 2) is an update to previously published compilations (Dyke et al., 2003a; Dyke, 2004; Dalton et al., 2020). All radiocarbon dates were calibrated using CALIB Rev. 8.1.0 (Stuiver and Reimer, 1993) and the IntCal20 calibration curve (Reimer et al., 2020), with the marine curve for marine samples (Heaton et al., 2020). Similar to Hughes et al. (2016), we reported the ages in calendar years, with the midpoint of all age ranges at 2-sigma, and errors as  $\pm$  half the total age range. This was chosen to capture all errors in the same way. The difference between our midpoint and the median was below 100 years in ~91% of the cases, between 100 and 200 years in ~8% of the cases, and between 200 and 330 years in ~1% of the cases. Thus, at our 0.5 kyr time-steps, the choice of median age or midpoint is moot. Ages and errors were rounded to the nearest 10 years.

Marine reservoir corrections were based on a synthesis of local reservoir corrections for the Arctic region (Coulthard et al., 2010), or more recent information from pairs of marine and terrestrial samples, if available. A more recent summary of marine reservoir corrections ( $\Delta R$ ) for North America was published after our census date and was therefore unavailable for use here (Pieńkowski et al., 2022). In the NADI-1 database, local  $\Delta R$  corrections were applied on a regional basis and typically range from 0.05 to 0.8 kyr (Supplementary Table 2). We acknowledge that  $\Delta R$  corrections in large-scale ice sheet reconstructions are a potential source of error, and we detail these concerns in Section 4.4.1.

Overall, approximately 38% of radiocarbon dates were from marine shells, many of which were samples specifically collected to ascertain local deglaciation and sea level change (e.g. England, 1996; Ó Cofaigh et al., 2000). Some marine shell samples were from marine sediment cores and can be used to directly constrain retreat of the ice margin (King, 1996; Pieńkowski et al., 2014). The remaining 62% of radiocarbon ages were from the terrestrial environment, largely basal dates from lake and peat cores (e.g. Richard and Labelle, 1989; Lacourse et al., 2019).

## 2.3. Compilation of luminescence database

Luminescence dating methods provide an age for the last exposure of sediment to sunlight. Thus, in general, they offer a minimum age constraint on ice retreat from a given region. The signal can be extracted in a laboratory either via optically or infrared stimulated luminescence (OSL and IRSL) methods. Thermoluminescence (heat-based) techniques can also be used, however they are prone to age underestimation due to anomalous fading (Huntley et al., 1985). We compiled 397 luminescence ages in our database (Supplementary Table 3). In most cases, these data relate to the establishment of proglacial lake beaches (Teller et al., 2018) or the establishment of stable sand dunes at some point (often immediately) following deglaciation (Wolfe et al., 2004; Munyikwa et al., 2017). However, some ages offer a more precise constraint on the ice margin position, for example, dates on beach ridges that formed at the margins of ice-dammed proglacial lakes can be related to former margins of the glacier (Teller et al., 2018). We make no adjustments or re-calculation of the luminescence ages from those presented in the original sources.

## 2.4. Compilation of uranium-series database

Uranium-series (U-Series) methods constrain the time elapsed since burial of a material. Here, we compiled two U-Series ages in our database (Supplementary Table 4). These data constrain the timing of ice advance in the northwestern margin of the Laurentide Ice Sheet (Lacelle et al., 2013).

## 2.5. Assessment of geochronological data

Once all geochronological data were assembled, we categorized each entry in terms of utility for constraining the ice margin (Table 1). Following the work of Hughes et al. (2016), we considered ‘ice-marginal’ data to be the most useful for directly constraining the timing and position of the ice margin. In our database, these data were largely cosmogenic nuclide ages. We categorized geochronological data as ‘deglacial’ if they very closely dated the emergence of the landscape from under the former ice sheet (e.g. kettle hole in a moraine). This is the same approach as taken with efforts to reconstruct European ice evolution (Hughes et al., 2016); however, we note some issues with this methodology in the Discussion. Overwhelmingly, 83% of our database consisted of ‘ice-free’ age constraints (mostly radiocarbon ages) that suggest the absence of ice with no indication of precisely when the ice sheet disappeared from the site (Fig. 4b). Finally, geochronological data were categorized as ‘advance’ if they constrain the timing of ice advance over a given area (e.g. radiocarbon ages from tree stumps buried under till; U-Series ages on a calcite concretion buried under till). Because our work is focused on the deglaciation of the NAISC, most ‘advance’ ages represent readvances or oscillations of the ice margin during retreat.

After individually assessing all geochronological data in terms of utility for constraining the ice margin (Table 1), we evaluated their reliability following quality assurance procedures for diverse geochronological databases outlined by Small et al. (2017) (see Table 2). Throughout this process, each data point was categorized as reliable (1), likely reliable (2) or unreliable (3). This ranking system addressed various concerns arising in the geochronological database, including

**Table 1**

Categories for geochronological data in terms of utility for constraining the ice margin. All geochronological data are detailed in [Supplementary Tables 1–4](#).

Category	Definition	Examples from the database	Relative presence in database
Ice marginal (ice-contact)	Directly dates the ice margin	Cosmogenic nuclide dating of a moraine; certain cases of radiocarbon ages on terrestrial plant macrofossils in basal lake sediments; certain cases of marine sediments containing drop stones; radiocarbon ages on shells contained in ice-contact delta sediments	Focused on certain regions; Uncommon (3%)
Deglacial	Very closely dates the landscape emergence from under the former ice sheet, ideally within 100s of years.	Radiocarbon dating of organic material that accumulated directly over till or other glacial feature, i.e. kettle holes, katabatic dunes.	Uncommon (6%)
Ice-free	Suggests the absence of ice with little or no indication of when the ice sheet retreated from the area (minimum-constraint on the ice margin).	Radiocarbon age on basal sediment in a lake core; radiocarbon age on animal bones.	Widespread and common (83%)
Advance	Constrains the timing of ice advance over a particular region	Radiocarbon age from tree stumps or other organic remains buried under till; U-Series age on calcite concretion buried under till.	Focused on certain regions; somewhat common (8%)

marine reservoir uncertainties in radiocarbon-dated shells, poorly clustered cosmogenic nuclide data and anomalous fading in luminescence ages. After scrutiny of the database, we consider 70% of geochronological data to be reliable or likely reliable (ranks 1 or 2), while 30% of the database is likely to be unreliable. Cosmogenic nuclide ages underwent a slightly different screening and ranking system and were recalculated as described in Section 2.1.

## 2.6. Constructing the NADI-1 ice margin sequence

The initial set-up for this work involved overlaying several databases onto a map. We first imported elevation data from the [United States Geological Survey's Center for Earth Resources Observation and Science \(EROS\) \(2010\)](#), which has a grid-spacing of 30 arc seconds ( $\sim 1$  km), as well as ocean bathymetry representing the continental shelf (less than 1000 m depth; <http://www.naturalearthdata.com/>). We then overlaid the Canadian Shield (Precambrian rock covering a large portion of Canada) as well as political boundaries for the United States and Canada. The political boundaries were included because they might reflect a shift in resolution of geological mapping or an abrupt map boundary, especially as it relates to the border between United States and Canada. We

then overlayed glacial geomorphological features onto our maps. At the continental scale, a key source of geomorphic data was the Glacial Map of Canada, which includes (but is not limited to) moraines, hummocky terrain, eskers, meltwater channels and flow features ([Prest et al., 1968](#)). We supplemented observations on the Glacial Map of Canada with ice flow indicators and landforms (i.e. lineations and striations) that are mapped in more recent regional and local studies (e.g. [Boulton and Clark, 1990](#); [Kleman et al., 2001](#); [Teller et al., 2005](#); [McMartin et al., 2012](#); [Barnett and Karrow, 2017](#); [McMartin et al., 2021](#); [Gauthier, 2022a](#)). For the glaciated United States, we use the glacial geological map of [Flint et al. \(1959\)](#) along with numerous studies of surficial mapping and geomorphology (e.g. [Leverett, 1902](#); [Clayton and Moran, 1982](#); [Stone and Borns, 1986](#); [Illinois State Geological Survey, 2004](#); [Martin et al., 2004](#); [Wisconsin Geological and Natural History Survey, 2011](#); [Blewett et al., 2014](#); [Johnson et al., 2016](#)). We then overlaid the checked geochronological data (described above in Sections 2.1–2.5). These data were color-coded on the maps for their utility to constrain the ice margin (see Table 1). As a final step in the set-up process, we divided the NAISC into 15 regions having similar glacial history (e.g. retreat patterns) to facilitate extensive regional discussions of the ice history (Supplementary Document 1). We then created 49 empty GIS shapefiles, spanning 0.5-kyr intervals from 25 to 1 ka.

As a first step in constructing the ice margins, cosmogenic nuclide data (when/where available) were used to anchor the ice position through the deglaciation sequence. Basal radiocarbon ages from terrestrial plant macrofossils in lakes were also given high priority for delineating the ice margin; this is discussed below. Although rare, if two different features in the same region yielded the same average age, the ice margin was placed at the midpoint. Because we re-calculated cosmogenic nuclide data (Section 2.1), our resulting pattern of ice retreat is sometimes slightly different from what is presented in the regional studies. However, these regional studies were nonetheless extensively consulted and used to infer the overall pattern of ice retreat and information specific to the ice margin behavior. For the Laurentide Ice Sheet, nunataks were recognized by consulting with the original publication as well as local geomorphological records. During deglaciation of the Cordilleran Ice Sheet, geomorphological evidence indicates that the high mountain peaks became ice free before the valleys, forming nunataks around the edge of the ice sheet, however, due to the complex topography of the Canadian Cordillera and lack of understanding on the ice sheet thickness ([Menounos et al., 2017](#); [Darvill et al., 2022](#); [Dulfer et al., 2022](#)), we chose to draw generalized ice margins without nunataks there.

We then turned our attention to available radiocarbon dates and other minimum-limiting data. We plotted these data on our maps in successive 0.5-kyr increments starting at 25 ka and moving toward progressively younger isochrones. For each isochrone, local studies were consulted, and the ice margin was drawn up-ice of radiocarbon dates. In some cases, we adopted the ice margin as suggested by relevant local studies (e.g. position of the Frontier Moraine; [Parent and Occhietti,](#)

**Table 2**

Ranking system for the geochronological database. Uranium-series data are excluded from this table because only two data points were available for this work (see [Supplementary Table 4](#)).

Rank	Examples from the database
1 (reliable)	<b>Radiocarbon:</b> Identified terrestrial plant fragments; animal bones; charcoal; insects. <b>Luminescence:</b> Dated feature yields a well-grouped age cluster with limited outliers; no anomalous fading. <b>Cosmogenic nuclide:</b> Dated feature yields a well-grouped age cluster with limited outliers.
2 (likely reliable)	<b>Radiocarbon:</b> Marine shell/foraminifera age that includes a local reservoir correction shell age that is based on down-core extrapolation. <b>Luminescence:</b> Invalid coordinates; errors not reported; any anomalous fading has been corrected. <b>Cosmogenic nuclide:</b> Dated feature yields a somewhat well-grouped age cluster with limited outliers.
3 <sup>a</sup> (unreliable)	<b>Radiocarbon:</b> unclear stratigraphic context; impacted by hardwater effects; high probability of sample contamination; unreported errors; deposit-feeding marine shells ( <a href="#">England et al., 2013</a> ); bull peat/sediment age; gyttja. <b>Luminescence:</b> anomalously old age in an otherwise well-grouped cluster; sample failed the dose recovery test; suspected post-depositional sediment mixing and/or poor solar resetting. <b>Cosmogenic nuclide:</b> Poor clustering of ages on a given feature; sample suffers from inheritance.

<sup>a</sup> Some ages are also considered unreliable (rank = 3) if they are deemed incorrect according to original author or subsequent analysis. See [Supplementary Tables 1–4](#) for further information.

1999). In select regions, the ice position was informed by varve chronologies, which offer precise constraint on ice retreat based on annual varve counts instead of radiometric geochronological constraints (e.g. Northeastern United States and Quebec; Antevs, 1925; Ridge et al., 2012). Finally, radiocarbon ages from organic materials buried below glacial deposits were used as maximum-limiting evidence for local ice re-advance (e.g. ~12 ka ice advance over Lake Superior; Lowell et al., 1999). Regardless of the methodology used to derive the ice margins, they were drawn in accordance with available moraines and/or ice-contact features, and we used eskers to infer direction of the retreat and subsequent retreat pattern/timing (e.g. glacial map of Canada; Prest et al., 1968; extensive esker mapping of Storrar et al., 2013).

As a last resort, if no reliable geochronological information was available in a region, we made informed decisions about the ice margin based on glaciological principles and assumptions. When adopting this method, we assumed a constant rate of retreat and drew the ice margin by consulting local maps. For example, we might have depicted a specific ice margin roughly following local topographic relief. A key location where there is a lack of certainty regarding the timing of ice extent is on the continental shelf around the Queen Elizabeth Islands (see Section 3.1). Geomorphological evidence from (Margold et al., 2015b) confirms the presence of large ice streams, and therefore an extension of the ice margin, on the continental shelf. However, the timing of this is not well constrained (see Margold et al., 2018 for a discussion of the local LGM ice extent in these regions). Moreover, we assume that ice extended to the continental shelf break over the entire extent of the Queen Elizabeth Islands and was not limited to areas where there is evidence for ice streaming. We assumed the LGM occurred at 25 ka, with progressive retreat toward the coastline. Finally, in some cases, local inferences were applied more broadly over distances of 200–500 km. For example, radiocarbon dates suggest the ice margin was stalled off the coast of Labrador at the continental shelf break until ~15 ka (see Section 3.3); we apply this assumption to the ice margin off the neighboring continental shelf. Although this approach has shortcomings, it offers a practical solution to portraying the ice margin in regions where no geochronological information is available. Very rarely, when no reliable radiocarbon ages were available for a given region, we sometimes cautiously considered radiocarbon ages derived from bulk organic material, assigned a reliability rank of 3, to glean something useful about the ice margin (e.g. configuration of ice margin based on an ice-marginal shell deposit; very broad deglacial time constraint based on the dating of basal lake organics). When this was the case, we adopted wider min-/max ice margins for the given area, and sometimes relied on linear interpolation between areas with reliable constraint and those without. We acknowledge there are uncertainties associated with this approach, however, our reasoning is that ‘something is better than nothing’ when very little data are available for constraining the ice margin. Supplementary Document 3 contains an overlay of ice margins from NADI-1 with geochronological data used for delineating the optimal ice margin – this visualization is useful for understanding the geochronological data available (or absent) in each region at a given time slice.

Once the optimal ice margin was finalized and fully described for each time-step, we turned our attention toward minimum and maximum ice extents. In regions where cosmogenic nuclide data were available, we use the youngest sample in the cluster as the minimum ice estimate and the oldest sample as the maximum ice extent, both rounded to the nearest 0.5 ka (excluding outliers; see Section 2.1). For example, if ‘Moraine X’ yielded 5 reliable (e.g. outliers removed) samples with ages of 14.6 ka, 17 ka, 13.2 ka, 14.2 ka and 15.5 ka, then the minimum/maximum errors on that feature would be 13 ka and 17 ka, respectively. Under this scenario, the following 3 actions were taken (i) the ice margin at 15 ka (average of samples) would be aligned to Moraine X, (ii) the minimum ice extent for 17 ka, 16.5 ka, 16 ka and 15.5 ka would be aligned to Moraine X, and (iii) the maximum ice extent for 14.5 ka and 14 ka would be aligned to Moraine X. This method was chosen to cover all uncertainties involved in cosmogenic nuclide dating. In regions

where the ice retreat was controlled only by minimum-limiting radiocarbon ages, we generally assigned the minimum and maximum ice extents as the ± 1-kyr isochrone. This approach accounted for uncertainties inherent to defining the ice margin using minimum-limiting radiocarbon ages, as well as any uncertainties in the radiocarbon database (including errors on the radiocarbon ages and uncertainties related to marine reservoir corrections). In regions where there was little constraint on the ice margin, we apply broader uncertainties. For example, the minimum/maximum ice extents for the Queen Elizabeth Islands between 25 ka and 15 ka were all placed at the coastline and shelf break, respectively, to account for our general uncertainty about the ice configuration during that interval (Section 3.1).

Rarely, the availability of multiple geochronological data types made the regional deglacial sequence more robust. In those cases, we modelled the minimum and maximum ice extents after the original publication. This was the case for the Southern Interior Plains, where cosmogenic nuclide dating and additional chronometers at several sites across the region offered tight constraint on ice dynamics that were strengthened by modelling (see Section 3.10; Norris et al., 2022). We adopted a similar approach for ice retreat across Alaska (Section 3.15), where our work was based on version 2 of the Alaska PaleoGlacier Atlas (Kaufman et al., 2011) and was merged with our interpretation of the remainder of the Cordilleran Ice Sheet.

### 3. Overview of ice retreat

In this section, we provide a brief overview of ice dynamics (largely retreat) across the NAISC between 25 ka and 1 ka. To facilitate discussion across the NAISC, we divide our work into 15 regions with similar glacial history (Fig. 1). We begin each subsection with an overview of deglacial landforms (Fig. 2), a broad statement on the overall approach for reconstructing the regional ice retreat, and a statement of uncertainty bounds for each region. The term ‘uncertainty bounds’ refers to the distance between the minimum and maximum ice estimates in each isochrone. We then provide a brief overview of key elements of the regional ice dynamics, citing essential publications and drawing attention to any databases that were fundamental to our work. Full details and justification for each ice margin (including minimum and maximum uncertainties) are available in Supplementary Document 1 and the location of all place names referred to in the descriptions below are shown in Figures SD1.1 to 1.15. We use the term ‘re-advance’ to refer to an oscillation of the ice margin that is often small (<100 m) and does not necessarily carry a climatic significance. A 49-panel figure showing all of NADI-1 is available in Supplementary Document 3 (with relevant geochronological data) and Supplementary Document 4 (without geochronological data). Optimal ice margins for 25–1 ka are overlaid in Fig. 5. Uncertainties across specific transects are shown in Fig. 6.

#### 3.1. Queen Elizabeth Islands

The Queen Elizabeth Islands hosted the Innuitian Ice Sheet (see Fig. 1 as well as England et al., 2006). This region is largely void of moraines (with some exceptions, see: England, 1978) but contains abundant eskers, meltwater channels (see Fig. 2 as well as Prest et al., 1968; Fulton, 1995; Dyke, 1999; Storrar et al., 2013) and widespread evidence of postglacial marine inundation along low-lying coastal regions (e.g. England, 1996; Ó Cofaigh et al., 2000). Our portrayal of ice retreat across the region is guided largely by these deglacial landforms as well as the age and location of radiocarbon dates (~380 total, largely marine shells). The uncertainty bounds remain constant at ~200 km from 25 to 15 ka as they are defined by the distance between the present-day coastline (minimum) and continental shelf break (maximum; see Fig. 6a, b and c). From 14.5 ka onwards, the uncertainty bounds are highly variable, with the largest uncertainty relating to the separation of the Laurentide and Innuitian ice sheets between 11.5 and 10.5 ka where the uncertainty bounds span 1000 km (see Fig. 6b and c).

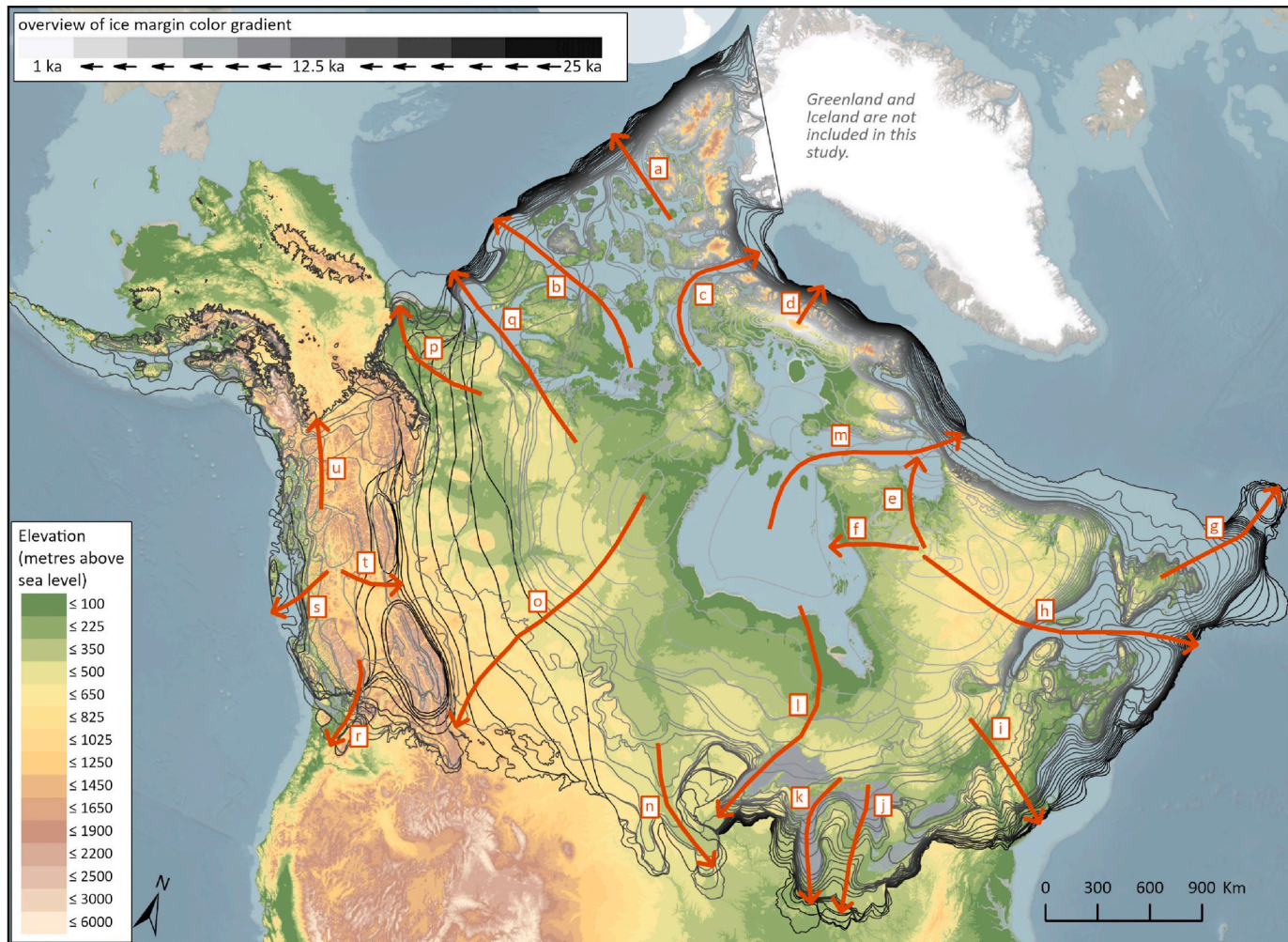


**Fig. 5.** All optimal NADI-1 margins from 25 ka to 1 ka. Orange arrows and boxes indicate flow lines for the uncertainty plots shown in Fig. 6. Some features (political boundaries, the Canadian Shield, lakes and rivers) have been omitted from this map to see the ice margin lines more easily. Note that we do not reconstruct the location of ice domes or saddles here or show how they migrated over time.

In terms of ice dynamics, between 25 ka and 14 ka in the Queen Elizabeth Islands, we show the ice margin at the continental shelf break and progressively retreating landward. This maximum ice extent and subsequent retreat is based on geomorphological evidence from Margold et al. (2015b) that suggests the presence of large ice streams on the continental shelf. We assume that ice extended to the continental shelf break over the entire CAA and was not limited to areas where there is evidence for ice streaming. Next, between 14 ka and 12 ka, we show a dramatic retreat of the western-most Innuitian ice as suggested by radiocarbon dates (largely from shells) from the coastline of Melville and surrounding islands (Hodgson, 1994; England et al., 2009; Nixon and England, 2014). A notable exception to this pattern is a re-advance of Laurentide ice (ice stream?) through McClintock Strait at 13 ka that deposited the Winter Harbour Till on southernmost Melville Island (constrained via radiocarbon ages on shells in till; Hodgson et al., 1984; Hodgson, 1994; England et al., 2009). Between 12 ka and 9.5 ka, widespread radiocarbon dating of marine shells (Ó Cofaigh et al., 2000; Atkinson and England, 2004; England et al., 2004), as well as marine coring and seafloor mapping around the broad Queen Elizabeth Islands (Pieńkowski et al., 2014; MacLean et al., 2017; Furze et al., 2018) suggest a dramatic retreat of ice toward the innermost areas of the archipelago. Innuitian ice separated from the westernmost Greenland Ice Sheet around 8 ka and this on-land retreat of the ice margin continued until 5 ka, where fragmented remains of Innuitian ice persisted in the

highland areas until present-day (present-day ice extent with nunataks removed; Natural Earth, 2021). Overall, our depiction of ice retreat over the Queen Elizabeth Islands is similar to England et al. (2006), however differs because of our assessment and calibration of radiocarbon ages, as well as our alignment of the 5 ka to 1 ka isochrones to a more recent digitization of present-day ice extent over the region (Natural Earth, 2021).

### 3.2. Baffin Island

The northeastern coast of Baffin Island (Fig. 1) is characterized by extensive fiords and cliffted islands, whereas the southwestern part of the island is low-lying, and was inundated by marine waters following deglaciation. Deglacial moraines and eskers are common, and generalized ice flow data suggest ice retreat occurred from all sides of Baffin Island inland to central regions (Fig. 2; Prest et al., 1968; Fulton, 1995; Kleman et al., 2001; Storrar et al., 2013). The deglaciation of Baffin Island is anchored by cosmogenic nuclide dating of 35 landscape features and is complemented by ~320 radiocarbon ages. The uncertainty bounds remain constant at ~100 km from 25 ka to 13 ka as they are defined by the distance between the present-day coastline (minimum) and continental shelf break (maximum; Fig. 6d). From 13 ka onwards, the uncertainty bounds remain small (<100 km), particularly in locations that still contain remnant ice today.

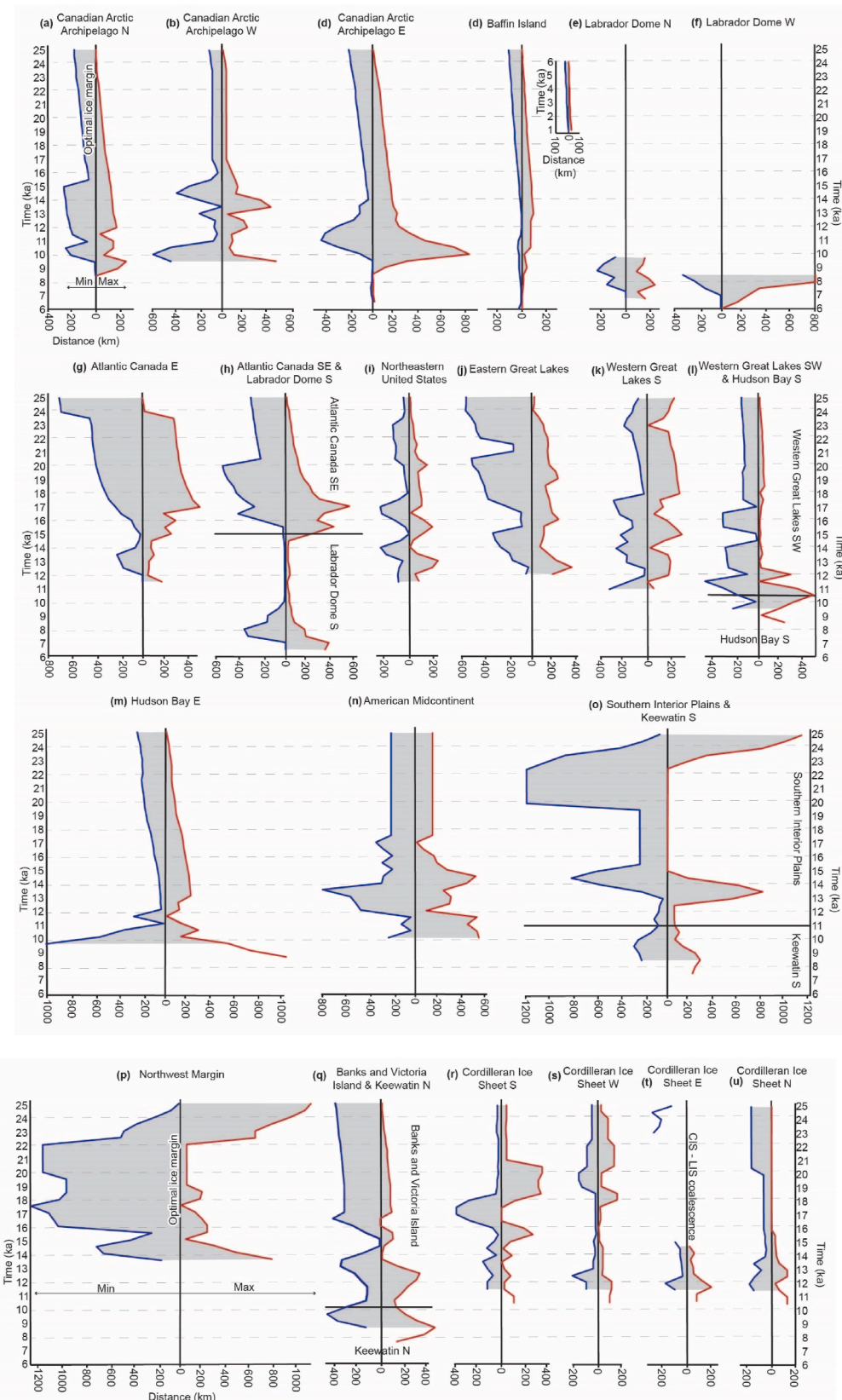


**Fig. 6.** Visualization of NADI-1 uncertainties. (a) to (u) graphs of time from 25 to 6 ka versus distance along a flowline from the optimal ice margin position (0 km) to the position of the maximum ice extent (red line) and minimum ice extent (blue line) for each region. Where a flowline crosses two regions, these regions are delineated in the graph by a horizontal black line. Note that for Baffin Island (graph d) time from 6 ka to present is also shown. The locations of the flowlines are shown in Fig. 5. Please note that we do not reconstruct the location of ice domes or saddles here or show how they migrated over time.

In terms of ice dynamics, between 25 ka and 15 ka, we show Baffin Island largely ice-covered, and the ice margin extended to the continental shelf break in Baffin Bay. Full glacial coverage of Baffin Island is supported by numerous cosmogenic nuclide dating studies along with geomorphic mapping (coverage in interstream/interfiord areas by largely non-erosive ice, see: Briner et al., 2003, 2005; 2009b, 2014). Extension to the continental shelf break at 25 ka is based on evidence of large ice streams (Margold et al., 2015b), the presence of a marine grounding line (Li et al., 2011), as well as evidence of an ice margin near the shelf break (Brouard and Lajeunesse, 2017; Jenner et al., 2018). We show the Clyde Foreland and northeastern coastal lowlands (Fig. 1) becoming ice-free starting at 15 ka, following cosmogenic nuclide dating of boulders in the local area (Briner et al., 2005; Davis et al., 2006b; Young et al., 2012). Deglaciation of Cumberland Peninsula began at 14.5 ka, and largely follows the cosmogenic dating of Margreth et al. (2017) and Corbett et al. (2016), as well as the work of Young et al. (2020, 2021). Starting at 13 ka, we show ice retreating through the fiords and sounds while being maintained in upland areas. The pattern of retreat across northeastern Baffin Island is based on cosmogenic nuclide dating of Sam Ford fjord (Briner et al., 2009a). Retreat of ice from Hall and Meta Incognita peninsulas is based largely on minimum-limiting radiocarbon ages and local surficial geology studies (i.e. Hodgson, 2003, 2005; Carboneau et al., 2012; Tremblay et al., 2013). The final phase of deglaciation started around 8 ka and is characterized by the collapse of ice over Foxe Basin and an ever-shrinking ice mass in the central regions of Baffin Island where the Barnes and Penny ice caps still persist.

### 3.3. Labrador Dome

The Labrador Dome was centered over the Canadian Shield in Labrador and Quebec (Fig. 1). Glacial geomorphological data suggest post-glacial marine inundation in coastal regions, and the subsequent inward receding ice left behind a myriad of eskers, moraines and glacial lake deposits (Fig. 2; Prest et al., 1968; Fulton, 1995; Storrar et al., 2013; Dubé-Loubert and Roy, 2017). Several different deglaciation histories have been proposed for this region (Kleman and Hättestrand, 1999; Veillette et al., 1999; Clark et al., 2000); our depiction of ice retreat is guided largely by cosmogenic nuclide dating of 15 landscape features (Carlson et al., 2007), along with the age and location of radiocarbon dates (~320 total, largely marine shells) and broadly follows the pattern of retreat suggested by Clark et al. (2000). The uncertainty bounds on the eastern margin of the Labrador Dome are low (<50 km; see Fig. 6h) between 14.5 ka and 10 ka as the ice margin retreats from the continental shelf break to the inner coast. The uncertainty bounds are much larger after 10 ka, reaching over 1000 km at 8.5 ka, which is related to the highly dynamic ice retreat in this region (Fig. 6e, f, and h).

In terms of the ice dynamics, at 25 ka we show Labrador ice extended onto the continental shelf edge, with a gradual retreat landward until 14.5 ka. The placement of the ice margin onto the continental shelf is supported by the presence of ice streams (Margold et al., 2015b), a marine grounding line (Li et al., 2011) and other ice margin evidence (Brouard and Lajeunesse, 2017; Jenner et al., 2018) from the shelf edge along the coast of Labrador and northward toward Baffin Island. Around 14 ka, geochronological evidence indicates ice retreated to the coastline near the Torngat Mountains, where the Saglek Moraines were dated to 14 ka (Clark et al., 2003). By 10 ka, we show the eastern margin of the Labrador Dome retreated to the Paradise Moraine ( $^{10}\text{Be}$  cosmogenic nuclide data; Ullman et al., 2016). Deposition of the North Shore Moraine and Sakami Moraine followed shortly afterward, as suggested by cosmogenic nuclide dating (Ullman et al., 2016). Between 8.5 ka and 6 ka, we show progressive reduction of the Labrador Dome that broadly follows the pattern of retreat suggested by Clark et al. (2000). This portrayal of ice retreat accommodates marine and terrestrial radiocarbon ages, especially along the shores of Hudson Bay (Lajeunesse, 2008), and is adjusted inward to accommodate re-entrants from glacial

lakes (Lac Payne and Lac Minto; Lauriol and Gray, 1987; Gray et al., 1993).

### 3.4. Atlantic Canada

Atlantic Canada is in easternmost Canada, adjacent to the Atlantic Ocean (Fig. 1). This region hosted a semi-independent ice mass, the Appalachian Ice Complex. Eskers, marine-based moraines and rib-like ridges suggest that ice retreated landward from an earlier position at the continental shelf break (Fig. 2; Prest et al., 1968; Stea et al., 1986; Fulton, 1995; Storrar et al., 2013). Our portrayal of ice retreat over this region is based largely on the age and location of radiocarbon dates (~710 total), along with local geomorphic mapping studies, and previous efforts to synthesize regional ice history. The uncertainty bounds remain constant from 25 ka to 17 ka as they are defined by the distance between the present-day coastline (minimum) and continental shelf break (maximum), with the width of the continental shelf varying between 200 and 700 km off the coast of Newfoundland and Nova Scotia (see Fig. 6g, and h). From 20 ka onwards the uncertainty bounds surrounding the deglaciation in the Laurentian Channel are large (~700 km; see Fig. 6h).

In terms of ice dynamics, between 25 ka and 17 ka, we assume ice over Atlantic Canada extended to the continental shelf break, and gradually retreated landward. The (undated) extension of the ice margin to the continental shelf break is supported by bathymetric data, seismic mapping, evidence of ice streams and side scan sonograms to map the Quaternary sediments on the continental shelf (King, 1996; Shaw et al., 2006; Todd et al., 2007; Roger et al., 2013; Margold et al., 2015a; Broom and Cameron, 2021). Next, cosmogenic nuclide dating of a high-elevation peak in western Newfoundland suggests significant thinning of the ice sheet by 18 ka (Gosse et al., 2006). Following the work of Shaw et al. (2006), we then show a pronounced embayment into the St. Lawrence Channel beginning around 17 ka, guided by radiocarbon ages from marine cores. By 14 ka, we show ice largely restricted to terrestrial areas. At 12.5 ka, we show a re-advance of ice over large parts of Atlantic Canada, which has been linked to the Younger Dryas (as studied extensively by Mott et al., 1986; Levesque et al., 1993; Stea et al., 2011). The regional extent of this re-advance is constrained by surficial mapping of the re-advance till, radiocarbon dating of buried organic material and paleoclimate indicators suggesting a short-lived climate oscillation (Jetté and Mott, 1989; Mott and Stea, 1994; Stea and Mott, 2005). Remnant ice over the Gaspe Peninsula also stabilized or underwent local re-advances of ~3 km along river valleys at that time (Hétu and Gray, 2000), and a similar re-advance occurred in coastal areas of western Newfoundland at 12 ka, as suggested by marine shells located in re-advance tills (Grant, 1969, 1992). These regional re-advances were short-lived, and, by 11 ka, we show a completely ice-free Atlantic Canada.

### 3.5. Northeastern United States and St. Lawrence Lowlands

The Northeastern United States and St. Lawrence Lowlands are located in the easternmost sector of the NAISC (Fig. 1). The region hosted a semi-independent ice mass, the Appalachian Ice Complex. This region contains numerous glacial features, including moraines, nunataks, and proglacial lake deposits with varve records (Fig. 2; Stone and Borns, 1986; Stanford, 1993; Ridge et al., 1992, 2012). Our interpretation of ice retreat across this region is anchored by cosmogenic nuclide dating of 24 landscape features and is complemented by radiocarbon dates (~550 total; largely marine shells and post-glacial organic material), OSL ages on post-glacial sediments and the New England Varve Chronology (Ridge et al., 2012). Due to the wealth of geochronological information in this region, the uncertainty bounds are relatively low throughout the deglaciation (between 40 km and 340 km; see Fig. 6i).

Cosmogenic nuclide dating suggests that ice in the Northeastern United States was at the local terminal moraines at 25 ka (Balco et al.,

2002; Corbett et al., 2017). Offshore, we show the 25-ka ice margin at the continental shelf break based on available geochronological data (Schlee, 1973; Schnitker et al., 2001). From 25 ka to 16.5 ka, we show a progressive retreat of the ice margin northwestward across the region, anchored by numerous cosmogenic nuclide ages on moraines (Balco et al., 2002; Balco and Schaefer, 2006; Hodgdon, 2016), a few minimum-limiting radiocarbon ages, and earlier work that integrated geomorphic mapping and ice retreat across the region (Stanford, 1993; Stanford et al., 2020). Between 16.5 ka and 13.5 ka, ice retreat continued, with large parts of low-lying coastal regions becoming ice-free and, initially, inundated with marine water (Borns et al., 2004). Retreat of the ice margin across the Northeastern United States through this interval is constrained largely by (i) cosmogenic nuclide dating of moraines and mountain peaks (Balco et al., 2009; Bierman et al., 2015; Davis et al., 2015; Hall et al., 2017; Bromley et al., 2015, 2020), and (ii) the new North American Varve Chronology (Ridge et al., 2012). There is also evidence of regional ice thinning around this time as suggested by the appearance and dating of nunataks (Davis et al., 2015; Koester et al., 2017). A final feature of ice retreat across this region is the collapse of ice from the St. Lawrence Lowlands at 12.5 ka, which resulted in a widespread marine inundation by the Champlain Sea (Occhietti and Richard, 2003; Richard and Occhietti, 2005). The ice margin then stagnated north of the region at the St. Narcisse moraine (Occhietti et al., 2011).

### 3.6. Eastern Great Lakes

The Eastern Great Lakes region is situated at the southeastern part of the NAISC and includes the area surrounding Lake Erie and east of Lake Michigan (Fig. 1). In terms of deglacial landforms, lobate moraines are a prominent feature of the landscape, with notably extensive moraines emanating outward from Lake Erie (Fig. 2; Goldthwait et al., 1967). Our depiction of the deglaciation of the Eastern Great Lakes is guided largely by radiocarbon dates (~710 total), along with extensive regional mapping of the aforementioned lake-border moraines. The uncertainty bounds are relatively large (between 550 km and 650 km) between 25 ka and 17.5 ka due to the lack of available constraints at these time-steps. From 17 ka onwards the uncertainty bounds range between 180 km and 370 km (see Fig. 6j).

Between 25 ka and 20 ka, we show a gradual retreat of the ice margin in the Eastern Great Lakes following a multiproxy analysis of ice dynamics (including chronology, stratigraphy, geomorphology and sedimentology associated with local moraine systems) by Heath et al. (2018), fitted to the location of mapped moraines in this region (Flint et al., 1959). In some regions the ice margin is poorly constrained and we align it with local chronological and geological work of Loope et al. (2018a) which suggests the maximum local ice extent was reached around 24 ka. From 19.5 ka to 16.5 ka, we show a gradual retreat of ice northward across the region. Starting at 16.5 ka, we show ice retreating toward the northeast into Lake Erie, which resulted in several successive ice-contact proglacial lakes (Barnett, 1985; Barnett and Karrow, 2018). Retreating ice then stabilized at the extensive Port Huron Moraine by 15.5 ka (Karrow et al., 2000), which resulted in a broad outwash plain to the west (Blewett et al., 1993; Schaetzl and Weisenborn, 2004; Schaetzl et al., 2017). Further retreat of ice into southwestern Ontario between 15 ka and 13 ka is guided by extensive geological and geochronological work in the region (Mulligan et al., 2018).

### 3.7. Western Great Lakes

The Western Great Lakes region is situated at the southern part of the NAISC and includes the area south and west of Lake Michigan, along with the area south of Lake Superior (Fig. 1). In terms of deglacial landforms, the region south of Lake Michigan is characterized by extensive lobate moraines and ice-walled lake plains (Fig. 2; Johnson et al., 1997; Clayton et al., 2008; Curry and Petras, 2011; Curry et al.,

2014). Our portrayal of the ice retreat from the Western Great Lakes is guided by cosmogenic nuclide dating of 11 landscape features (south of Lake Superior), 119 post-glacial sites dated via OSL or luminescence methods and minimum-limiting radiocarbon ages (~220 data points). The uncertainty bounds in this region vary between 150 km and 400 km (Fig. 6k and l). Occasionally, around Lake Superior, the uncertainty bounds are much smaller (<50 km), where the ice margin position is well constrained by cosmogenic nuclide ages.

In terms of ice dynamics, south of Lake Michigan, we show ice reaching its maximum extent at 23 ka following maximum-limiting radiocarbon ages on sub-till organic material (largely wood and plant macrofossils; Curry and Petras, 2011; Heath et al., 2018). We then show a northward retreat of the ice margin, anchored by the position of mapped moraines and supported by radiocarbon dating on organic material contained in ice-walled lake plain deposits (Johnson et al., 1997; Curry et al., 2010; Curry and Petras, 2011). The ice margin reached the modern-day southern coastline of Lake Michigan by 17.5 ka, and gradually retreated northward afterward. South of Lake Superior, we show the ice configuration between 25 ka and 22 ka at the local terminal moraines as suggested by cosmogenic nuclide dating of boulders by Colgan et al. (2002) and Ullman et al. (2015). Starting at 22 ka, we show a gradual retreat of the ice margin eastward toward Lake Michigan and northward toward Lake Superior, anchored by additional cosmogenic nuclide dating work from the aforementioned studies. Retreat eastward toward Lake Michigan was interrupted by a pronounced re-advance at 14 ka (Two Creeks forest bed; Lowell et al., 1999). By 12 ka, the ice margin had retreated northward into Lake Superior. We finally show a brief southward re-advance toward the southern shoreline of Lake Superior at 11.5 ka as determined by the radiocarbon dating of buried forests near Marquette, Michigan (Lake Gribben forest bed; Hughes and Merry, 1978; Lowell et al., 1999).

### 3.8. Hudson Bay

The Hudson Bay region comprises an extensive area of central Canada, spanning both marine and terrestrial environments (Fig. 1). Deglacial landforms consist of extensive moraines, eskers and proglacial lake sediments (Fig. 2; Prest et al., 1968; Storrar et al., 2013; Gauthier, 2022a). Our interpretation of ice retreat across the region is guided largely by these deglacial features, the age and location of radiocarbon dates (~250 total; largely marine shells) and recent studies that have tracked ice retreat across this region (Roy et al., 2015; Gauthier et al., 2020). The uncertainty bounds remain constant at 260 km in the area of the Hudson Strait sill between 25 ka and 11 ka as they are defined by the distance between the present-day coastline (minimum) and continental shelf break (maximum; see Fig. 6m). From 10.5 ka to 8.5 km the uncertainty bounds are high, spanning up to 1500 km at 9.5 ka, which reflects the dynamic nature of ice retreat through Hudson Strait and across Hudson Bay at these time-steps (Fig. 6l and m; Laymon, 1991; Stravers et al., 1992; McMartin et al., 2013).

Our depiction of the deglaciation of the Hudson Bay region begins at 12 ka. At that time, over Quebec, we assume a constant rate of retreat and align the ice margin to mapped moraines (Occhietti, 1980; Bolduc, 1995; Govare, 1995; Occhietti et al., 2011), guided by minimum-limiting radiocarbon ages. Closer to the Quebec/Ontario border, our ice margins follow the reconstructions of Veillette (1994), which are based largely on evidence from glacial lakes that occupied a re-entrant of the interlobate zone as the ice sheet retreated (along with the deposition of the Harricana Interlobate moraine; Hardy, 1977; Vincent and Hardy, 1977; Veillette, 1988; Breckenridge et al., 2012). At 9 ka, we show a brief re-advance, mapped after Godbout et al. (2019) and references therein (e.g. Boissonneau, 1966; Paulen, 2001; Roy et al., 2011; Breckenridge et al., 2012; Veillette et al., 2017). Next, at 8 ka, we show a fully collapsed ice sheet over Hudson Bay, the timing of which is correlated to the final drainages of glacial Lake Agassiz and Lake Ojibway (Gauthier et al., 2020; Brouard et al., 2021). Southwest of

Hudson Bay, the retreat of ice over Manitoba and adjacent areas of Ontario is largely informed by the recent deglaciation work of Gauthier et al. (2022) and correlated to earlier work on varves by Breckenridge et al. (2004) and Breckenridge (2007). Following Gauthier et al. (2022), we show a re-advance into Manitoba at 11 ka, resulting in the prominent Pas moraine. By 8.5 ka, we show the final stand of ice over Hudson Bay.

### 3.9. American midcontinent

The American Midcontinent, situated along the southern margin of the NAISC (Fig. 1), hosted two key ice stream lobes during deglaciation (James and Des Moines lobes). The glacial history of this region is preserved in several prominent hummocky moraines and the deglacial record is extensively documented in regional mapping projects (Fig. 2; Ruhe, 1952; Kemmis et al., 1981; Harris, 1998; Lusardi et al., 2011; Mickelson and Attig, 2017). Generally, the lateral extent of these ice streams is well defined, based on lateral moraines, shear moraines, and transition from streamlined to non-streamlined terrain. However, the frontal position of the ice streams is subject to uncertainty because they are known to have oscillated (Patterson, 1997a; Lusardi et al., 2011). Our depiction of ice retreat across the American Midcontinent is guided by cosmogenic nuclide dating of 13 landscape features, 45 post-glacial sites dated via OSL or luminescence methods, as well as the age and location of radiocarbon dates (~180 total). The uncertainty bounds remain constant at 350 km from 25 ka to 16 ka, reflecting the stability of the ice margin, or the scale of the oscillation of the ice stream fronts, at, or near, the maximum position in this region at this time (see Fig. 6n). From 15.5 ka to 10 ka the uncertainties bounds are much larger, reaching over 1000 km at 13.5 ka, but generally, they vary between 460 km and 850 km during these time-steps.

In terms of ice dynamics, between 25 ka and 18.5 ka, we align ice in the eastern American Midcontinent with the extent of a till that is mapped in southwestern Minnesota (Ruhe, 1969; Kemmis et al., 1981). Although somewhat speculative, this ice configuration is supported by a unique matrix texture and lithology in the surface till (Patterson, 1997a, 1997b; Lusardi et al., 2011). To the west of Lake Superior, ice retreat is anchored to cosmogenic nuclide dating of successive moraines (Lowell et al., 2021). At 17 ka, we show a short-lived ice advance of the Des Moines lobe into Iowa that terminated at the well-studied Bemis moraine (Clayton and Moran, 1982; Hallberg and Kemmis, 1986). Next, between 17 ka and 12.5 ka, we show a progressive retreat in a northward direction, interspersed by periodic ice re-advances that resulted in the formation of moraines (Kemmis et al., 1981). One exception was a short-lived (~100 yr) prominent (~200 km) eastward advance of the Grantsburg sublobe at 15.5 ka (Cooper, 1935; Wright et al., 1973; Johnson and Hemstad, 1998). The St. Louis sublobe also advanced as others retreated, and the Red River lobe, which occupied the same valley as Des Moines lobe but originated from a different ice stream, is another example. Finally, retreat of ice from the western region is tracked by cosmogenic nuclide dating of associated boulders by Heath et al. (2020).

### 3.10. Southern Interior Plains

The Southern Interior Plains region is located in west-central Canada (Fig. 1). In terms of deglacial landforms, the landscape includes hummocky terrain, glacial lake sediments and sand dunes built from reworked glacial lake sediments, outwash plains and moraines (see Fig. 2 as well as Prest et al., 1968; Fulton, 1995; Atkinson et al., 2016; Wolfe et al., 2016; Norris et al., 2017; Utting and Atkinson, 2019). Our portrayal of ice retreat across this region is guided by cosmogenic nuclide dating of 7 landscape features, 76 post-glacial dune sites dated via OSL or other luminescence methods, and by radiocarbon dates (~240 total). The uncertainty bounds are large (1200 km) between 25 ka and 20 ka due to the sparse coverage of ages that date ice advance across the region (see Fig. 6o). Between 19.5 ka and 15.5 ka uncertainty bounds remain constant at 220 km, due to the stability of the ice margin

at, or near, its maximum position in this region at this time. During the initial ice retreat (between 15 ka and 14 ka) the uncertainty bounds become large again (sometimes spanning 1150 km), reflecting the dynamic nature of ice retreat at this time and from 12.5 ka onwards the uncertainty bounds are small (~150 km), where the ice margin position is well constrained by cosmogenic nuclide ages.

In terms of ice dynamics, between 25 ka and 15.5 ka, we show the ice margin extended to the maximum extent of till in Montana, as supported by extensive mapping of glacial deposits (Fullerton et al., 2004). This ice position is supported by cosmogenic nuclide dating of ice rafted boulders in glacial Lake Musselshell, which were derived from the Laurentide Ice Sheet (Davis et al., 2006a). Next, at 15 ka, we show the initial detachment of the Laurentide and Cordilleran ice sheets, demarcated by cosmogenic nuclide dating of the Foothills Erratics Train (Jackson et al., 1997; Margold et al., 2019; Clark et al., 2022b). Cosmogenic nuclide dating in northeastern British Columbia suggests that the 14-ka interval is the first time where the Cordilleran and Laurentide ice sheets were separated along their entire length (Clark et al., 2022b). We then show rapid retreat of the ice margin northeastward across the Southern Interior Plains based on mapping of glacial landform features (Evans et al., 2014; Norris et al., 2017; Atkinson et al., 2014, 2018) and OSL dates from post-glacial aeolian sand and dune fields (Wolfe et al., 2007; Munyikwa et al., 2011). Finally, we show ice at or near the Cree Lake moraine between 13 ka and 11.5 ka as supported by multiple 10Be cosmogenic nuclide dates at three separate sites (Norris et al., 2022).

### 3.11. Keewatin dome

The Keewatin Dome was a key feature of the NAISC that was situated on the Canadian Shield west of Hudson Bay (Fig. 1). The glacial geomorphological record includes a myriad of eskers, along with moraine ridges, meltwater channels and glacial lake deposits (Fig. 2; Prest et al., 1968; McMartin and Henderson, 2004; Storrar et al., 2013; Hodder et al., 2016; McMartin et al., 2020). Our depiction of ice retreat across this region is anchored only by cosmogenic nuclide dating of 2 landscape features and is supported by ~90 radiocarbon ages. The uncertainty bounds of this region range between 200 km and 700 km, reflecting an overall lack of geochronological constraints (Fig. 6o and q).

Cosmogenic nuclide dating of boulders suggest that retreat of the Keewatin ice margin slowed at the western limit of the Canadian Shield around 13 ka to 12 ka (Reyes et al., 2022). Following this relative slow down, the deglaciation of Keewatin resumed at 11 ka until 7.5 ka; however, the pace of retreat is largely assumed since there are few geochronological constraints over the region. Our depiction of ice retreat through this interval is based on (i) recent mapping of the glacial geomorphology and surficial geology in eastern Keewatin (McMartin et al., 2021), (ii) ensuring a perpendicular placement relative to eskers (Prest et al., 1968; Storrar et al., 2013), and (iii) alignment of the 9-ka ice margin to the McAlpine and Chantrey moraines (Prest et al., 1968). By 7.5 ka, we show final remnant ice over Keewatin, which is based on recent landform mapping and glacioisostatic uplift of deposits containing marine shells along the western coast of Hudson Bay (Dredge and McMartin, 2007; McMartin et al., 2015).

### 3.12. Northwestern margin

The Northwestern Margin occupies the northwestern extremity of the Laurentide Ice Sheet, largely within the Northwest Territories south to its southerly border at 60°N with British Columbia and Alberta (Fig. 1). In terms of deglacial landforms, this region is characterized by hummocky terrain with some eskers, meltwater channels, moraine ridges and glacial streamlined landforms (Fig. 2; Prest et al., 1968; Fulton, 1995; Storrar et al., 2013; Evans et al., 2021; Dulfer et al., 2023). Our portrayal of ice retreat across the Northwestern Margin is guided by cosmogenic nuclide dating of five landscape features, five IRSL and four OSL ages on preglacial dune sands which provide a maximum constrain

on the advance, seven OSL ages on postglacial sands which provide a minimum constraint on deglaciation, and ~90 radiocarbon dates that offer minimum age constraints on ice retreat. This region has the largest uncertainty bounds of any region within the NAISC. The uncertainty bounds exceed 1000 km at most time-steps, with the exception of the 15.5 ka, 15 ka, and 14.5 ka time-steps, where the uncertainty bounds are reduced to 500 km, 820 km, and 850 km respectively (see Fig. 6p). This uncertainty reflects an overall lack of geochronological control on the timing of ice advance and retreat across the Northwestern Margin.

Between 25 ka and 17 ka very little is known about the timing of ice advance in the Northwestern Margin, although the spatial extent of the local maximum is well-defined by surficial mapping studies (e.g. Duk-Rodkin, 1999, 2022). We show the ice margin advancing from a reduced extent between 25 and 22.5 ka, and then through to 18.5 ka at the same position as the Sitidgi Stade (mapped from moraines; see Hughes, 1987; Rampton, 1988), which is roughly 100–150 km inland of the present-day coastline. The formation of lakes in the unglaciated Bluefish, Bell and Old Crow basins to the west of the Richardson Mountains is dependent on the Laurentide Ice Sheet blocking the preglacial drainage to the east from these basins (Kennedy et al., 2010). Accordingly, the presence of these lakes from 22 ka onwards suggests that the Northwestern Margin was at or near the local maximum position along the Richardson Mountains at this time. Starting at 18.5 ka, we show the ice beginning to slowly advance to the local maximum ice extent, which occurs at 17.5 ka. During the local maximum ice extent the ice margin extended to the continental shelf break in the Beaufort Sea, as indicated by undated seismic reflection data from the Beaufort Sea (Batchelor et al., 2014; King, 2015; MacLean et al., 2015; O'Regan et al., 2018) as well as corroborative evidence for an ice advance from the stratigraphic record along the coastline (Toker Point Stadial; Rampton, 1988) and the entirety of Herschel Island being a glacial thrust mass on North Yukon Coastal Plain (Rampton, 1988). Along the Richardson and Mackenzie mountain ranges, the maximum extent is based on surficial mapping work (Duk-Rodkin, 1999, 2022). The 17.5 ka age of this ice advance is suggested by nine OSL dates of sub-till sand deposits along the shoreline, suggesting ice advance must have occurred after 18.5 ka (Murton et al., 2015). Starting at 17.0 ka, deglaciation of the Northwestern Margin had begun, based on cosmogenic nuclide dating of boulders in the central Mackenzie Mountains (Stoker et al., 2022). A short-lived local Last Glacial Maximum is supported by OSL dates from pre-Laurentide and postglacial sands in the Mackenzie Delta region (Bateman and Murton, 2006; Murton et al., 2007, 2015). Finally, from 16 ka to 13 ka, we show the ice margin retreating gradually eastward, following (i) the outermost ridges of hummocky terrain belts (mapped by Evans et al., 2021); (ii) moraines (Sitidgi Stade moraines; Hughes, 1987; Rampton, 1988), (iii) the topographic relief of the Mackenzie Basin, damming of several glacial lakes (e.g. glacial Lake Mackenzie; Smith, 1992; Couch and Eyles, 2008), and (iv) cosmogenic nuclide dating of erratic boulders in the middle reaches of the Mackenzie River and on the ridges of the Franklin Mountains immediately east of it (Stoker et al., 2022).

### 3.13. Banks and Victoria islands

Banks and Victoria islands are located at the northwesternmost extent of the Laurentide Ice Sheet (Fig. 1). The glacial history of this region is preserved in landscape-scale lineations, shoreline marine inundation, hummocky terrain, meltwater channels and eskers (see Fig. 2 as well as Fyles, 1963; Prest et al., 1968; Dyke et al., 2003b; Storrar and Stokes, 2007; Stokes et al., 2006, 2009; Lakeman and England, 2013). Our interpretation of ice retreat over this region is guided largely by the age and location of minimum-limiting radiocarbon dates (~190 total, largely marine shells). The uncertainty bounds for Amundsen Gulf (south of Banks and Victoria islands) remain constant at 400 km from 25 ka to 16.5 ka as they are defined by the distance between the present-day coastline (minimum) and continental shelf break (maximum; see Fig. 6q). From 16 ka to 14 ka the uncertainty bounds are

between 250 km and 50 km, when the optimal ice margin is located at the present-day coastline. From 13.5 ka onwards the uncertainty bounds vary widely between 250 km and 700 km, reflecting uncertainties in the geochronological constraints during these time-steps.

In terms of ice dynamics, we show a fully glaciated Banks and Victoria islands between 25 ka and 15 ka, with ice extending to the continental shelf break at 25 ka and progressively retreating until 15 ka. This ice extent is based on geomorphological evidence from Margold et al. (2015b) that suggests the presence of large ice streams (and therefore the extension of the ice margin) on the continental shelf, as well as seismic surveys and mapping of the continental shelf in the Beaufort Sea (Batchelor et al., 2012; King et al., 2014). More recent work places the M'Clure Ice Stream to within 8 km of the shelf edge (Batchelor et al., 2016). Because the lines of evidence are undated, maximum ice extent is not well constrained and is herein assumed to be at 25 ka. Next, starting at 14.5 ka, we show progressive deglaciation of Banks Island, following extensive radiocarbon dating of postglacial marine shells and geomorphic mapping (England et al., 2009; Lakeman and England, 2012, 2013). By 13 ka, ice began retreating eastward across Victoria Island, and several moraines on the southwestern peninsulas suggest cycles of advance/stagnation that likely correspond to the Younger Dryas (Dyke and Savelle, 2000; Dyke et al., 2003b). Finally, between 12 ka and 10 ka, we show retreat across Victoria Island that is largely interpolated and follows the general position of mapped moraines, where available, as well as maintaining the ice margin perpendicular to eskers (Fyles, 1963; Storrar and Stokes, 2007). Inuitian and Laurentide ice had fully separated by 10.5 ka.

### 3.14. Cordilleran Ice Sheet

The Cordilleran Ice Sheet occupied the westernmost region of the NAISC, bordering the Pacific Ocean (Fig. 1). Deglacial landforms include a variety of eskers, meltwater channels, incised glacial lake sediments, and perched deltas (see Fig. 2 as well as Prest et al., 1968; Margold et al., 2011; Dulfer and Margold, 2021). Our depiction of the deglaciation of this region is anchored by cosmogenic nuclide dating of 38 landscape features and is complemented by ~580 radiocarbon ages. The uncertainty bounds for the Cordilleran Ice Sheet are generally small, varying between 30 km and 350 km at all time steps (see Fig. 6r, s, t, and u). The smallest uncertainty occurs between 17.5 ka and 13 ka along the Pacific Coast, where the position of the ice margin is constrained by numerous cosmogenic nuclide exposure sites (see Fig. 6s). The relatively small uncertainty bounds for the northern and western sectors of the Cordilleran Ice Sheet likely reflect the smaller size of the region when compared with regions across the Laurentide Ice Sheet, rather than the robustness of the geochronological constraints.

The margins of the Cordilleran Ice Sheet reached their local LGM extent asynchronously. Between 25 ka and 24.5 ka we show a fragmented Cordilleran Ice Sheet that was gradually building toward its maximum extent. A not-yet-fully coalesced ice sheet during this interval is suggested by numerous radiocarbon ages on organic material located below till (Fulton, 1971; Clague et al., 1980; Naughton et al., 2003). The exception is the northern margin of the Cordilleran Ice Sheet, where radiocarbon ages from the Yukon indicate ice advance occurred prior to 25 ka (Jackson and Harrington, 1991). We show the Cordilleran and Laurentide ice sheets coalesced east of the Rocky Mountains at 22.5 ka and Cordilleran ice at its maximum western extent, midway along the continental shelf, around 20 ka (following a hiatus in deposition of mammal bones on Prince of Wales Island; Lesnek et al., 2018; Shaw et al., 2020). The maximum extension of the western margin of the Cordilleran Ice Sheet was short-lived. Retreat, which began at 18.5 ka, is largely anchored to cosmogenic nuclide dating of boulders by Darvill et al. (2018, 2022) as well as Lesnek et al. (2018, 2020b). The maximum southern extension of the Cordilleran Ice Sheet was also short-lived, with a maximum around 17.5 ka (Porter and Swanson, 1998; Cosma et al., 2008; Taylor et al., 2014; Balbas et al., 2017) and retreat

beginning before 16 ka. Retreat of the Puget Lobe at the southwest margin of the ice sheet is supported by numerous radiocarbon ages on sub-till and post-glacial organic material and local cosmogenic nuclide dates (Porter and Swanson, 1998; Borchers et al., 2016; Balbas et al., 2017). Similarly, we show the northern margin retreating after 16 ka, albeit the timing of initial retreat is sparsely dated, particularly in the Mackenzie Mountains (Stroeven et al., 2010; Menounos et al., 2017). Deglaciation of the Cordilleran Ice Sheet involved complex frontal retreat of glaciers through the mountainous terrain accompanied by ice-sheet thinning (Margold et al., 2013, 2014; Clague, 2017; Menounos et al., 2017; Dulfer et al., 2021; Darvill et al., 2022). Following separation of the Cordilleran and Laurentide ice sheets at 14 ka, ice persisted over the Rocky Mountains for a further 2 ka based on cosmogenic nuclide ages from opposite sides of the mountain range (Dulfer et al., 2021; Clark et al., 2022b). At 11.5 ka, we use, and expand on, a geomorphology-based reconstruction of the central sector of the Cordilleran Ice Sheet during a regional readvance of the ice sheet in the late glacial by Dulfer et al. (2022). From 10 ka onward, the extent of ice is likely less than or equal to the present-day distribution. Therefore, we stop the reconstruction of the Cordilleran Ice Sheet at 10 ka.

### 3.15. Alaska

We reconstructed ice margins across Alaska differently than elsewhere. Instead of working from the primary data, we interpolated between the few ice extents that are depicted in version 2 of the Alaska PaleoGlacier Atlas (Kaufman et al., 2011), which provides a detailed overview of the disintegration of ice over the Alaska region (<http://akatlas.geology.buffalo.edu/>). In terms of ice dynamics, prominent moraine systems encircle high-elevation mountain ranges in this region, which suggest that, at the Last Glacial Maximum, Alaska was not fully glaciated. Rather, local mountain glaciers extended laterally, leaving many lower-elevation regions ice-free (e.g. Wahrhaftig, 1958; Hamilton, 1994; Mann and Peteet, 1994; Ely et al., 2016). We show maximum ice extent over high-elevation areas between 25 ka and 18.5 ka, including local ice over the Brooks Range, Ahklun Mountains and the Alaska Range. We then show a gradual reduction of ice over the Alaska Range, as well as ice remaining over the Brooks Range and Ahklun Mountains until 14 ka. Finally, from 12 to 1 ka, we show remnant ice over the high elevation regions of the Alaska Range.

## 4. Discussion

Our reconstruction of the deglaciation of the NAISC between 25 and 1 ka represents the first version of North American Deglaciation Isochrones, NADI-1. This work – complete with uncertainty bounds for each isochrone – applies the same standards used to reconstruct Eurasian ice sheets and creates a geochronological database of comparable quality (Hughes et al., 2016; Clark et al., 2022a). This is a first step towards a reconstruction of NAISC evolution at a similar level of precision as the Eurasian ice sheets, but does not include all the aspects of some of these reconstructions (e.g. ice divide locations or Bayesian age sequence modelling along ice-sheet-sector-scale transects; Clark et al., 2022a). The paucity of geochronological constraints in some regions and the size of the NAISC means that our understanding of the deglaciation is of a lesser detail, as highlighted by our uncertainty bounds. The reconstruction of Eurasian ice sheets, in particular the British-Irish Ice Sheet, provides a framework for future versions of the NADI database, which we discuss further in Section 4.6.

There are some important limitations to this work. First, we implore users of these maps to consider that the ice margin could have been anywhere between the minimum and maximum ice extents. This is because, in some regions, the optimal ice margin is indeed a ‘best guess’ (e.g. interpolated or aligned with distinct features of glacial geomorphology) and there are large expanses where no chronological constraints exist. These issues have been fully accounted for in the

minimum and maximum ice extents. We also stress that, in many regions, our work suggests that retreat of the ice margin was near-continuous; however, in some cases ice retreat may have been interrupted by minor readvances. This applies to most of the isochrones except for specifically identified stillstands (see Supplementary Document 1). Thus, the NADI-1 ice margins should be viewed as “snapshots” of the ice margin at given time intervals, and do not necessarily represent stepwise retreat.

We generated several additional figures to aid in the discussion of our work. The deglaciation of the NAISC occurred in tandem with increased insolation in high northern latitudes (Berger and Loutre, 1991), which is known to drive retreat of ice sheets in the Northern Hemisphere. Therefore, we plot insolation data and other relevant proxy data in Fig. 7. In Fig. 8, we highlight the diachronous nature of the Last Glacial Maximum. Finally, an overview of all NADI-1 timesteps is shown in Fig. 9 and the complete NADI-1 is available in Supplementary Document 3 (with relevant geochronological data) and Supplementary Document 4 (without geochronological data). Shapefiles, additional visualizations and spreadsheets of geochronological data are also available in the Supplemental Documents and Tables.

### 4.1. Assessment of uncertainty

The explicit quantification of uncertainties in the form of minimum and maximum isochrones within NADI-1 provides a substantial revision on the previous generations of the NAISC ice margin chronology (e.g. Dyke, 2004; Dalton et al., 2020). Capturing this uncertainty in ice margin position is also necessary to constrain and validate numerical ice sheet modelling (Tarasov et al., 2012; Stokes et al., 2015). Fig. 6 portrays the uncertainty bounds along flowlines in each region of the NAISC, highlighting several regions where the uncertainty in the ice margin position is high (>1000 km), including the Queen Elizabeth Islands between 10.5 ka and 10 ka, Labrador Dome between 8.5 ka and 8 ka, Hudson Bay between 9.5 and 8.5 ka, American Midcontinent at 13.5 ka, Southern Interior Plains between 25 and 20 ka as well as 14.5 and 13.5 ka, and Northwest Margin at all time steps between 25 ka and 16 ka as well as 14 ka. These high uncertainties often occur across regions that are characterized by highly dynamic and rapid ice retreat. However, it should be noted that the uncertainty bounds not only reflect the availability of geochronological data, but they are also dependent on the size of the region (and thus the total length of the flowline). For example, across the Cordilleran Ice Sheet the flowlines do not exceed 700 km, and therefore, it is not possible for the uncertainty along this ice margin retreat route to be as large as those recorded for several regions of the Laurentide Ice Sheet, irrespective of the available chronology.

### 4.2. Calculations of areal extent

The NADI-1 isochrones suggest that North American ice sheets reached their maximum areal extent (15,470,000 km<sup>2</sup>) at 22 ka. We note, however, the significant uncertainties on the 22-ka ice margin, especially as much of the marine sector of the NASIC is unconstrained by geochronological data. More broadly, the areal extent between 22.5 and 19.5 ka remained essentially at a plateau in the range of 15,400,000 km<sup>2</sup> (Fig. 7), which corresponds to a time of relative depletion of the Greenland GRIP δ<sup>18</sup>O record ice core (Rasmussen et al., 2014; Seierstad et al., 2014), a similar depletion of the δD record from the Antarctic EPICA ice core (Stenni et al., 2001) and reduced insolation at 65°N (Laskar et al., 2004).

The areal extent of the NAISC then decreased progressively until it was essentially an order of magnitude smaller following the collapse of Laurentide ice over Hudson Bay at ~8 ka (~1,802,000 km<sup>2</sup>). This collapse occurred during a time of δ<sup>18</sup>O enrichment in the Greenland GRIP ice core (Rasmussen et al., 2014; Seierstad et al., 2014) and a similar enrichment of the δD record from the Antarctic EPICA ice core (Stenni et al., 2001). After 8 ka, the NAISC consisted mostly of small

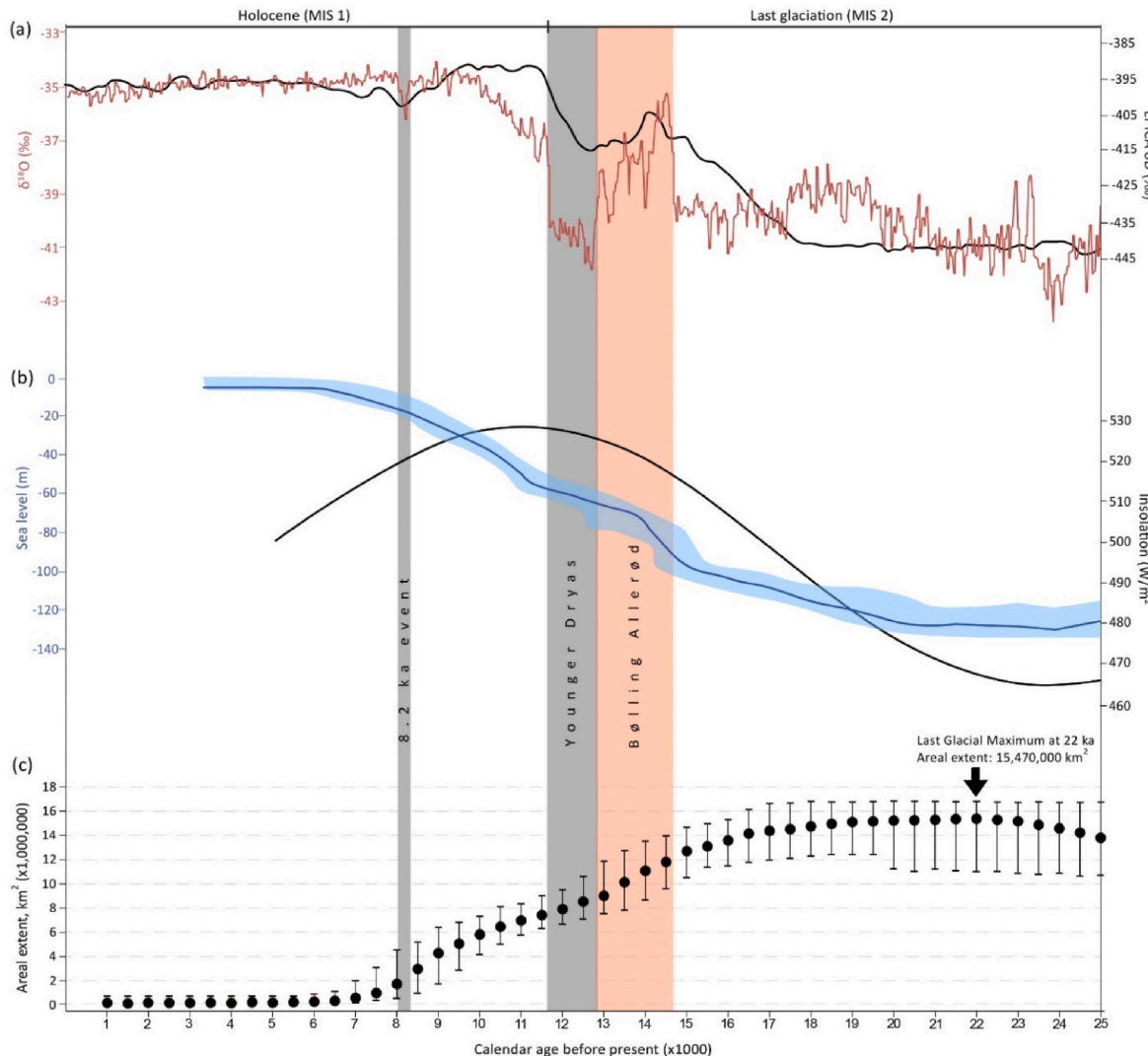


**Fig. 7.** (a)  $\delta^{18}\text{O}$  record from the Greenland GRIP ice core (red; Rasmussen et al., 2014; Seierstad et al., 2014) and  $\delta\text{D}$  (deuterium) record from the Antarctic EPICA ice core (black) smoothed with a 500-year running average (Stenni et al., 2001). (b) Relative sea level curve from 22 ka to 3 ka (blue) from Carlson and Clark (2012) based on a compilation of far-field sites extended to 25 ka using the sea level stack of Spratt and Lisiecki (2016) and mean summer insolation at 65°N (black; Laskar et al., 2004). (c) Areal extent of the North American Ice Sheet Complex (Laurentide, Cordilleran and Innuitian ice sheets) from 25 ka to 1 ka. Black dots represent the optimal ice margin whereas error bars represent minimum and maximum ice extents.

independent ice bodies that gradually decreased in area until they reached  $<200,000 \text{ km}^2$  at 3 ka. Overall, these areal estimates compare well with data reported in other literature, where the LGM is considered to be ~21 ka (minimum in the marine  $\delta^{18}\text{O}$  record; Martinson et al., 1987), to sometime between 25 ka and 21 ka (minimum global mean sea level, based on a variety of empirical and modelling efforts; Yokoyama et al., 2000; Peltier and Fairbanks, 2006), to as early as 26.5 ka (assessment of geochronological data to determine the largest ice extent; Clark et al., 2009).

We focus our attention herein on areal extent because there is significant complexity in converting areal extent to volume of ice. For example, some of the land-terminating ice streams near the southern margin of the Laurentide Ice Sheet slowly lost volume over time but maintained a near-constant areal extent. This delays the exposure of the subglacial landscape even where supraglacial debris is thin to absent. In Ham and Attig (1996), debris-covered masses of stagnant ice became separated from the active ice (fans emanate on all sides). They persist if conditions are cold enough for their survival.

#### 4.3. Comparison between NADI-1 and earlier radiocarbon-based efforts

A comparison between NADI-1 and previous radiocarbon work (Dyke, 2004; Dalton et al., 2020) is shown in Supplementary Document 5. By virtue of including a broader geochronological database and the latest available mapping and glacial geomorphic studies, our work represents a more complete deglacial chronology than previous efforts (Bryson et al., 1969; Dyke, 2004; Dalton et al., 2020). The most immediate difference between NADI-1 and earlier radiocarbon-based attempts is the refinement of ice sheet evolution in regions where cosmogenic nuclide methods have been applied. Notable examples include (i) better constraint on the recession of ice across Northeastern United States and the St. Lawrence Lowlands (Section 3.5; key studies: Balco and Schaefer, 2006; Balco et al., 2002, 2009; Corbett et al., 2019); (ii) enhanced information on ice dynamics in western Lake Superior (Section 3.9; key study: Lowell et al., 2021); (ii) a more refined understanding of the unzipping of the Laurentide and Cordilleran ice sheets (Sections 3.10 and 3.14; Margold et al., 2019; Clark et al., 2022b), and; (iv) better constraint on the expansion and subsequent recession of the Cordilleran Ice Sheet (Section 3.14; key studies: Darvill et al., 2018,

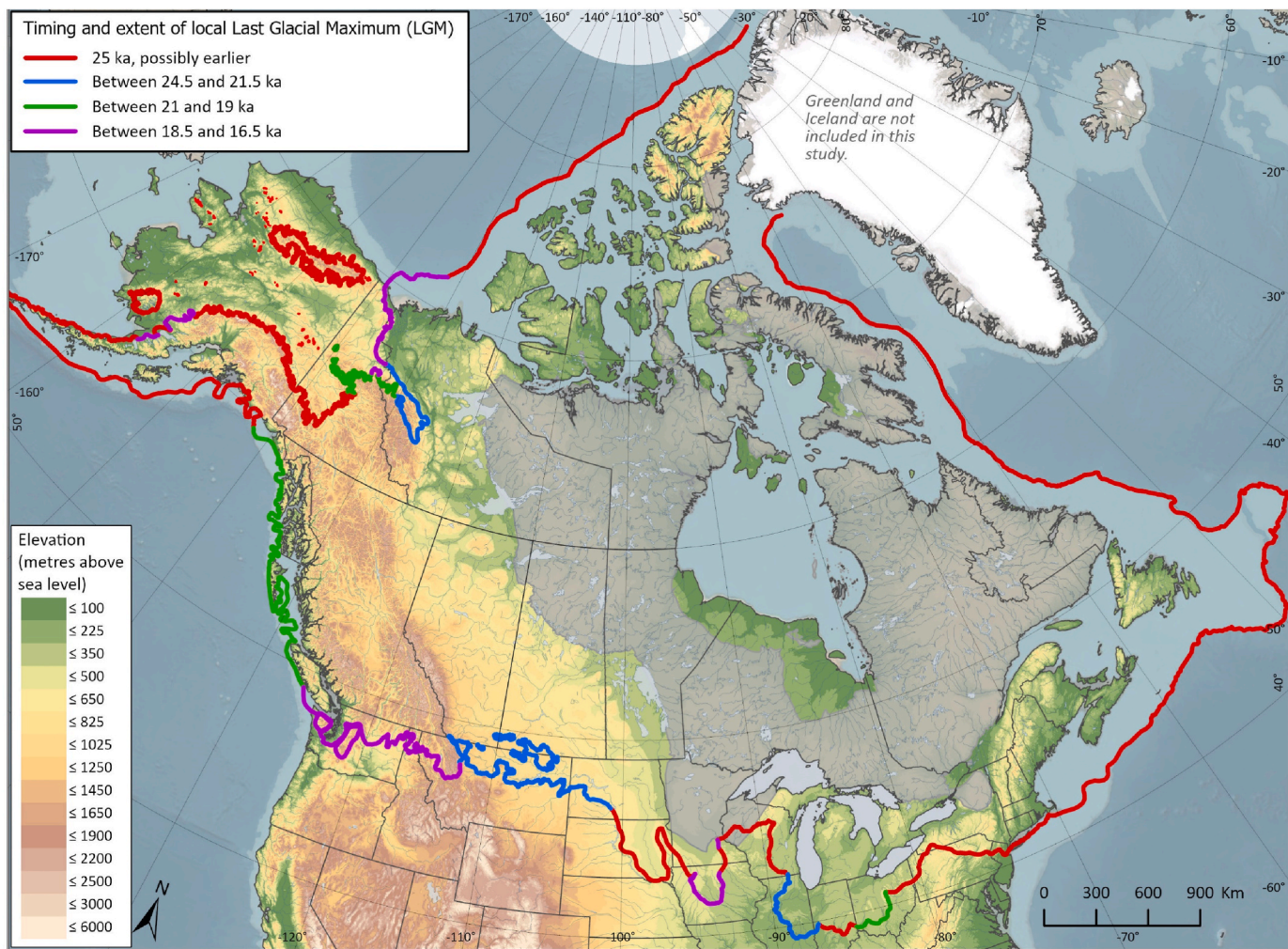


**Fig. 8.** The timing and extent of the local Last Glacial Maximum (LGM) across the North American Ice Sheet Complex (NAISC). Note the asynchronous nature of this local maximum extent, with some regions attaining their maximum extent prior to 25 ka and others between 18.5 and 16.5 ka.

2022; Lesnek et al., 2018, 2020b; Dulfer et al., 2021). An in-depth comparison between these studies is not possible here. However, we note that, across most timesteps and regions, the isochrones from previous radiocarbon work (Dyke, 2004; Dalton et al., 2020) are captured in our minimum and maximum ice extents (Supplementary Document 5).

#### 4.4. Outstanding issues with NADI-1

Regrettably, some relevant studies and data were unintentionally omitted from consideration in NADI-1. These papers were brought to our attention very late during the development of NADI-1 or in the review process. For transparency, we document these omissions in Supplementary Document 6. These studies should be prioritized for inclusion in NADI-2. Below, we outline some additional lingering issues that remain following our work on NADI-1.

##### 4.4.1. Improving ice-margin information from radiocarbon ages

Radiocarbon ages are by far the most widely available type of data for reconstructing the position of NAISC margins through time. Like other recent efforts to reconstruct continental ice sheets (e.g. Hughes et al., 2016; Clark et al., 2022a), our work places a greater emphasis on some radiocarbon ages for delineation of the ice margin (i.e. those on terrestrial plant macrofossils in basal lake sediments). However, as detailed in Section 2.5, most radiocarbon ages (83%) offer little or no indication of precisely when the ice sheet retreated from the area. Is it

possible to glean additional ice-margin data from these age constraints? For example, given that some of them relate to peatland and lacustrine deposits with associated paleoclimate data (largely via pollen and chironomids; Richard and Labelle, 1989; Fortin and Gajewski, 2016; Hargan et al., 2020), it might be possible to extract useful information about the distance to the neighboring ice margin. Studies that examine the establishment of vegetation on recently deglaciated landscapes (known as the ecesis) might be useful in this regard (e.g. McCarthy and Luckman, 1993; Gorham et al., 2007). It may also be worthwhile to investigate the role of lacustrine fauna, which may more closely date early deglaciation than terrestrial vegetation (Smith, 2000).

Another issue is local marine reservoir corrections ( $\Delta R$ ). These corrections are influenced by several factors, including ocean circulation and regional biological processes (Stuiver et al., 1986; Stuiver and Reimer, 1993). Accordingly, they are not static over time and can vary considerably when influenced by a variety of effects of a retreating ice sheet and changing ocean circulation. Our  $\Delta R$  corrections are based on dedicated studies over broad regions of North America (Coulthard et al., 2010). However, there remain significant unknowns in this database that only become apparent upon finding paired marine and terrestrial radiocarbon ages. For example, while we rely largely on the  $\Delta R$  corrections suggested by Coulthard et al. (2010) for Arctic Canada, we adopt significantly higher  $\Delta R$  values for certain areas of and time-slices in the Northeastern United States and the St. Lawrence River owing to regional workers finding paired marine and terrestrial material for



**Fig. 9.** Maps showcasing the 49 timesteps in NADI-1. Note that ice is restricted to the Canadian Arctic from 5.5 ka to 1 ka, and the maps are therefore truncated. In the Supplementary Data, the complete NADI-1 chronology is available in PDF, GIF and shapefile formats, together with additional visualizations and spreadsheets of geochronological data.

radiocarbon dating (Occhietti and Richard, 2003; Richard and Occhietti, 2005; Thompson et al., 2011). In these cases, the  $\Delta R$  was increased from 1 to 1.8 kyrs, as a result of poor circulation in the Champlain Sea, an inland sea that filled the St. Lawrence Lowlands immediately following deglaciation (Occhietti and Richard, 2003; Richard and Occhietti, 2005). This effectively shifted the deglaciation of this region to almost 1-kyrs later than previously documented. Highly variable  $\Delta R$  values also likely occurred following deglaciation of Hudson Bay and Arctic Canada and finding paired marine and terrestrial radiocarbon ages (Vickers et al., 2010) should remain a key priority in these areas. An alternative approach might be assigning  $\Delta R$  corrections for specific time intervals, instead of a patchwork approach based on regional studies. This approach was discussed by Clark et al. (2022a) when reconstructing the expansion and retreat of the last British–Irish Ice Sheet. However, in large-scale ice sheet reconstructions  $\Delta R$  corrections remain “a problem with no perfect solution” (Clark et al., 2022a).

#### 4.4.2. Challenges in developing a cosmogenic nuclide database for use on a continental scale

One of the key differences between NADI-1 and the previous generations of ice margin chronology for the NAISC (Dyke et al., 2003a; Dyke, 2004; Dalton et al., 2020) is the integration of cosmogenic nuclide exposure ages to directly date the ice margin position (Gosse and Phillips, 2001; Balco, 2011). Our  $^{10}\text{Be}$  and  $^{26}\text{Al}$  cosmogenic nuclide data were extracted from *expage*, which is a global database that has been compiled over a number of years. The *expage* calculator (version 201912; <https://expage.github.io/calculator.html>) allows us to treat continental-scale cosmogenic nuclide data in a uniform manner, applying the same production rate, scaling model, and glacio-isostatic adjustment (GIA) correction calculation across the database.

There is currently no uniformly accepted method for calculating exposure ages, with authors using a range of production rates, scaling models, and corrections (e.g. for GIA, snow cover, and erosion). As a result, calculated deglacial exposure ages may differ by  $> 1$  ka (generally between 0 and 10% of the calculated age), depending on the chosen calculation method. In some regions, the choice of calculation approach has led to incompatible deglacial chronologies (Ullman et al., 2016; Young et al., 2020; Clark et al., 2022b; Reyes et al., 2022; Stoker et al., 2022). In the Northwest Territories, Stoker et al. (2022) found the choice of production rate, which is the rate at which cosmogenic nuclides are produced at a site where the age is known, has the largest influence on the calculated exposure age. Exposure ages calculated using the Arctic production rate which is influenced by the local GIA effect (Young et al., 2013) are  $\sim 8.5\%$  older than those calculated using the ‘primary’ calibration dataset of Borchers et al. (2016). Alternatively, using the Arctic production rate value, which has been corrected to remove the uplift component, as originally suggested by Young et al. (2013), would likely result in ages that are only a few percent older. Here we use a time-dependent spallation production rate with reference  $^{10}\text{Be}$  and  $^{26}\text{Al}$  production rates based on global average from calibration studies published 2009–2019 (see Table S1 in Supplementary Document 2 for the list of the calibration sites).

The choice of scaling model, which scales the production rate from a known site to the sample site, taking into account several factors, such as latitude and elevation, has a lesser effect on the calculated exposure age ( $\sim 2\%$  difference; Stoker et al., 2022). Here we use the nuclide-specific  $^{10}\text{Be}$  and  $^{26}\text{Al}$  LSD production rate scaling and geomagnetic framework from Lifton et al. (2014). The LSD production rate scaling is based on simulated cosmic ray flux and is physically the most advanced production rate scaling model at this time, with empirical data supporting the lack of geographic bias for the production rate scaling (Balco, 2020) and the nuclide-specific scaling for  $^{10}\text{Be}$  and  $^{26}\text{Al}$  (Halsted et al., 2021).

Past erosion of the sampled surface and shielding by snow and vegetation cover can affect the accumulation of cosmogenic nuclides, resulting in a calculated exposure age which underestimates the true deglaciation age of the sampled surface (Gosse and Phillips, 2001;

Schildgen et al., 2005; Plug et al., 2007). Some exposure age calculators allow you to apply corrections for these uncertainties based on independent field observations or local climate data (e.g. Balco et al., 2008). However, given that our database is on a continental-scale, we are unable to apply uniform corrections for surface weathering and snow and vegetation cover. These processes do have a large effect at particular sample sites, for example, in the Rocky Mountains where there is significant present-day snow cover that has probably had a shielding effect on the boulders (Dulfer et al., 2021). In such cases, calculated exposure ages are likely to be younger than the true deglaciation age. Where this is suspected, it has been noted in Supplementary Document 1.

The LSD scaling model assumes that atmospheric pressure has remained stable over time. However, atmospheric pressure can vary due to (1) elevation changes due to GIA (Jones et al., 2019); and (2) variations in atmospheric mass distribution over time (Staiger et al., 2007). These two processes work against each other, although the extent to which they offset each other is debated (Balco, 2020; Young et al., 2020). There is currently no universally accepted method for accounting for these processes, and the community remains divided, with some authors reporting GIA-corrected ages and others not. However, as recent work has shown that the effect of variations in atmospheric mass distribution over time is likely an order of magnitude lower than that of the GIA generated effects (Cuzzone et al., 2016; Ullman et al., 2016; Dulfer et al., 2021), and as the effect of GIA on the North American continental crust is reasonably well modelled (Peltier et al., 2015; Lambeck et al., 2017), we choose to apply a uniform correction for GIA to our cosmogenic nuclide database here.

#### 4.4.3. Difficulties in merging disparate ice margins

A challenge in working on continental-scale ice dynamics is the need to merge differing interpretations of ice sheet retreat based on the application of various geochronological methods. Notably, across central-western Canada in the 13-ka isochrone, our work combines the age of the Cree Lake Moraine (dated via comogenic nuclide methods; Norris et al., 2022) with the radiocarbon-based ice margins farther east (Gauthier et al., 2022). Although typically considered as minimum-limiting, radiocarbon ages in this case more closely relate to the ice marginal position because the ice margin is necessary to impound local glacial lakes (i.e. glacial Lake Hind; Gauthier, 2022b; Gauthier et al., 2022). The resulting ice margin is irregular across the landscape, effectively bisecting the eastern Cree lake Moraine In order to connect with the more southerly ice margins to the east (Fig. 5). This ice configuration is the function of merging these two different interpretations and is ultimately not glacially viable and this remains unfixed. These concerns are illustrated in a recent paper by Fisher and Breckenridge (2022) who examined the timing of drainage of glacial Lake Agassiz, which was directly controlled by this receding ice margin. The authors argue that the age of the Cree Lake Moraine (dated via comogenic nuclide methods; Norris et al., 2022) would result in an opening of the northwestern outlet earlier than previously proposed by Fisher and Breckenridge (2022). We stress that our minimum and maximum ice extents were designed to capture any of these uncertainties. However, we agree this issue needs to be addressed since the drainage of glacial Lake Agassiz is directly linked to the configuration of the ice margin.

Another region where we had difficulty in merging two disparate margins was the Northwestern Margin. In that region, the NADI-1 reconstruction suggests ice reached its altitudinal limit along the Richardson Mountains around 22 ka. However, evidence from the coastline suggests its northern aerial limit was only reached around 17.5 ka (Bateman and Murton, 2006; Murton et al., 2015). The delay in reaching the northern areal limit is difficult to reconcile since, glaciologically, ice flow to the Richardson Mountains would require extension to the continental shelf break. Modelling work might offer some insights into a more realistic ice margin in this case. Minimum and maximum uncertainties are generous in this region through this interval to account for these concerns.

#### 4.5. Key events in the ice margin sequence

Here we provide a brief overview of key deglacial events in the ice margin sequence. We briefly summarize our findings as they relate to the timing of ice advance across western North America, the asynchronous nature of local LGMs, the opening of the ice-free corridor, and the collapse of ice over Hudson Bay.

##### 4.5.1. The advance of the western Laurentide and Cordilleran ice sheets

Chronological constraints on ice sheet advance are more uncertain than those on ice retreat because the evidence is more difficult to find, and research is generally focused on ice retreat (see Fig. 4). While NADI-1 is also largely focused on constructing isochrones that capture the timing of ice retreat across the NAISC, we start our reconstruction at 25 ka, when the Cordilleran and Laurentide ice sheets were not yet coalesced, which means that NADI-1 also presents a reconstruction of ice advance in these areas. The ice advance phase of the Laurentide Ice Sheet is relatively poorly constrained, and its understanding relies heavily on numerical ice sheet modelling (Stokes et al., 2012). Of particular importance here is the nature of ice-buildup, for example, whether local ice masses in upland areas played a role in the pattern and timing of ice advance to the local maximum (Ives, 1957; Williams, 1978, 1979; Bromwich et al., 2002). Our key data point for timing the Laurentide advance towards the Cordillera is a single radiocarbon age on a horse bone near Edmonton of 25.6 ka that indicates ice free conditions at this time (Young et al., 1994; Heintzman et al., 2016). We thus show ice advancing across the Interior Plains ('Northwestern Margin' and 'Southern Interior Plains' sectors of this reconstruction) from 25 ka until the coalescence of the Cordilleran and Laurentide ice sheets at 22.5 ka. This represented, for the first time in the Quaternary, a coalescence of the Laurentide and Cordilleran ice sheets (Batchelor et al., 2019). At the same time, we show ice advancing outwards from the Rocky Mountains based on several maximum-limiting radiocarbon ages from the Rocky Mountain Trench and the Interior Plateau (Dyck et al., 1965; Lowdon et al., 1971; Clague, 1980). We acknowledge that the uncertainty bounds on ice advance in these regions are large and that further quantitative dating is required to reduce this uncertainty. The relatively late advance to the maximum position of the western Laurentide Ice Sheet likely reflects the long response time of MIS 3 Labrador and Keewatin ice masses to the global cooling that led to the LGM (Kleman et al., 2010; Batchelor et al., 2019; Gowan et al., 2021; Dalton et al., 2022), as well as the large distances the ice margin had to advance between the ice domes and across the Interior Plains. The westward expansion of Laurentide ice can also be seen in the early Maskwa phase for the Des Moines lobe in the Buffalo Corridor (Ross et al., 2009).

##### 4.5.2. Asynchronous last glacial maximum

The maximum extent in different sectors of global ice sheets did not occur synchronously. Ice sheet build-up is influenced by a variety of factors in Greenland (Sinclair et al., 2016), the Eurasian Ice Sheet Complex (Hughes et al., 2016) and the Patagonian Ice Sheet (Davies et al., 2020). Similarly, the local LGM across the NAISC was asynchronous in nature, with some regions attaining their maximum extent prior to 25 ka and others as late as between 18.5 and 17.5 ka (Fig. 8). The earliest documented local LGM occurred along parts of the southern margin of the Laurentide Ice Sheet at ~27 ka (Curry et al., 2018; Loope et al., 2018b). We show the maximum extent of the marine terminating margins of the Innuitian Ice Sheet and eastern Laurentide Ice Sheet as also occurring by 25 ka, although this needs to be confirmed by quantitative dating methods. This is not dissimilar to regions of the British-Irish Ice Sheet where the close geographic proximity of ice source areas to the narrow continental shelf allowed the maximum extent in some regions to be reached rapidly (Clark et al., 2022a). Contrastingly, the Northwest Margin of the Laurentide Ice Sheet reached its local maximum position as late as ~17.5 ka (Richardson Mountains; Kennedy et al., 2010; Lacelle et al., 2013; Murton et al., 2015). This may be a

result of the relatively late coalescence of the Cordilleran and Laurentide ice sheets at ~22.5 ka and large distances between this ice source area and the maximum ice margin position in the Northwest Territories. A moisture deficit and/or shifting continental air masses may have also played a role in this late coalescence (Manabe and Broccoli, 1985; Kageyama and Valdes, 2000).

The Cordilleran Ice Sheet also exhibited an asynchronous LGM (Fig. 8), as suggested by numerous ice advance radiocarbon ages on organic material located below till (Clague, 1980; Clague et al., 1980; Porter and Swanson, 1998; Ward and Thomson, 2004; Mathewes and Clague, 2017). The northern sector of the Cordilleran Ice Sheet, over Yukon and Alaska, reached its maximum ice extent prior to 25 ka (Jackson and Harington, 1991) and Cordilleran ice reached its maximum western extent around 20 ka following a hiatus in deposition of mammal bones on Prince of Wales Island (Blaise et al., 1990; Cosma et al., 2008; Lesnek et al., 2018). However, the maximum southern extent occurred much later, with the maximum extent of the Purcell Trench lobe at 18.5 ka, the Juan de Fuca and Okanagan lobes at 18 ka, and finally the Puget lobe at 17.5 ka (Porter and Swanson, 1998; Cosma et al., 2008; Taylor et al., 2014; Balbas et al., 2017). The mechanism behind this late southern advance of the Cordilleran to its local LGM position, which occurs while other sectors of the ice sheet are already in retreat, has long been considered enigmatic. This late advance is out of phase with the alpine glacial maximum in the surrounding Olympic and Cascade mountains that occurred at ~25 ka (Thackray, 2008; Riedel et al., 2010; Riedel, 2017). Given that mountain glaciers are sensitive indicators of environmental change and respond rapidly to climate forcing (Oerlemans, 2005), the late advance of the southern Cordilleran margin is possibly not a reflection of changes in atmospheric circulation and precipitation over time, but rather, changes in the internal dynamics of the ice sheet. It follows that this late advance may also be related to the coalescence of the Cordilleran and Laurentide ice sheets at ~22.5 ka and formation of the ice saddle causing variations in ice flow across the Cordillera.

##### 4.5.3. Opening of the ice-free corridor

The timing of the opening of the ice-free corridor is a critical concern for human and animal migration between eastern Beringia and continental North America south of the ice sheets (Bednarski, 2008; Heintzman et al., 2016; Becerra-Valdivia and Higham, 2020), as well as for the sea-level rise during Meltwater Pulse 1A (Gregoire et al., 2016; Lin et al., 2021). Our work suggests the detachment of the Laurentide and Cordilleran ice sheets took place gradually via southerly and northerly 'unzipping' of the ice masses. The initial detachment of the southern portion is demarcated by the Foothills Erratics Train, which was dated to 15 ka, preceded by an earlier lowering of the Laurentide Ice Sheet surface at its contact with the Rocky Mountain front (Margold et al., 2019; Clark et al., 2022b). The northern portion has its early ice sheet surface lowering dated to 17.0 ka, with ice remaining in the central Mackenzie Valley until ~15 ka (Stoker et al., 2022). We show the completed unzipping of the corridor at 14 ka, following a recently published transect of cosmogenic nuclide ages (Clark et al., 2022b). However, the cosmogenic nuclide ages available for the ice-free corridor region are subject to uncertainty associated with the age calculation roughly at the order of 10% of the calculated age (see Section 4.4.2). While different assessments of the opening of the ice-free corridor vary from early (after 16 ka; Potter et al., 2018) to late (between 15 and 14 ka; Pedersen et al., 2016), this is covered within the uncertainty bounds of our ice margin chronology (i.e. by the minimum and maximum ice extent) dictated by the uncertainties in the primary data. However, careful cleaning of the radiocarbon dates (Froese et al., 2019) along with incorporation of the <sup>10</sup>Be and OSL ages, produces a consistent intermediate model (Norris et al., 2022). This intermediate model is consistent with bison genetic data that indicates a full unzipping by 13.2 ka (Heintzman et al., 2016).

#### 4.5.4. Collapse of ice over Hudson Bay

The collapse of ice over Hudson Bay resulted in abrupt freshwater input into the North Atlantic and is potentially responsible for triggering the 8.2 ka cooling event that is recognized in sites across the Northern Hemisphere (Barber et al., 1999; Gregoire et al., 2012; Matero et al., 2017; Carlson et al., 2021). Following extensive analysis of local landforms and radiocarbon ages by Gauthier et al. (2020) we show the final stand of ice over Hudson Bay at 8.5 ka, with the collapse at  $8.11 \pm 0.19$  ka. This collapse occurred parallel to a two-step drainage of impounded glacial lakes, which is supported by new shoreline records (Godbout et al., 2020).

#### 4.6. Future work

##### 4.6.1. Regions with poor geochronological control

Our work on NADI-1 highlights numerous regions across the NAISC where ice dynamics remain poorly understood due to a lack of geochronological control. These regions should be a focus of future work. Notably, the advance of the western margin of the Laurentide Ice Sheet is sparsely dated (uncertainty bounds  $>1000$  km). Thus, studies in the Southern Interior Plains and Northwestern Margin regions should focus on dating ice advance toward the local last glacial maximum. Known sedimentary sections could be targeted for this work (e.g. Evans et al., 2021). The availability of new geochronological methods encourages us to revisit previously described sedimentary sections (Duk-Rodkin and Hughes, 1992; Smith, 1992). This approach has been successfully applied by Evans et al. (2021) in the Smoking Hills region.

In addition, the timing of extension of ice cover to the Canadian continental shelf break along much of the NAISC perimeter at the LGM remains almost entirely unknown, except for regions of past ice streaming where we have sufficient seismic coverage. Priority areas for study include the Queen Elizabeth Islands, the Laurentide Ice Sheet off the coast of Baffin Island, Labrador, and Newfoundland. New studies should focus on dating marine sedimentary sequences from the continental shelf and slope (see Andrews, 1998; Stokes et al., 2015).

Ice retreat across the islands of the Queen Elizabeth Islands is largely anchored on ice free radiocarbon dates from marine shells. This introduces uncertainties related to local marine reservoir corrections that could be reduced by applying different dating techniques in this region, such as cosmogenic exposure dating or improved regional, marine reservoir corrections (Pieńkowski et al., 2022). It is also notable that large regional moraines are not found in many parts of Canada, notably the Queen Elizabeth Islands. The glaciological reason for this is unknown but may be possible to explore via modelling.

Key undated moraine sequences that record the maximum position of the southern margin of the Laurentide Ice Sheet and its subsequent retreat, including moraines surrounding Lake Erie, Lake Michigan and the Des Moines Lobe, could be targeted using quantitative techniques, such as cosmogenic exposure dating. Moreover, the timing of ice retreat across most of central mainland Canada could be better constrained by dating quartz-bearing erratics, which are present at many sites (e.g. Reyes et al., 2022). Future work could prioritize key undated moraines in the Keewatin region (McAlpine and Chantrey moraines). The Mackenzie Mountains in the Northwest Territories and the Yukon are other regions that have almost no geochronological control on the timing of ice advance or retreat for both the Cordilleran and Laurentide ice sheets. Future studies should be focused on collecting organic material below till for radiocarbon dating, dating ice retreat using cosmogenic nuclides or OSL dating at sites with subtil sand deposits.

To gain a better understanding of the pattern and timing of ice retreat across the interior of the Cordilleran Ice Sheet, the rate of ice sheet thinning during deglaciation needs to be quantified. This could be achieved using the “dipstick” method, which uses cosmogenic nuclide dates from a vertical transect to determine thinning rates. Such methods have been applied to determine thinning of some large global ice sheets such as Antarctica (Stone et al., 2003; Small et al., 2019) and Patagonia

(e.g. Boex et al., 2013), but have yet only been applied regionally in North America (Koester et al., 2017).

Finally, we note that many of the places with poor geochronological control, for example the Mackenzie Mountains and most of the Canadian Arctic (north of  $60^{\circ}$ N), are very remote, making it logically and financially challenging, if not prohibitive, to collect data over large areas of the country. Collaboration with industry (mining) may provide opportunities for sampling locally around isolated development sites, as may collaboration with larger government-run field geology programs (e.g. the Geol. Surv. Can's GEM program).

##### 4.6.2. Future directions of NADI-1

Below we suggest several ways NADI-1 can be expanded to gain a better understanding of the NAISC evolution through time. First, future work could involve the development of a multi-chronometer Bayesian framework to reconstruct the ice margin chronology. This methodology uses a statistical approach to examine geochronological data along a well-dated transect, resulting in an ice evolution scenario (and associated minimum and maximum ice extents) that is based in statistics rather than expert judgement. Bayesian modelling was recently applied to the British-Irish Ice Sheet (Clark et al., 2022a) and has been used in several recent regional-scale studies across the Laurentide Ice Sheet. (Lowell et al., 2021; Norris et al., 2022; Stoker et al., 2022). The future application of this method across the entire NAISC would benefit from targeted fieldwork and sampling along transects spanning all regions of the NAISC with sampling strategies that are specifically catered to facilitate this approach, as well as a good independent understanding of the pattern of retreat (including any re-advances) from geomorphic and surficial geology data. The sampling strategies undertaken by the BRITICE-CHRONO project (<https://britice-chrono.sites.sheffield.ac.uk/home>) would be good to imitate, although adjustments would be necessary to account for the larger size of the NAISC and overall lack of infrastructure in many regions.

Moreover, in future efforts to refine the deglaciation of the NAISC, there is a potential to better resolve some of the coding of the radiocarbon database. For example, we considered geochronological data ‘deglacial’ if they closely dated the landscape emergence from under the former ice sheet (e.g. kettle hole in a moraine). However post-glacial landscape emergence may vary by hundreds or thousands of years (Dyke and Evans, 2003), which is a source of an added uncertainty in our reconstruction. In areas containing ice-walled lake plains, this offset can be constrained to some extent by the age of plant microfossils in the lake sediment, with consideration for the age of vegetative colonization (Curry and Petras, 2011). This issue confounds an accurate portrayal of the terrestrial-terminating ice streams, in particular the Des Moines and James lobes, where downwasting of stagnant ice occurred rather than retreat of an active ice margin. As another example, the assessment of reliability of radiocarbon ages may be in need of refinement. Our ranking system (reliable – likely reliable – unreliable) leads to many radiocarbon ages derived from bulk material being categorized as unreliable (rank = 3) even though they sometimes (often?) contain at least some insight into the ice margin. This approach leads to some regions having virtually no geochronological constraints on the ice margin. While a ranking of ‘unreliable’ is merited in some cases (especially historical ages that used bulk organics), there are downsides to this approach, and it could be argued that even radiocarbon ages derived from bulk organic materials are better than no constraints over a given region. Future work on NADI isochrones should be focused on more detailed assessment of the utility of such ages and perhaps an expansion of the assessment criteria for geochronological data.

Finally, future iterations of NADI could focus on reconstructing the evolution of glacial lakes over time (which was the case with the earlier, purely radiocarbon-based ice margin chronology of Dyke et al., 2003a; Dyke, 2004). The glacial lakes that formed along the retreating margins of the NAISC during deglaciation likely directly influenced ice dynamics (Utting and Atkinson, 2019; Sutherland et al., 2020) and held large

amounts of freshwater that had the potential to catastrophically drain into the ocean (Teller et al., 2002; Hanson et al., 2012; Norris et al., 2021). However, the addition of glacial lakes into the ice retreat chronology will have to be squared with the minimum and maximum uncertainty bounds for each time-step.

## 5. Conclusion

Understanding the dynamics of the NAISC is critical to many facets of Quat. Res., including studies of sea level change, global isostatic adjustment, and availability of migration route(s) to the North American continent. Here, we present the first version of NADI-1, which consists of a fully documented series of maps showing deglaciation of the NAISC from 25 to 1 ka in 0.5-kyr intervals (49 maps in total). A wealth of data and visualizations accompany this manuscript: All NADI-1 ice margins are presented in Fig. 9, and we also present various visualizations and additional analyses in the Supplementary Data, including extensive documentation of ice margin decisions (Supplementary Document 1) and additional details on the cosmogenic nuclide dataset (Supplementary Document 2). Moreover, NADI-1 maps are available in PDF and GIF format with and without relevant geochronological data (Supplementary Document 3 and 4, respectively), and a comparison between NADI-1 and previous reconstructions of North American ice sheet dynamics (Supplementary Document 5). Supplementary Tables 1–4 contain all relevant geochronological data, and the NADI-1 shapefiles are also available open access at <https://doi.org/10.5281/zenodo.8161764>. To ensure transparency, we provide a list of studies and data that we unintentionally omitted from our work (Supplementary Data 6). Our work is based on the interpretation of primary data, includes a diverse and thoroughly documented geochronological database, and is presented in calendar years. Importantly, we include optimal, minimum, and maximum ice extents along with extensive documentation and justification for the placement of each ice margin.

## 6. Key references used to constrain NADI-1

The NADI-1 isochrones were constructed using data from many studies. To acknowledge the importance of these primary studies, we include a list of key references here with full citations at the end of the manuscript. This list is not comprehensive; it includes only those studies where data have been specifically used to constrain the ice margin at some point during the 25–1 ka interval (i.e. those studies cited in Supplementary Document 1).

Ali et al. (2012), Allard and Seguin (1985), Allard and Tremblay (1981), Alley and Young (1978), Anderson (2005), Anderson and Macpherson (1994), Anderson et al. (1997, 2008), Andrews (1966, 1976), Andrews and Drapier (1967), Andrews and Miller (1972), Andrews et al. (1970, 1996, 1998, 1999), Antevs (1925), Anundsen et al. (1994), Ashworth et al. (1981), Atkinson (2003), Atkinson and England (2004), Atkinson et al. (2014, 2016, 2018), Attig et al. (1985, 2011), Atwater (1986), Balbas et al. (2017), Balco and Schaefer (2006), Balco et al. (2002, 2009), Barnett (1979, 1985, 1988a, 1988b), Barnett and Forbes (1972), Barnett and Karrow (2017), Barrie and Piper (1982), Barrie et al. (1987), Barrie and Conway (1999), Batchelor et al. (2012, 2014), Bateman and Murton (2006), Batterson et al. (1993), Bauer et al. (2020), Bednarski (1986, 1995, 2008), Beierle and Smith (1998), Bell et al. (2001, 2003), Berger and Eyles (1994), Berry and Drimmie (1982), Bettis and Hoyer (1986), Bettis et al. (1996), Bierman et al. (2015), Björck (1985), Black and Rubin (1968), Blais-Stevens et al. (1999), Blaise et al. (1990), Blake (1956, 1966, 1982, 1983, 1987, 1988, 1992), Bleuer (1974), Blewett and Rieck (1987), Blewett et al. (1993, 2014), Bobrowsky (1989), Bobrowsky and Rutter (1992), Boissonneau (1966, 1968), Bolduc (1995), Bonifay and Piper (1988), Booth et al. (2003), Borchers et al. (2016), Borns et al. (2004), Bouchard (1980), Breckenridge (2007, 2013), Breckenridge and Phillips (2010), Breckenridge et al. (2004, 2012, 2021), Briner and Kaufman (2008), Briner et al.

(2005, 2007, 2009), Broecker and Kulp (1957), Bromley et al. (2015, 2020), Brookes (1974, 1977), Broom and Cameron (2021), Broster and Dickinson (2015), Brouard and Lajeunesse (2017), Brouard et al. (2021), Brown et al. (2006), Bruegger (2016), Bruneau and Gray (1997), Brush (1967), Burgis (1970), Cadwell (1989), Calhoun (1906), Calkin (1970), Calkin and Miller (1977), Carboneau et al. (2012), Carlson et al. (2007), Carrara (1995), Carrara et al. (1996), Carson et al. (2012), Chauvin (1977), Christiansen (1971, 1979), Clague (1977, 1980a,b, 1984, 1987, 1988), Clague and James (2002), Clague et al. (1980, 1988, 1997, 2021), Clark (1985), Clark and Clague (2021), Clark et al. (2000, 2003, 2008, 2022), Clayton (1966), Clayton and Attig (1989), Clayton and Moran (1982), Coleman (1922, 1973), Colgan et al. (2002), Colman et al. (2020), Conley (1986), Cooper (1935, 1979), Corbett et al. (2017, 2019), Cosma et al. (2008), Cowan (1975), Craig (1965), Crandell (1963), Crowl (1980), Crump et al. (2019, 2020), Cumming et al. (1992), Curry and Petras (2011), Curry et al. (2010, 2014, 2018), Cwynar (1988), Dadswell (1974), Daigneault (2008), Daigneault and Occhietti (2006), Darvill et al. (2018, 2022), David and Lebus (1985), Davis (1999), Davis et al. (1975, 2006a,b, 2015), deVries and Dreimanis (1960), Dieffenbacher-Krall and Nurse (2005), Dieffenbacher-Krall et al. (2016), Dionne (1977), Dionne and Coll (1995), Dionne and Occhietti (1996), Dredge (2004), Dredge and Cowan (1989), Dredge and McMartin (2007), Dredge et al. (1995, 1998), Driver et al. (1996), Dubé-Loubert et al. (2018, 2021), Dubois et al. (1985, 1988), Dubois Verret (2015), Duckworth (1979), Duk-Rodkin (1999, 2022), Duk-Rodkin et al. (1996), Dulfer et al. (2021, 2022), Dyck and Fyles (1963, 1964), Dyck et al. (1965a,b, 1966), Dyke (1979, 1984, 1998), Dyke and Hooper (2001), Dyke and Savelle (2000), Dyke et al. (1991, 2003), Eamer et al. (2017), Easterbrook (1992), El-Guellaq et al. (2015), Elmore et al. (2013), Elson (1956), England (1976, 1990, 1997, 1999), England et al. (2000, 2004, 2008, 2009), Engstrom and Hansen (1985), Evans (1990), Evans et al. (2014, 2021), Falconer et al. (1965), Fisher et al. (2009, 2019), Flint et al. (1959), Fortier and Allard (2004), Franz et al. (2016), Fréchette and de Vernal (2009), Frielle and Clague (2002), Fuller (1914), Fullerton (1980), Fullerton et al. (2004), Fulton (1971, 1991), Fulton and Hodgson (1979), Furze et al. (2018), Fyles (1963), Gajewski et al. (1993), Gauthier et al. (2020, 2022), Genries et al. (2012), Gipp and Piper (1989), Glover et al. (2011), Godbout et al. (2017, 2019), Goldthwait et al. (1907, 1958, 1961), Gorokhovich et al. (2018), Gosse et al. (2006), Govare (1995), Grant (1969, 1992), Gratton et al. (1984), Gray and Hétu (1981), Gray et al. (1993), Hall et al. (2017), Hallberg and Kemmis (1986), Hansel and Mickelson (1988), Hansel et al. (1985), Hanson (2003), Hardy (1977), Haugerud (2021), Heath et al. (2018, 2020), Hebdah et al. (2008, 2022), Hein and Mudie (1991), Heinrichs et al. (2002), Heintzman et al. (2016), Henderson (1974), Hétu and Gray (2000), Heusser (1973), Heyman et al. (2011), Hickman and Schweger (1996), Hill et al. (1985), Hillaire-Marcel (1976), Hillaire-Marcel et al. (1981), Hobbs et al. (1990), Hodgdon (2016), Hodgson and Haselton (1974), Hodgson (1981, 1985, 1994, 2003, 2005), Hodgson and Vincent (1984), Hodgson et al. (1984), Hooke and Hanson (2017), Hooyer (2007), Houde-Poirier (2014), Hughes and Merry (1978), Hughes (1972, 1987), Hyvärinen (1985), Jackson and Harrington (1991), Jackson et al. (1991, 1997, 2017), Jacobs et al. (1985), Jelgersma (1962), Jenner et al. (2018), Jennings (1993, 1996, 1998, 2011, 2015, 2018), Jetté and Mott (1989), Johnson and Hemstad (1998), Johnson and Mooers (1998), Johnson et al. (1971, 1999, 2016), Josenhans and Zevenhuizen (1990), Karrow (1963, 1974, 1987a,b, 1988), Karrow et al. (2000), Kaufman and Williams (1992), Kaufman et al. (2011), Kaye (1964, 1972), Kelly et al. (2016), Kemmis et al. (1981), Kennedy et al. (2010), Kerr (1996), Kerr et al. (2021), King (1969, 1985, 1987, 1996, 2015), King and Buckley (1967), King et al. (2014), Klassen (1967, 1972, 1983, 1986, 1987, 1993, 1994), Klassen et al. (1992), Knaebel (2006), Koch et al. (2007), Koester et al. (2017), Kovánen and Easterbrook (2001, 2002a, 2002b), Krzyszkowski and Karrow (2001), Kulig (1996), Labelle and Richard (1981), Lacelle et al. (2007, 2013), LaFarge-England et al. (1991), Lajeunesse and Allard

- (2003), Lajeunesse and St-Onge (2008), Lakeman and England (2012, 2013), Lakeman et al. (2018), Lamb (1980), Lamoureux and England (2000), Landmesser et al. (1982), Larsen (1996), Larson (2011), Lauriol (1982), Lauriol and Gray (1987), Lavoie and Richard (2000), Lavoie et al. (2013), Lemmen (1989), Leopold et al. (1982), Lepper et al. (2007, 2011), Lesnek et al. (2018, 2020), Leverett and Taylor (1915), Leverington et al. (2000), Levesque et al. (1993), Lewis et al. (2011), Leydet et al. (2018), Li et al. (2011), Little (2006), Liu et al. (2014), Liverman (1994), Liverman et al. (2006), Loope et al. (2010, 2012, 2018), Lowdon and Blake (1968, 1970, 1973, 1975, 1978, 1980, 1981), Lowdon et al. (1967, 1971), Lowell et al. (1999, 2005, 2009, 2021), Luehmann et al. (2013), Lundstrom (2013), Lusardi et al. (2011), Mackay and Mathews (1973), MacLean et al. (2015, 2017), MacPherson (1996), Maher and Mickelson (1996), Maher et al. (1998), Manley (1996), Manley and Jennings (1996), Manley and Miller (2001), Marcoux and Richard (1995), Margold et al. (2013, 2014, 2015a,b, 2019), Margreth et al. (2017), Martin et al. (2004), Mathewes and Clague (2017), Matile and Keller (2004), Matsch and Schneider (1986), Matthews (1967), Mayle and Cwynar (1995), Mayle et al. (1993a, 1993b), McCallum and Wittnerberg (1968), McHenry and Dunlop (2016), McLaren and Barnett (1978), McMarn (1994), McMarn et al. (2015, 2021), McNeely (1989, 2002, 2006), McNeely and Atkinson (1995), McNeely and Brennan (2005), McNeely and Jorgensen (1993), McNeely and McCuaig (1991), Menounos et al. (2009, 2017), Miller (1979, 1980), Miller et al. (1977, 2002, 2005), Monaghan et al. (1986), Montelli et al. (2017), Mooers and Lehr (1997), Moore et al. (2001), Moorman (1998), Mott (1973, 1977), Mott and Stea (1993), Mott et al. (1986), Muhs et al. (2013, 2018), Muller and Calkin (1993), Mulligan et al. (2018), Munyikwa et al. (2011, 2017), Murton (2009), Murton et al. (2010, 2015, 2017), Narancic et al. (2016), Naughton et al. (2003), Nelson (1982), Nielsen (1980, 1988), Nixon and England (2014), Nixon et al. (2014), Norris et al. (2017, 2022), Nutz et al. (2015), O'Regan et al. (2018), Ó Cofaigh et al. (2000), Occhietti (1980), Occhietti and Richard (2003), Occhietti et al. (2011), Packalen et al. (2014), Pair and Rodrigues (1993), Parent and Occhietti (1999), Patterson and Wright (1998), Patterson (1994, 1997a,b, 1999a,b), Paulen (2001), Pedersen et al. (2016), Peltier et al. (2015), Peterson (1986), Pieńkowski et al. (2014), Pigati et al. (2010), Pilote et al. (2018), Piper and Fehr (1991), Plouffe (2000), Porreca et al. (2018), Porter and Swanson (1998), Prest (1963, 1968, 1973), Prest et al. (1968), Prichonnet (1995), Prior (1991), Pritchard (2006), Proudfoot and St. Croix (1987), Quinn and Goldthwait (1979), Rampton (1988), Rampton et al. (1984), Rappol (1993), Reasoner et al. (1994), Rech et al. (2012), Rémillard et al. (2016), Reyes et al. (2022), Rice et al. (2019), Richard and Occhietti (2005), Richard et al. (1982, 1997), Ridge (2000), Ridge et al. (2012), Riedel (2017), Riedel et al. (2010, 2021), Ritchie (1977), Rittenour et al. (2015), Rodrigues et al. (1993), Roger et al. (2013), Ross et al. (2009), Roy et al. (2011), Rubin and Suess (1955), Ruhe (1969, 1983), Rutherford et al. (1984), Ryder et al. (1991), Rydningen et al. (2013), Saarnisto (1974), Savelle and Dyke (2014), Savoie and Richard (1979), Schaetzl and Weisenborn (2004), Schaetzl et al. (2017), Schlee (1973), Schnitker et al. (2001), Schreiner (1984), Seaman (1989, 2006), Seaman and McCoy (2008), Senici et al. (2015), Setterholm (1995), Sevon and Braun (2000), Shapiro et al. (2004), Sharpe and Russell (2016), Sharpe and Russell (2019), Shaw et al. (2000, 2006, 2017, 2020), Shaw and Longva (2017), Short (1981), Simard et al. (2003), Smith (1992, 1999), Smith and Fisher (1993), Sookhan et al. (2018), Spear and Cwynar (1997), Spooner (1998), Spooner et al. (2005), St-Onge and McMarn (1995), Stalker (1956, 1962), Stanford (1993), Stanford et al. (2020), Stanley and Marshall (2015), Stea (2011), Stea and Mott (1989, 1998, 2005), Stea et al. (1992, 1998, 2003, 2011), Steig et al. (1998), Stoker et al. (2022), Stone and Borns (1986), Stone et al. (2002), Storrar and Stokes (2007), Stravers and Syvitski (1991), Stravers et al. (1992), Stroeve et al. (2010, 2014), Stuiver and Borns (1975), Suess (1954), Sun (1993), Sun and Teller (1997), Swartz et al. (2015), Syverson and Colgan (2011), Taylor (1913), Taylor et al. (2014), Teller et al. (2005, 2018, 2020), Terasmae (1980), Terasmae and Matthews (1980), Thackray (2008), Thomas et al. (1973, 2010), Thompson (1999), Todd et al. (1999), Todd and Shaw (2012), Todd et al. (2007), Totten (1976), Tremblay et al. (2013), Tripsanas and Piper (2008), Tucker (1974), Tulenko et al. (2022), Ullman et al. (2015, 2016), Veillette (1988, 1994), Veillette and Cloutier (1993), Veillette et al. (2017), Vickers et al. (2010), Vincent (1982), Vincent and Hardy (1977, 1979), Walters (2013), Walton et al. (1961), Ward and Thomson (2004), Ward et al. (2003), Waters et al. (2015), Wayne (1965), Welsted and Young (1980), Westgate (1968), White (1968, 1984), White and Totten (1979), White et al. (1969), Williams et al. (2015), Willman and Frye (1970), Winn (1977), Wisconsin Geological and Natural History Survey (2011), Wolfe and Butler (1994), Wolfe et al. (2007), Wood et al. (2010), Woywitka (2019), Wright (1976, 1972), Wright and Ruhe (1965), Wright et al. (1973), Young et al. (1994, 2009, 2012, 2013, 2020, 2021a, 2021b).

## Author contributions

Manuscript conceptualization by MM and ASD. Methods and approach developed by MM and ASD, with the guidance of ALCH and JH. Data compilation by ASD and JH. Mapping, detailed description, and justification of ice margins led by ASD with regional contributions from MM, DGF, SLN, and BJS (western and NW Laurentide); HED and JJC (Cordilleran); MSG (Manitoba and Hudson Bay) and CEJ (American Midcontinent). Writing of manuscript led by ASD with input from all co-authors.

## Declaration of competing interest

The authors declare that they have no known competing financial interests or personal relationships that could have appeared to influence the work reported in this paper.

## Data availability

All data used in this study have been attached to the submission

## Acknowledgements

This project was funded by a Czech Science Foundation (GAČR) Junior grant to MM (19-21216Y). Additional funding to ASD was obtained from Charles University's International Post-Doc Research Fund. We also gratefully acknowledge productive conversations and collaboration at PALSEA, a working group of the International Union for Quaternary Sciences (INQUA) and Past Global Changes (PAGES), which in turn received support from the Swiss Academy of Sciences Chinese Academy of Sciences. We also thank Sam Kelley, Lev Tarasov and Alberto Reyes for productive conversations, as well as reviewers Rod Smith and Chris Clark for constructive feedback that greatly improved this manuscript.

## Appendix A. Supplementary data

Supplementary data to this article can be found online at <https://doi.org/10.1016/j.quascirev.2023.108345>.

**Supplementary Document 1.** Justification document that details the reconstruction of NADI-1 ice margins from 25 to 1 ka across all 15 regions examined in this manuscript. This document also contains regional maps, summary tables of cosmogenic nuclide data and justification for minimum, and maximum ice extent estimates.

**Supplementary Document 3.** A series of maps that overlay the ice margins from NADI-1 with relevant geochronological data for each optimal ice margin (PDF format).

**Supplementary Document 4.** Sequence of 49 maps showing the NADI-1 isochrones from 25 to 1 ka (PDF format).

**Supplementary Document 5.** Sequence of 49 maps showing the

NADI-1 overlaid with the isochrones of Dalton et al. (2020) and Dyke (2004) (PDF format).

**Supplementary Document 6.** Relevant studies that were unintentionally omitted from NADI-1.

**Supplementary Document 7.** A series of maps that overlay the ice margins from NADI-1 with relevant geochronological data for each optimal ice margin (GIF format)

**Supplementary Document 8.** Sequence of 49 maps showing the NADI-1 isochrones from 25 to 1 ka (GIF format).

**Supplementary Document 9.** Sequence of 49 maps showing the NADI-1 overlaid with the isochrones of Dalton et al. (2020) and Dyke (2004) (GIF format).

**Supplementary Table 1.** Cosmogenic nuclide database.

**Supplementary Table 2.** Radiocarbon database.

**Supplementary Table 3.** Luminescence database.

**Supplementary Table 4.** Uranium-thorium database.

**Supplemental Shapefiles.** NADI-1 map files. There are 588 files in total: 49 time-steps x 3 files per timestep (optimal/min/max) = 147 individual shapefiles and their respective 147 .prj, .dbf and .shx files. These shapefiles are also available at <https://doi.org/10.5281/zenodo.8161764>.

**Supplementary Document 2.** Additional information regarding the cosmogenic nuclide dataset.

## References

- Andrews, J.T., 1998. Abrupt changes (Heinrich events) in late Quaternary North Atlantic marine environments: a history and review of data and concepts. *J. Quat. Sci.* 13, 3–16.
- Antevs, E., 1925. Retreat of the Last Ice-Sheet in Eastern Canada. *Geol. Surv. Can Memoir* 146, p. 142.
- Argus, D.F., Peltier, W.R., Drummond, R., Moore, A.W., 2014. The Antarctica component of postglacial rebound model ICE-6G\_C (VM5a) based on GPS positioning, exposure age dating of ice thicknesses, and relative sea level histories. *Geophys. J. Int.* 198, 537–563.
- Atkinson, N., England, J., 2004. Postglacial emergence of Amund and Ellef Ringnes islands, Nunavut: implications for the northwest sector of the Inuitian ice sheet. *Can. J. Earth Sci.* 41, 271–283.
- Atkinson, N., Utting, D.J., Pawley, S.M., 2014. Glacial Landforms of Alberta, Canada; Scale 1:1,000,000. Alberta Energy Regulator AER/AGS Map 604.
- Atkinson, N., Pawley, S., Utting, D.J., 2016. Flow-pattern evolution of the Laurentide and Cordilleran ice sheets across west-central Alberta, Canada: implications for ice sheet growth, retreat and dynamics during the last glacial cycle. *J. Quat. Sci.* 31, 753–768.
- Atkinson, N., Utting, D.J., Pawley, S.M., 2018. An Update to the Glacial Landforms Map of Alberta. Alberta Energy Regulator. AER/AGS Open File Report, p. 24, 2018-08.
- Balbas, A.M., Barth, A.M., Clark, P.U., Clark, J., Caffee, M., O'Connor, J., Baker, V.R., Konrad, K., Bjornstad, B., 2017. <sup>10</sup>Be dating of late Pleistocene megafloods and Cordilleran Ice Sheet retreat in the northwestern United States. *Geology* 45, 583–586.
- Balco, G., 2011. Contributions and unrealized potential contributions of cosmogenic-nuclide exposure dating to glacier chronology, 1990–2010. *Quat. Sci. Rev.* 30, 3–27.
- Balco, G., 2020. Glacier change and paleoclimate applications of cosmogenic-nuclide exposure dating. *Annu. Rev. Earth Planet Sci.* 48, 21–48.
- Balco, G., Schaefer, J.M., 2006. Cosmogenic-nuclide and varve chronologies for the deglaciation of southern New England. *Quat. Geochronol.* 1, 15–28.
- Balco, G., Stone, J.O.H., Porter, S.C., Caffee, M.W., 2002. Cosmogenic-nuclide ages for new England coastal moraines, Martha's Vineyard and Cape Cod, Massachusetts, USA. *Quat. Sci. Rev.* 21, 2127–2135.
- Balco, G., Stone, J.O., Lifton, N.A., Dunai, T.J., 2008. A complete and easily accessible means of calculating surface exposure ages or erosion rates from <sup>10</sup>Be and <sup>26</sup>Al measurements. *Quat. Geochronol.* 3, 174–195.
- Balco, G., Briner, J., Finkel, R.C., Rayburn, J.A., Ridge, J.C., Schaefer, J.M., 2009. Regional beryllium-10 production rate calibration for late-glacial northeastern North America. *Quat. Geochronol.* 4, 93–107.
- Barber, D.C., Dyke, A., Hillaire-Marcel, C., Jennings, A.E., Andrews, J.T., Kerwin, M.W., Bilodeau, G., McNeely, R., Southon, J., Morehead, M.D., Gagnon, J.M., 1999. Forcing of the cold event of 8,200 years ago by catastrophic drainage of Laurentide lakes. *Nature* 400, 344–348.
- Barnett, P.J., 1985. Glacial retreat and lake levels, north-central Lake Erie basin, Ontario. In: Karrow, P.F., Calkin, P.E. (Eds.), *Quaternary Evolution of the Great Lakes: Geological Association of Canada Special Paper* 30, pp. 185–194.
- Barnett, P.J., Karrow, P.F., 2017. Ice-marginal sedimentation and processes of diamictite deposition in large proglacial lakes, Lake Erie, Ontario, Canada. *Can. J. Earth Sci.* 55, 846–862.
- Barnett, P.J., Karrow, P.F., 2018. Ice-marginal sedimentation and processes of diamictite deposition in large proglacial lakes, Lake Erie, Ontario, Canada. *Can. J. Earth Sci.* 55, 846–862.
- Batchelor, C.L., Dowdeswell, J.A., Pietras, J.T., 2012. Variable history of Quaternary ice sheet advance across the Beaufort Sea margin. *Arctic Ocean. Geol.* 41, 131–134.
- Batchelor, C.L., Dowdeswell, J.A., Pietras, J.T., 2014. Evidence for multiple Quaternary ice advances and fan development from the Amundsen Gulf cross-shelf trough and slope, Canadian Beaufort Sea margin. *Mar. Petrol. Geol.* 52, 125–143.
- Batchelor, C.L., Dowdeswell, J.A., Dowdeswell, E.K., Todd, B.J., 2016. A subglacial landform assemblage on the outer shelf of M'Clure Strait, Canadian Arctic, ploughed by iceberg keels. *Geol. Soc. Lond. Mem.* 46, 337–340.
- Batchelor, C.L., Margold, M., Krapp, M., Murton, D.K., Dalton, A.S., Gibbard, P.L., Stokes, C.R., Murton, J.B., Manica, A., 2019. The configuration of Northern Hemisphere ice sheets through the Quaternary. *Nat. Commun.* 10, 3713.
- Bateman, M.D., Murton, J.B., 2006. The chronostratigraphy of Late Pleistocene glacial and periglacial aeolian activity in the Tuktoyaktuk Coastlands, NWT, Canada. *Quat. Sci. Rev.* 25, 2552–2568.
- Becerra-Valdivia, L., Higham, T., 2020. The timing and effect of the earliest human arrivals in North America. *Nature* 584, 93–97.
- Bednarzki, J.M., 2008. Landform assemblages produced by the Laurentide Ice Sheet in northeastern British Columbia and adjacent Northwest Territories — constraints on glacial lakes and patterns of ice retreat. *Can. J. Earth Sci.* 45, 593–610.
- Berger, A., Loutre, M.F., 1991. Insolation values for the climate of the last 10 million years. *Quat. Sci. Rev.* 10, 297–317.
- Bierman, P.R., 1994. Using in situ produced cosmogenic isotopes to estimate rates of landscape evolution: a review from the geomorphic perspective. *J. Geophys. Res. Solid Earth* 99, 13885–13896.
- Bierman, P.R., Marsella, K.A., Patterson, C., Davis, P.T., Caffee, M., 1999. Mid-Pleistocene cosmogenic minimum-age limits for pre-Wisconsinan glacial surfaces in southwestern Minnesota and southern Baffin Island: a multiple nuclide approach. *Geomorphology* 27, 25–39.
- Bierman, P.R., Davis, P.T., Corbett, L.B., Lifton, N.A., Finkel, R.C., 2015. Cold-based Laurentide ice covered new England's highest summits during the last glacial maximum. *Geology* 43, 1059–1062.
- Blaise, B., Clague, J.A., Mathewes, R.W., 1990. Time of maximum late Wisconsin glaciation, West Coast of Canada. *Quat. Res.* 34, 282–295.
- Blewett, W.L., Winters, H.A., Rieck, R.L., 1993. New age control on the Port Huron moraine in northern Michigan. *Phys. Geogr.* 14, 131–138.
- Blewett, W.L., Drzyzga, S.A., Sherrod, L., Wang, H., 2014. Geomorphic relations among glacial Lake Algonquin and the Munising and Grand Marais moraines in eastern upper Michigan, USA. *Geomorphology* 219, 270–284.
- Boex, J., Fogwill, C., Harrison, S., Glasser, N.F., Hein, A., Schnabel, C., Xu, S., 2013. Rapid thinning of the late Pleistocene Patagonian ice sheet followed migration of the southern Westerlies. *Sci. Rep.* 3, 2118.
- Boissonneau, A.N., 1966. Glacial history of northeastern Ontario: the Cochrane-Hearst area. *Can. J. Earth Sci.* 3, 559–578.
- Bolduc, A.M., 1995. Landforms in the Laurentians of Southern Quebec: Implications for the Deglaciation History Of the Laurentide Ice Sheet: CANQUA-CGRG Joint Meeting, St. John's, Newfoundland, Program, Abstracts and Field Guides. CA5.
- Borchers, B., Marrero, S., Balco, G., Caffee, M., Goehring, B., Lifton, N., Nishizumi, K., Phillips, F., Schaefer, J., Stone, J., 2016. Geological calibration of spallation production rates in the CRONUS-Earth project. *Quat. Geochronol.* 31, 188–198.
- Borns Jr., H.W., Doner, L.A., Dorion, C.C., Jacobson Jr., G.L., Kaplan, M.R., Kreutz, K.J., Lowell, T.V., Thompson, W.B., Weddle, T.K., 2004. The deglaciation of Maine, U.S.A. In: Ehlers, J., Gibbard, P.L. (Eds.), *Quaternary Glaciations – Extent and Chronology, Part II: North America*. Elsevier, Amsterdam, pp. 89–109.
- Boulton, G.S., Clark, C.D., 1990. A highly mobile Laurentide ice sheet revealed by satellite images of glacial lineations. *Nature* 346, 813–817.
- Breckenridge, A., 2007. The Lake Superior varve stratigraphy and implications for eastern Lake Agassiz outflow from 10,700 to 8900 cal ybp (9.5–8.0 <sup>14</sup>C ka). *Palaeogeogr. Palaeoclimatol. Palaeoecol.* 246, 45–61.
- Breckenridge, A., Johnson, T.C., Beske-Diehl, S., Mothersill, J.S., 2004. The timing of regional Lateglacial events and post-glacial sedimentation rates from Lake Superior. *Quat. Sci. Rev.* 23, 2355–2367.
- Breckenridge, A., Lowell, T.V., Stroup, J.S., Evans, G., 2012. A review and analysis of varve thickness records from glacial Lake Ojibway (Ontario and Quebec, Canada). *Quat. Int.* 260, 43–54.
- Breckenridge, A., Lowell, T.V., Peteet, D., Watrus, N., Moretto, M., Norris, N., Dennison, A., 2021. A new glacial varve chronology along the southern Laurentide Ice Sheet that spans the Younger Dryas–Holocene boundary. *Geology* 49, 283–288.
- Briner, J.P., Miller, G.H., Davis, P.T., Bierman, P.R., Caffee, M., 2003. Last Glacial Maximum ice sheet dynamics in Arctic Canada inferred from young erratics perched on ancient tors. *Quat. Sci. Rev.* 22, 437–444.
- Briner, J.P., Miller, G.H., Davis, P.T., Finkel, R.C., 2005. Cosmogenic exposure dating in arctic glacial landscapes: implications for the glacial history of northeastern Baffin Island, Arctic Canada. *Can. J. Earth Sci.* 42, 67–84.
- Briner, J.P., Miller, G.H., Davis, P.T., Finkel, R.C., 2006. Cosmogenic radionuclides from fiord landscapes support differential erosion by overriding ice sheets. *Geol. Soc. Am. Bull.* 118, 406–420.
- Briner, J.P., Bini, A.C., Anderson, R.S., 2009a. Rapid early Holocene retreat of a Laurentide outlet glacier through an Arctic fjord. *Nat. Geosci.* 2, 496–499.
- Briner, J.P., Davis, P.T., Miller, G.H., 2009b. Latest Pleistocene and Holocene glaciation of Baffin Island, Arctic Canada: key patterns and chronologies. *Quat. Sci. Rev.* 28, 2075–2087.
- Briner, J.P., Lifton, N.A., Miller, G.H., Refsnider, K., Anderson, R., Finkel, R., 2014. Using in situ cosmogenic <sup>10</sup>Be, <sup>14</sup>C, and <sup>26</sup>Al to decipher the history of polythermal ice sheets on Baffin Island, Arctic Canada. *Quat. Geochronol.* 19, 4–13.

- Bromley, G.R.M., Hall, B.L., Thompson, W.B., Kaplan, M.R., Garcia, J.L., Schaefer, J.M., 2015. Late glacial fluctuations of the Laurentide Ice Sheet in the White Mountains of Maine and New Hampshire, U.S.A. *Quat. Res.* 83, 522–530.
- Bromley, G.R.M., Hall, B.L., Thompson, W.B., Lowell, T.V., 2020. Age of the Berlin moraine complex, New Hampshire, USA, and implications for ice sheet dynamics and climate during Termination 1. *Quat. Res.* 94, 80–93.
- Bromwich, D.H., Toracinta, E.R., Wang, S.-H., 2002. Meteorological perspective on the initiation of the Laurentide Ice Sheet. *Quat. Int.* 95–96, 113–124.
- Broom, L., Cameron, G.D.M., 2021. Surficial geology and seabed features of Flemish Cap, offshore Island of Newfoundland, Newfoundland and Labrador. *Geol. Surv. Can. Open File* 8827, 27.
- Brouard, E., Lajeunesse, P., 2017. Maximum extent and decay of the Laurentide Ice Sheet in western Baffin Bay during the Last glacial episode. *Sci. Rep.* 7, 10711.
- Brouard, E., Roy, M., Godbout, P.-M., Veillette, J.J., 2021. A framework for the timing of the final meltwater outbursts from glacial Lake Agassiz-Ojibway. *Quat. Sci. Rev.* 274, 107269.
- Bryson, R.A., Wendland, W.M., Ives, J.D., Andrews, J.T., 1969. Radiocarbon isochrones on the distintegration of the Laurentide Ice Sheet. *Arct. Alp. Res.* 1, 1–14.
- Carboneau, A.S., Allard, M., LeBlanc, A.M., L'Héroult, E., Mate, D., Oldenborger, G.A., Gosselin, P., Sladen, W.E., 2012. Surficial geology and periglacial features, Pangnirtung, Nunavut. *Geol. Surv. Can. Can. Geosci. Map* 65.
- Carlson, A.E., Clark, P.U., 2012. Ice sheet sources of sea level rise and freshwater discharge during the last deglaciation. *Rev. Geophys.* 50, RG4007.
- Carlson, A.E., Clark, P.U., Raisbeck, G.M., Brook, E.J., 2007. Rapid Holocene deglaciation of the Labrador Sector of the Laurentide Ice Sheet. *J. Clim.* 20, 5126–5133.
- Carlson, A.E., Reyes, A.V., Sillett, K., Wilcken, K.M., Rood, D.H., 2021. Southwest Greenland ice-sheet retreat during the 8.2 ka cold event. *Quat. Sci. Rev.* 268, 107101.
- Catania, G.A., Stearns, L.A., Moon, T.A., Enderlin, E.M., Jackson, R.H., 2020. Future evolution of Greenland's marine-terminating outlet glaciers. *J. Geophys. Res.: Earth Surf.* 125, e2018JF004873.
- Ceperley, E.G., Marcott, S.A., Rawling, J.E., Zoet, L.K., Zimmerman, S.R.H., 2019. The role of permafrost on the morphology of an MIS 3 moraine from the southern Laurentide Ice Sheet. *Geology* 47, 440–444.
- Chmeleff, J., von Blanckenburg, F., Kossett, K., Jakob, D., 2010. Determination of the  $^{10}\text{Be}$  half-life by multicollector ICP-MS and liquid scintillation counting. *Nucl. Instrum. Methods Phys. Res. Sect. B Beam Interact. Mater. Atoms* 268, 192–199.
- Clague, J.J., 1980. Late Quaternary geology and geochronology of British Columbia, Part 1: Radiocarbon dates. *Geol. Surv. Can. Paper* 80-13, 33 p.
- Clague, J.J., 2017. Deglaciation of the Cordillera of Western Canada at the end of the Pleistocene. *Cuadernos de Investigación Geográfica* 43, 449.
- Clague, J.J., Armstrong, J.E., Mathews, W.H., 1980. Advance of the Late Wisconsin Cordilleran Ice Sheet in Southern British Columbia since 22,000 Yr B.P. *Quat. Res.* 13, 322–326.
- Clark, P.U., Mix, A.C., 2002. Ice sheets and sea level of the Last Glacial Maximum. *Quat. Sci. Rev.* 21, 1–7.
- Clark, P.U., Tarasov, L., 2014. Closing the sea level budget at the Last Glacial Maximum. *Proc. Natl. Acad. Sci. USA* 111, 15861–15862.
- Clark, C.D., Knight, J.K., T Gray, J., 2000. Geomorphological reconstruction of the Labrador sector of the Laurentide Ice Sheet. *Quat. Sci. Rev.* 19, 1343–1366.
- Clark, P.U., Brook, E.J., Raisbeck, G.M., Yiou, F., Clark, J., 2003. Cosmogenic  $^{10}\text{Be}$  ages of the Sagle Moraines, Torngat Mountains, Labrador. *Geol.* 31, 617–620.
- Clark, P.U., Dyke, A.S., Shakun, J.D., Carlson, A.E., Clark, J., Wohlfarth, B., Mitrovica, J.X., Hostettler, S.W., McCabe, A.M., 2009. The Last Glacial Maximum. *Science* 325, 710–714.
- Clark, C.D., Ely, J.C., Greenwood, S.L., Hughes, A.L.C., Meehan, R., Barr, I.D., Bateman, M.D., Bradwell, T., Doole, J., Evans, D.J.A., Jordan, C.J., Monteys, X., Pellicer, X.M., Sheehy, M., 2018. BRITICE Glacial Map, version 2: a map and GIS database of glacial landforms of the last British-Irish Ice Sheet. *Boreas* 47, 11–27.
- Clark, C.D., Ely, J.C., Hindmarsh, R.C.A., Bradley, S., Ignéczí, A., Fabel, D., Ó Cofaigh, C., Chiverrell, R.C., Scourse, J., Benetti, S., Bradwell, T., Evans, D.J.A., Jordan, C.J., Monteys, X., Burke, M., Callard, S.L., Medaldea, A., Saher, M., Small, D., Smedley, R.K., Gasson, E., Gregoire, L., Gandy, N., Hughes, A.L.C., Ballantyne, C., Bateman, M.D., Bigg, G.R., Doole, J., Dove, D., Duller, G.A.T., Jenkins, G.T.H., Livingstone, S.L., McCarron, S., Moreton, S., Pollard, D., Praeg, D., Sejrup, H.P., Van Landeghem, K.J., Wilson, P., 2022a. Growth and retreat of the last British-Irish Ice Sheet, 31 000 to 15 000 years ago: the BRITICE-CHRONO reconstruction. *Boreas*. <https://doi.org/10.1111/bor.12594> n/a.
- Clark, J., Carlson, A.E., Reyes, A.V., Carlson, E.C.B., Guillaume, L., Milne, G.A., Tarasov, L., Caffee, M., Wilcken, K., Rood, D.H., 2022b. The age of the opening of the Ice-Free Corridor and implications for the peopling of the Americas. *Proc. Natl. Acad. Sci. USA* 119, e2118558119.
- Clayton, L., Moran, S.R., 1982. Chronology of Late Wisconsinan Glaciation in Middle North America. *Quat. Sci. Rev.* 1, 55–82.
- Clayton, L., Attig, J.W., Ham, N.R., Johnson, M.D., Jennings, C.E., Syverson, K.M., 2008. Ice-walled-lake plains: Implications for the origin of hummocky glacial topography in middle North America. *Geomorphology* 97, 237–248.
- Colgan, P.M., Bierman, P.R., Mickelson, D.M., Caffee, M., 2002. Variation in glacial erosion near the southern margin of the Laurentide Ice Sheet, south-central Wisconsin, USA: Implications for cosmogenic dating of glacial terrains. *Geol. Soc. Am. Bull.* 114, 1581–1591.
- Cooper, W.S., 1935. The history of the upper Mississippi River in late Wisconsin and postglacial time. *Minn. Geol. Surv. Bull.* 26, 116.
- Corbett, L.B., Bierman, P.R., Davis, P.T., 2016. Glacial history and landscape evolution of southern Cumberland Peninsula, Baffin Island, Canada, constrained by cosmogenic  $^{10}\text{Be}$  and  $^{26}\text{Al}$ . *Geol. Soc. Am. Bull.* 128, 1173–1192.
- Corbett, L.B., Bierman, P.R., Stone, B.D., Caffee, M.W., Larsen, P.L., 2017. Cosmogenic nuclide age estimate for Laurentide Ice Sheet recession from the terminal moraine, New Jersey, USA, and constraints on latest Pleistocene ice sheet history. *Quat. Res.* 87, 482–498.
- Corbett, L.B., Bierman, P.R., Wright, S.F., Shakun, J.D., Davis, P.T., Goehringer, B.M., Halsted, C.T., Koester, A.J., Caffee, M.W., Zimmerman, S.R., 2019. Analysis of multiple cosmogenic nuclides constrains Laurentide Ice Sheet history and process on Mt. Mansfield, Vermont's highest peak. *Quat. Sci. Rev.* 205, 234–246.
- Cosma, T.N., Hendy, I.L., Chang, A.S., 2008. Chronological constraints on Cordilleran Ice Sheet glaciomarine sedimentation from core M02-2496 off Vancouver Island (western Canada). *Quat. Sci. Rev.* 27, 941–955.
- Couch, A.G., Eyles, N., 2008. Sedimentary record of glacial Lake Mackenzie, Northwest Territories, Canada: Implications for Arctic freshwater forcing. *Palaeogeogr. Palaeoclimatol. Palaeoecol.* 268, 26–38.
- Coulthard, R.D., Furze, M.F.A., Pierkowski, A.J., Nixon, F.C., England, J.H., 2010. New marine  $\Delta\text{R}$  values for Arctic Canada. *Quat. Geochronol.* 5, 419–434.
- Crump, S.E., Anderson, L.S., Miller, G.H., Anderson, R.S., 2017. Interpreting exposure ages from ice-cored moraines: A Neoglacial case study on Baffin Island, Arctic Canada. *J. Quat. Sci.* 32, 1049–1062.
- Curry, B., Petras, J., 2011. Chronological framework for the deglaciation of the Lake Michigan lobe of the Laurentide Ice Sheet from ice-walled lake deposits. *J. Quat. Sci.* 26, 402–410.
- Curry, B.B., Konen, M.E., Larson, T.H., Yansa, C.H., Hackley, K.C., Alexanderson, H., Lowell, T.V., 2010. The DeKalb mounds of northeastern Illinois as archives of deglacial history and postglacial environments. *Quat. Res.* 74, 82–90.
- Curry, B.B., Hajic, E.R., Clark, J.A., Befus, K.M., Carrell, J.E., Brown, S.E., 2014. The Kankakee Torrent and other large meltwater flooding events during the last deglaciation, Illinois, USA. *Quat. Sci. Rev.* 90, 22–36.
- Curry, B.B., Lowell, T.V., Wang, H., Anderson, A.C., 2018. Revised time-distance diagram for the Lake Michigan Lobe, Michigan Subepisode, Wisconsin Episode, Illinois, USA. In: Kehew, A.E., Curry, B.B. (Eds.), *Quaternary Glaciation of the Great Lakes Region: Process, Landforms, Sediments, and Chronology*. Geological Society of America Special Paper 530, pp. 69–101.
- Cuzzone, J.K., Clark, P.U., Carlson, A.E., Ullman, D.J., Rinterknecht, V.R., Milne, G.A., Lunkka, J.-P., Wohlfarth, B., Marcott, S.A., Caffee, M., 2016. Final deglaciation of the Scandinavian Ice Sheet and implications for the Holocene global sea-level budget. *Earth Planet Sci. Lett.* 448, 34–41.
- Dalton, A.S., Margold, M., Stokes, C.R., Tarasov, L., Dyke, A.S., Adams, R.S., Allard, S., Arends, H.E., Atkinson, N., Attig, J.W., Barnett, P.J., Barnett, R.L., Batterson, M., Bernatchez, P., Borns, H.W., Breckenridge, A., Briner, J.P., Brouard, E., Campbell, J. E., Carlson, A.E., Clague, J.J., Curry, B.B., Daigneault, R.-A., Dubé-Loubert, H., Easterbrook, D.J., Franzl, D.A., Friedrich, H.G., Funder, S., Gauthier, M.S., Gowen, A.S., Harris, K.L., Hétu, B., Hooyer, T.S., Jennings, C.E., Johnson, M.D., Kehew, A.E., Kelley, S.E., Kerr, D., King, E.L., Kjeldsen, K.K., Knaebel, A.R., Lajeunesse, P., Lakeman, T.R., Lamothé, M., Larson, P., Lavoie, M., Loope, H.M., Lowell, T.V., Lusardi, B.A., Manz, L., McMartin, I., Nixon, F.C., Occhietti, S., Parkhill, M.A., Piper, D.J.W., Pronk, A.G., Richard, P.J.H., Ridge, J.C., Ross, M., Roy, M., Seaman, A., Shaw, J., Stea, R.R., Teller, J.T., Thompson, W.B., Thorleifson, L.H., Utting, D.J., Veillette, J.J., Ward, B.C., Weddle, T.K., Wright, H.E., 2020. An updated radiocarbon-based ice margin chronology for the last deglaciation of the North American Ice Sheet Complex. *Quat. Sci. Rev.* 234, 106223.
- Dalton, A.S., Stokes, C.R., Batchelor, C.L., 2022. Evolution of the Laurentide and Inuitian ice sheets prior to the Last Glacial Maximum (115 ka to 25 ka). *Earth Sci. Rev.* 224, 103875.
- Darvill, C.M., Menounos, B., Goehringer, B.M., Lian, O.B., Caffee, M.W., 2018. Retreat of the western Cordilleran Ice Sheet margin during the last deglaciation. *Geophys. Res. Lett.* 45, 9710–9720.
- Darvill, C.M., Menounos, B., Goehringer, B.M., Lesnek, A.J., 2022. Cordilleran Ice Sheet stability during the last deglaciation. *Geophys. Res. Lett.* 49, e2021GL097191.
- Davies, B.J., 2022. Cryospheric Geomorphology: Dating Glacial Landforms II: radiometric techniques. In: Haritashaya, U. (Ed.), *Treatise on Geomorphology*. Elsevier, pp. 249–280.
- Davies, B.J., Darvill, C.M., Lovell, H., Bendle, J.M., Dowdeswell, J.A., Fabel, D., García, J.-L., Geiger, A., Glasser, N.F., Gheorghiu, D.M., Harrison, S., Hein, A.S., Kaplan, M.R., Martin, J.R.V., Mendelova, M., Palmer, A., Pelto, M., Rodés, Á., Sagredo, E.A., Smedley, R.K., Smellie, J.L., Thorndycraft, V.R., 2020. The evolution of the Patagonian Ice Sheet from 35 ka to the present day (PATICE). *Earth Sci. Rev.* 204, 103152.
- Davis, N.K., Locke, W.W., Pierce, K.L., Finkel, R.C., 2006a. Glacial Lake Musselshell: Late Wisconsin slackwater on the Laurentide ice margin in central Montana, USA. *Geomorphology* 75, 330–345.
- Davis, P.T., Briner, J.P., Coulthard, R.D., Finkel, R.W., Miller, G.H., 2006b. Preservation of Arctic landscapes overridden by cold-based ice sheets. *Quat. Res.* 65, 156–163.
- Davis, P.T., Bierman, P.R., Corbett, L.B., Finkel, R.C., 2015. Cosmogenic exposure age evidence for rapid Laurentide deglaciation of the Katahdin area, west-central Maine, USA, 16 to 15 ka. *Quat. Sci. Rev.* 116, 95–105.
- Dawson, G.M., 1890. On the glaciation of the northern part of the Cordillera, with an attempt to correlate the events of the glacial period in the Cordillera and Great Plains. *The American Geologist* 6, 153–162.
- Dredge, L.A., McMartin, I., 2007. Surficial Geology, Wager Bay, Nunavut, Scale 1:100 000. *Geol. Surv. Can. A Series Map* 2111A.

- Dubé-Loubert, H., Roy, M., 2017. Development, evolution and drainage of glacial Lake Naskaupi during the deglaciation of north-central Quebec and Labrador. *J. Quat. Sci.* 32, 1121–1137.
- Duk-Rodkin, A., 1999. Glacial Limits Map of Yukon. Department of Indian and Northern Development, Canada. Exploration and Geological Services Division. Geoscience Map 1999-2.
- Duk-Rodkin, A., 2022. Glacial Limits, Mackenzie Mountains and Foothills, Northwest Territories, Canada, vol. 8891. *Geol. Surv. Can Open File*.
- Duk-Rodkin, A., Hughes, O., 1992. Pleistocene Montane Glaciations in the Mackenzie Mountains, Northwest Territories. *Géogr. Phys. Quaternaire* 46, 69–83.
- Dulfer, H.E., Margold, M., 2021. Glacial geomorphology of the central sector of the Cordilleran Ice Sheet, Northern British Columbia, Canada. *J. Maps* 17, 1–15.
- Dulfer, H.E., Margold, M., Engel, Z., Braucher, R., Team, A., 2021. Using  $^{10}\text{Be}$  dating to determine when the Cordilleran Ice Sheet stopped flowing over the Canadian Rocky Mountains. *Quat. Res.* 102, 1–12.
- Dulfer, H.E., Margold, M., Darvill, C.M., Stroeve, A.P., 2022. Reconstructing the advance and retreat dynamics of the central sector of the last Cordilleran Ice Sheet. *Quat. Sci. Rev.* 284, 107465.
- Dulfer, H.E., Stoker, B.J., Margold, M., Stokes, C.R., 2023. Glacial geomorphology of the northwest Laurentide Ice Sheet on the northern Interior Plains and western Canadian Shield, Canada. *J. Maps* 1–18.
- Dyck, W., Fyles, J.G., Blake, W.J., 1965. *Geol. Surv. Can Radiocarbon Dates IV*. *Geol. Surv. Can. Pap.* 65–4, 23.
- Dyke, A.S., 1999. Last Glacial Maximum and deglaciation of Devon Island, Arctic Canada: support for an Innuittian ice sheet. *Quat. Sci. Rev.* 18, 393–420.
- Dyke, A.S., 2004. An outline of North American deglaciation with emphasis on central and northern Canada. In: Ehlers, J., Gibbard, P.L. (Eds.), *Quaternary Glaciations - Extent and Chronology, Part II*. Elsevier, pp. 373–424.
- Dyke, A.S., Evans, D.J.A., 2003. Ice-marginal terrestrial landsystems: Northern Laurentide and Innuittian ice sheet margins. In: Evans, D.J.A. (Ed.), *Glacial Landsystems*, pp. 143–165.
- Dyke, A.S., Prest, V.K., 1987. Late Wisconsinan and Holocene history of the Laurentide Ice Sheet. *Géogr. Phys. Quaternaire* 41, 237–263.
- Dyke, A.S., Savelle, J.M., 2000. Major end moraines of Younger Dryas age on Wollaston Peninsula, Victoria Island, Canadian Arctic: implications for paleoclimate and for formation of hummocky moraine. *Can. J. Earth Sci.* 37, 601–619.
- Dyke, A.S., Moore, A., Robertson, L., 2003a. Deglaciation of North America: Thirty-two digital maps at 1:7,000,000 scale with accompanying digital chronological database and one poster (two sheets) with full map series. *Geol. Surv. Can. Open File* 1574. <https://doi.org/10.4095/214399>.
- Dyke, A.S., St-Onge, D.A., Savelle, J.M., 2003b. Deglaciation of southwestern Victoria Island and adjacent Arctic mainland, Nunavut-Northwest Territories. *Geol. Surv. Can. Map* 2027A scale 1:500,000.
- Ely, J.C., Gribble, E.A., Clark, C.D., 2016. The glacial geomorphology of the western Cordilleran ice sheet and Ahklun ice cap, Southern Alaska. *J. Maps* 12, 415–424.
- England, J., 1978. The glacial geology of northeastern Ellesmere Island, N.W.T., Canada. *Can. J. Earth Sci.* 15, 603–617.
- England, J., 1996. Glacier dynamics and paleoclimatic change during the last glaciation of eastern Ellesmere Island, Canada. *Can. J. Earth Sci.* 33, 779–799.
- England, J.H., Atkinson, N., Dyke, A.S., Evans, D.J.A., Zreda, M., 2004. Late Wisconsinan buildup and wastage of the Innuittian Ice Sheet across southern Ellesmere Island, Nunavut. *Can. J. Earth Sci.* 41, 39–61.
- England, J., Atkinson, N., Bednarski, J., Dyke, A.S., Hodgson, D.A., Ó Cofaigh, C., 2006. The Innuittian Ice Sheet: configuration, dynamics and chronology. *Quat. Sci. Rev.* 25, 689–703.
- England, J.H., Furze, M.F.A., Doupé, J.P., 2009. Revision of the NW Laurentide Ice Sheet: implications for paleoclimate, the northeast extremity of Beringia, and Arctic Ocean sedimentation. *Quat. Sci. Rev.* 28, 1573–1596.
- England, J., Dyke, A.S., Coulthard, R.D., McNeely, R., Aitken, A., 2013. The exaggerated radiocarbon age of deposit-feeding molluscs in calcareous environments. *Boreas* 42, 362–373.
- United States Geological Survey's Center for Earth Resources Observation and Science (EROS), 2010. 30 Arc-Second DEM of North America. <https://databasin.org/datasets/d2198be9d2264de19cb93fe6a380b69c>.
- Evans, D.J.A., Young, N.J.P., Ó Cofaigh, C., 2014. Glacial geomorphology of terrestrial-terminating fast flow lobes/ice stream margins in the southwest Laurentide Ice Sheet. *Geomorphology* 204, 86–113.
- Evans, D.J.A., Smith, I.R., Gosse, J.C., Galloway, J.M., 2021. Glacial landforms and sediments (landsystem) of the Smoking Hills area, Northwest Territories, Canada: Implications for regional Pliocene – Pleistocene Laurentide Ice Sheet dynamics. *Quat. Sci. Rev.* 262, 106958.
- Fame, M.L., Spotila, J.A., Owen, L.A., Shuster, D.L., 2019. Consistent slow exhumation in a late Cenozoic glaciated landscape: The Presidential and Carter ranges of the White Mountains in New Hampshire, USA. *Geomorphology* 345, 106842.
- Fisher, T.G., Breckenridge, A., 2022. Relative lake level reconstructions for glacial Lake Agassiz spanning the Herman to Campbell levels. *Quat. Sci. Rev.* 294, 107760.
- Flint, R.F., 1943. Growth of North American ice sheet during the Wisconsin age. *Geol. Soc. Am. Bull.* 54, 325–362.
- Flint, R.F., Colton, R.B., Goldthwait, R.P., Willman, H.B., 1959. Glacial Map of the United States East of the Rocky Mountains. Geological Society of America, New York.
- Fortin, M.-C., Gajewski, K., 2016. Multiproxy paleoecological evidence of Holocene climatic changes on the Boothia Peninsula, Canadian Arctic. *Quat. Res.* 85, 347–357.
- Froese, D.G., Young, J.M., Norris, S.L., Margold, M., 2019. Availability and Viability of the Ice-free Corridor and Pacific Coast Routes for the Peopling of the Americas. *Soc. Am. Archaeol.: Archaeological Record* 19, 27–33.
- Fullerton, D.S., Colton, R.B., Bush, C.A., Straub, A.W., 2004. Map showing spatial and temporal relations of mountain and continental glaciations on the Northern Plains, primarily in northern Montana and northwestern North Dakota. *Scientific Investigations Map 2843. Version 1.0*.
- Fulton, R.J., 1971. Radiocarbon Geochronology of Southern British Columbia. *Geol. Surv. Can. Paper* 71–37, p. 28.
- Fulton, R.J., 1995. Surficial materials of Canada. *Geol. Surv. Can. "A" Series Map 1880A* scale: 1:5,000,000.
- Furze, M.F.A., Pieńkowski, A.J., McNeely, M.A., Bennett, R., Cage, A.G., 2018. Deglaciation and ice shelf development at the northeast margin of the Laurentide Ice Sheet during the Younger Dryas chronozone. *Boreas* 47, 271–296.
- Fyles, J.G., 1963. Surficial geology of Victoria and Stefansson Islands, District of Franklin. *Geol. Surv. Can. Bull.* 107, 1–38.
- Gauthier, M.S., 2022a. Digital Compilation of Surficial Point and Line Features for Manitoba, Including Ice-Flow Data. Manitoba Natural Resources and Northern Development Manitoba Geological Survey, p. 5. *GeoFile 1-2022*.
- Gauthier, M.S., 2022b. Using radiocarbon ages on organics affected by freshwater—a geologic and archaeologic update on the freshwater reservoir ages and freshwater diet effect in Manitoba, Canada. *Radiocarbon* 64, 253–264.
- Gauthier, M.S., Kelley, S.E., Hodder, T.J., 2020. Lake Agassiz drainage bracketed Holocene Hudson Bay Ice Saddle collapse. *Earth Planet Sci. Lett.* 544, 116372.
- Gauthier, M.S., Breckenridge, A., Hodder, T.J., 2022. Patterns of ice recession and ice stream activity for the MIS 2 Laurentide Ice Sheet in Manitoba, Canada. *Boreas* 51, 274–298.
- Gilbert, A., Flowers, G.E., Miller, G.H., Refsnider, K.A., Young, N.E., Rudić, V., 2017. The projected demise of Barnes Ice Cap: Evidence of an unusually warm 21st century Arctic. *Geophys. Res. Lett.* 44, 2810–2816.
- Godbout, P.-M., Roy, M., Veillette, J.J., 2019. High-resolution varve sequences record one major late-glacial ice readvance and two drainage events in the eastern Lake Agassiz-Ojibway basin. *Quat. Sci. Rev.* 223, 105942.
- Godbout, P.-M., Roy, M., Veillette, J.J., 2020. A detailed lake-level reconstruction shows evidence for two abrupt lake drawdowns in the late-stage history of the eastern Lake Agassiz-Ojibway basin. *Quat. Sci. Rev.* 238, 106327.
- Goldthwait, R.P., White, G.W., Forsyth, J.L., 1967. Glacial Map of Ohio - United States Geological Survey Miscellaneous Geological Inventory Map 316.
- Gorham, E., Lehman, C., Dyke, A., Janssens, J., Dyke, L., 2007. Temporal and spatial aspects of peatland initiation following deglaciation in North America. *Quat. Sci. Rev.* 26, 300–311.
- Gosse, J.C., Phillips, F.M., 2001. Terrestrial in situ cosmogenic nuclides: theory and application. *Quat. Sci. Rev.* 20, 1475–1560.
- Gosse, J.C., Bell, T., Gray, J.T., Klein, J., Yang, G., Finkel, R., 2006. Using Cosmogenic Isotopes to Interpret the Landscape Record of Glaciation: Nunataks in Newfoundland? Blackwell Publishing.
- Govare, É., 1995. *Géomorphologie et paléoenvironnements de la région de Charlevoix, Québec, Canada* [PhD thesis]. Université de Montréal, p. 425.
- Gowan, E.J., Zhang, X., Khosravi, S., Rovere, A., Stocchi, P., Hughes, A.L.C., Gyllencreutz, R., Mangerud, J., Svendsen, J.I., Lohmann, G., 2021. Global ice sheet reconstruction for the past 80000 years. *Nat. Commun.* 12, 1199.
- Grant, D.R., 1969. Late Pleistocene readvance of piedmont glaciers in western Newfoundland. *Marit. Sediments* 5, 126–128.
- Grant, D.R., 1992. Quaternary Geology of St. Anthony-Blanc-Sablon Area, Newfoundland and Quebec. *Geol. Surv. Can Memoir* 427, p. 60.
- Gray, J., Lauriol, B., Bruneau, D., Ricard, J., 1993. Postglacial emergence of Ungava Peninsula, and its relationship to glacial history. *Can. J. Earth Sci.* 30, 1676–1696.
- Gregoire, L.J., Payne, A.J., Valdes, P.J., 2012. Deglacial rapid sea level rises caused by ice-sheet saddle collapses. *Nature* 487, 219–222.
- Gregoire, L.J., Otto-Bliesner, B., Valdes, P.J., Ivanovic, R., 2016. Abrupt Bølling warming and ice saddle collapse contributions to the Meltwater Pulse 1a rapid sea level rise. *Geophys. Res. Lett.* 43, 9130–9137.
- Hall, B.L., Borns, H.W., Bromley, G.R.M., Lowell, T.V., 2017. Age of the Pineo Ridge System: Implications for behavior of the Laurentide Ice Sheet in eastern Maine, U.S. A., during the last deglaciation. *Quat. Sci. Rev.* 169, 344–356.
- Hallberg, G.R., Kemmis, T.J., 1986. Stratigraphy and correlation of the glacial deposits of the Des Moines and James lobes and adjacent areas in North Dakota, South Dakota, Minnesota, and Iowa. *Quat. Sci. Rev.* 5, 65–68.
- Halsted, C.T., Bierman, P.R., Balco, G., 2021. Empirical evidence for latitude and altitude variation of the in situ cosmogenic  $^{26}\text{Al}/^{10}\text{Be}$  production ratio. *Geosciences* 11, 402.
- Ham, N.R., Attig, J.W., 1996. Ice wastage and landscape evolution along the southern margin of the Laurentide Ice Sheet, north-central Wisconsin. *Boreas* 25, 171–186.
- Hamilton, T.D., 1994. Late Cenozoic Glaciation of Alaska. *Geological Society of America, Boulder, Colorado*.
- Hanson, M.A., Lian, O.B., Clague, J.J., 2012. The sequence and timing of large late Pleistocene floods from glacial Lake Missoula. *Quat. Sci. Rev.* 31, 67–81.
- Hardy, L., 1977. La déglaciation et les épisodes lacustre et marin sur le versant québécois des basses terres de la baie de James. *Géogr. Phys. Quaternaire* 31, 261–273.
- Hargan, K.E., Finkelstein, S.A., Rühland, K.M., Packalen, M.S., Dalton, A.S., Paterson, A.M., Keller, W., Smol, J.P., 2020. Post-glacial lake development and paleoclimate in the central Hudson Bay Lowlands inferred from sediment records. *J. Paleolimnol.* 64, 25–46.
- Harris, K.L., 1998. Computer-assisted lithostratigraphy. In: Patterson, C.J., Wright, H.E.J. (Eds.), *Contributions to Quaternary Studies in Minnesota: Minnesota Geological Survey Report of Investigations*, vol. 49, pp. 179–191.
- Heath, S.L., Loope, H.M., Curry, B.B., Lowell, T.V., 2018. Pattern of southern Laurentide Ice Sheet margin position changes during Heinrich Stadials 2 and 1. *Quat. Sci. Rev.* 201, 362–379.

- Heath, S.L., Lowell, T.V., Hall, B.L., 2020. Surface exposure dating of the Pierre Sublobe of the James Lobe, Laurentide Ice Sheet. *Quat. Res.* 97, 88–98.
- Heaton, T.J., Köhler, P., Butzin, M., Bard, E., Reimer, R.W., Austin, W.E.N., Bronk Ramsey, C., Grootes, P.M., Hughen, K.A., Kromer, B., Reimer, P.J., Adkins, J., Burke, A., Cook, M.S., Olsen, J., Skinner, L.C., 2020. Marine20—The marine radiocarbon age calibration curve (0–55,000 cal BP). *Radiocarbon* 62, 779–820.
- Heintzman, P.D., Froese, D., Ives, J.W., Soares, A.E.R., Zazula, G.D., Letts, B., Andrews, T.D., Driver, J.C., Hall, E., Hare, P.G., Jass, C.N., MacKay, G., Southon, J.R., Stiller, M., Woywitka, R., Suchard, M.A., Shapiro, B., 2016. Bison phylogeography constrains dispersal and viability of the Ice Free Corridor in western Canada. *Proc. Natl. Acad. Sci. USA* 113, 8057–8063.
- Hétu, B., Gray, J., 2000. Les étapes de la déglaciation dans le nord de la Gaspésie (Québec) : les marges glaciaires des dryas ancien et récent. *Géogr. Phys. Quaternaire* 54, 5–40.
- Heyman, J., Stroeven, A.P., Harbor, J.M., Caffee, M.W., 2011. Too young or too old? Evaluating cosmogenic exposure dating based on an analysis of compiled boulder exposure ages. *Earth Planet. Sci. Lett.* 302, 71–80.
- Hodder, T.J., Ross, M., Menzies, J., 2016. Sedimentary record of ice divide migration and ice streams in the Keewatin core region of the Laurentide Ice Sheet. *Sediment. Geol.* 338, 97–114.
- Hodgdon, T., 2016. Developing a Chronology for Thinning of the Laurentide Ice Sheet in New Hampshire during the Last Deglaciation [B.Sc Thesis. Department of Geology, University of New Hampshire, p. 46, 46].
- Hodgson, D.A., 1994. Episodic ice streams and ice shelves during retreat of the northwesternmost sector of the late Wisconsinan Laurentide Ice Sheet over the central Canadian Arctic Archipelago. *Boreas* 23, 14–28.
- Hodgson, D.A., 2003. Surficial Geology, Frobisher Bay, Baffin Island, Nunavut. *Geol. Surv. Can. "A" Series Map 2042A*.
- Hodgson, D.A., 2005. Quaternary geology of western Meta Incognita Peninsula and Iqaluit area, Baffin Island, Nunavut. *Geol. Surv. Can. Bull.* 582, 82.
- Hodgson, D.A., Vincent, J.S., Fyles, J.G., 1984. Quaternary geology of central Melville Island, Northwest Territories. *Geol. Surv. Can. 25. Paper 83-16*.
- Horberg, L., Anderson, R.C., 1956. Bedrock Topography and Pleistocene Glacial Lobes in Central United States. *J. Geol.* 64, 101–116.
- Hughes, O.L., 1987. Late Wisconsinan Laurentide glacial limits of Northwestern Canada: the Tutsieta Lake and Kelly Lake phases. *Geol. Surv. Can. 19. Paper 85-25*.
- Hughes, L., Merry, W.J., 1978. Marquette Buried Forest 9,850 Years Old [conference Abstract]. American Association for the Advancement of Science no. 12-14 February 1978.
- Hughes, A.L.C., Gyllencreutz, R., Lohne, Ø.S., Mangerud, J., Svendsen, J.I., 2016. The last Eurasian ice sheets – a chronological database and time-slice reconstruction, DATED-1. *Boreas* 45, 1–45.
- Huntley, D.J., Godfrey-Smith, D.I., Thewalt, M.L.W., 1985. Optical dating of sediments. *Nature* 313, 105–107.
- Illinois State Geological Survey, 2004. Woodfordian Moraines of Illinois (Vector Digital Data). Illinois State Geological Survey, Champaign, Illinois.
- Ives, J.D., 1957. Glaciation of the Torngat Mountains, Northern Labrador. *Arctic* 10, 67–87.
- Jackson, L., Harrington, C., 1991. Middle Wisconsinan mammals, stratigraphy, and sedimentology at the Ketza River site, Yukon Territory. *Géogr. Phys. Quaternaire* 45, 69–77.
- Jackson, L.E., Phillips, F.M., Shimamura, K., Little, E.C., 1997. Cosmogenic  $^{36}\text{Cl}$  dating of the Foothills Erratics Train, Alberta, Canada. *Geology* 25, 195–198.
- Jenner, K.A., Campbell, D.C., Piper, D.J.W., 2018. Along-slope variations in sediment lithofacies and depositional processes since the Last Glacial Maximum on the northeast Baffin margin, Canada. *Mar. Geol.* 405, 92–107.
- Jetté, H., Mott, R., 1989. Palynostratigraphie du tardiglaciaire et de l'Holocène de la région du lac Chance Harbour, Nouvelle-Écosse. *Géogr. Phys. Quaternaire* 43, 27–38.
- Johnson, M.D., Hemstad, C., 1998. Glacial Lake Grantsburg: A short-lived lake recording the advance and retreat of the Grantsburg sublobe. Contributions to Quaternary studies in Minnesota: Minn. Geol. Surv. Rep. Invest. 49, 49–60.
- Johnson, W.H., Hansel, A.K., Bettis, E.A., Karrow, P.F., Larson, G.J., Lowell, T.V., Schneider, A.F., 1997. Late Quaternary temporal and event classifications, Great Lakes region, North America. *Quat. Res.* 47, 1–12.
- Johnson, M.D., Adams, R.S., Gowen, A.S., Harris, K.L., Hobbs, H.C., Jennings, C.E., Knaebel, A.R., Lusardi, B.A., Meyer, G.N., 2016. Quaternary lithostratigraphic units of Minnesota. Minn. Geol. Surv. Rep. Invest. 68, 262.
- Jones, R.S., Whitehouse, P.L., Bentley, M.J., Small, D., Dalton, A.S., 2019. Impact of glacial isostatic adjustment on cosmogenic surface-exposure dating. *Quat. Sci. Rev.* 212, 206–212.
- Kageyama, M., Valdes, P.J., 2000. Impact of the North American ice-sheet orography on the Last Glacial Maximum eddies and snowfall. *Geophys. Res. Lett.* 27, 1515–1518.
- Karrow, P.F., 1963. Pleistocene Geology of the Hamilton-Galt Area. Ontario Department of Mine Geological Report No. 16, p. 68 (+ maps).
- Karrow, P.F., Dreimanis, A., Barnett, P.J., 2000. A Proposed Diachronic Revision of Late Quaternary Time-Stratigraphic Classification in the Eastern and Northern Great Lakes Area. *Quat. Res.* 54, 1–12.
- Kaufman, D.S., Young, N.E., Briner, J.P., Manley, W.F., 2011. Alaska PaleoGlacier Atlas Version 2. [http://instaar.colorado.edu/groups/QGISL/ak\\_paleoglacier\\_atlas/downloads/index.html](http://instaar.colorado.edu/groups/QGISL/ak_paleoglacier_atlas/downloads/index.html).
- Kemmis, T.J., Hallberg, G.R., Lutenegger, A.J., 1981. Depositional environments of glacial sediments and landforms on the Des Moines Lobe, Iowa. *Iowa Geol. Surv. Guidebook Series No. 6* 132.
- Kennedy, K.E., Froese, D.G., Zazula, G.D., Lauriol, B., 2010. Last Glacial Maximum age for the northwest Laurentide maximum from the Eagle River spillway and delta complex, northern Yukon. *Quat. Sci. Rev.* 29, 1288–1300.
- King, L.H., 1996. Late Wisconsinan ice retreat from the Scotian Shelf. *Geol. Soc. Am. Bull.* 108, 1056–1067.
- King, E.L., 2015. Late glaciation in the eastern Beaufort Sea: contrasts in shallow depositional styles from Amundsen Gulf, Banks Island Shelf and M'Clure Strait, ArcticNet. In: 2015 Annual Scientific Meeting: Oral Presentation Abstracts, Vancouver, Canada.
- King, E.L., Lakeman, T.R., Blasco, S., 2014. The Shallow Geologic Framework of the Banks Island Shelf, Eastern Beaufort Sea: Evidence for Glaciation of the Entire Shelf and Multiple Shelf Edge Geohazards [abstract], Arctic Change 2014 (Ottawa, Canada).
- Kleman, J., Hätteström, C., 1999. Frozen-bed Fennoscandian and Laurentide ice sheets during the Last Glacial Maximum. *Nature* 402, 63–66.
- Kleman, J., Marchant, D., Borgström, I., 2001. Geomorphic evidence for late glacial ice dynamics on southern Baffin Island and in outer Hudson Strait, Nunavut, Canada. *Arctic Antarct. Alpine Res.* 33, 249–257.
- Kleman, J., Jansson, K., De Angelis, H., Stroeven, A.P., Hätteström, C., Alm, G., Glasser, N., 2010. North American Ice Sheet build-up during the last glacial cycle, 115–21kyr. *Quat. Sci. Rev.* 29, 2036–2051.
- Koester, A.J., Shakun, J.D., Bierman, P.R., Davis, P.T., Corbett, L.B., Braun, D., Zimmerman, S.R., 2017. Rapid thinning of the Laurentide Ice Sheet in coastal Maine, USA, during late Heinrich Stadial 1. *Quat. Sci. Rev.* 163, 180–192.
- Korschinek, G., Bergmaier, A., Faestermann, T., Gerstmann, U.C., Knie, K., Rugel, G., Wallner, A., Dillmann, I., Dollinger, G., von Gostomski, C.L., Kossert, K., Maiti, M., Poutivtsev, M., Remmert, A., 2010. A new value for the half-life of  $^{10}\text{Be}$  by Heavy-Ion Elastic Recoil Detection and liquid scintillation counting. *Nucl. Instrum. Methods Phys. Res. Sect. B Beam Interact. Mater. Atoms* 268, 187–191.
- Lacelle, D., Lauriol, B., Zazula, G., Ghaleb, B., Utting, N., Clark, I.D., 2013. Timing of advance and basal condition of the Laurentide Ice Sheet during the last glacial maximum in the Richardson Mountains, NWT. *Quat. Res.* 80, 274–283.
- Lacourse, T., Beer, K.W., Craig, K.B., Canil, D., 2019. Postglacial wetland succession, carbon accumulation, and forest dynamics on the east coast of Vancouver Island, British Columbia, Canada. *Quat. Res.* 92, 232–245.
- Lajeunesse, P., 2008. Early Holocene deglaciation of the eastern coast of Hudson Bay. *Geomorphology* 99, 341–352.
- Lakeman, T.R., England, J.H., 2012. Paleoglaciological insights from the age and morphology of the Jesse moraine belt, western Canadian Arctic. *Quat. Sci. Rev.* 47, 82–100.
- Lakeman, T.R., England, J.H., 2013. Late Wisconsinan glaciation and postglacial relative sea-level change on western Banks Island, Canadian Arctic Archipelago. *Quat. Res.* 80, 99–112.
- Lal, D., 1991. Cosmic ray labeling of erosion surfaces: *in situ* nuclide production rates and erosion models. *Earth Planet. Sci. Lett.* 104, 424–439.
- Lambeck, K., Purcell, A., Zhao, S., 2017. The North American Late Wisconsin ice sheet and mantle viscosity from glacial rebound analyses. *Quat. Sci. Rev.* 158, 172–210.
- Larsen, N.K., Funder, S., Kjær, K.H., Kjeldsen, K.K., Knudsen, M.F., Linge, H., 2014. Rapid early Holocene ice retreat in West Greenland. *Quat. Sci. Rev.* 92, 310–323.
- Laskar, J., Robutel, P., Joutel, F., Gastineau, M., Correia, A.C.M., Levrard, B., 2004. A long-term numerical solution for the insolation quantities of the Earth. *Astron. Astrophys.* 428, 261–285.
- Lauriol, B., Gray, J.T., 1987. The decay and disappearance of the Late Wisconsin Ice Sheet in the Ungava Peninsula, Northern Quebec, Canada. *Arct. Alp. Res.* 19, 109–126.
- Haymon, C.A., 1991. Marine episodes in Hudson Strait and Hudson Bay, Canada, during the Wisconsin Glaciation. *Quat. Res.* 35, 53–62.
- Leger, T.P.M., Clark, C.D., Huynh, C., Jones, S., Ely, J.C., Bradley, S.L., Diemont, C., Hughes, A.L.C., 2023. A Greenland-wide empirical reconstruction of paleo ice-sheet retreat informed by ice extent markers: PaleoGrIS version 1.0. *Clim. Past Discuss* 2023, 1–97.
- Lesnek, A.J., Briner, J.P., Lindqvist, C., Baichtal, J.F., Heaton, T.H., 2018. Deglaciation of the Pacific coastal corridor directly preceded the human colonization of the Americas. *Sci. Adv.* 4 eaar5040.
- Lesnek, A.J., Briner, J.P., Baichtal, J.F., Lyles, A.S., 2020a. New constraints on the last deglaciation of the Cordilleran Ice Sheet in coastal Southeast Alaska. *Quat. Res.* 1–21.
- Lesnek, A.J., Briner, J.P., Baichtal, J.F., Lyles, A.S., 2020b. New constraints on the last deglaciation of the Cordilleran Ice Sheet in coastal Southeast Alaska. *Quat. Res.* 96, 140–160.
- Leverett, F., 1902. Glacial formations and drainage features of the Erie and Ohio basins. *United States Geol. Surv. Monograph* 41.
- Levesque, A.J., Mayle, F.E., Walker, I.R., Cwynar, L.C., 1993. A previously unrecognized late-glacial cold event in eastern North America. *Nature* 361, 623–626.
- Li, G., Piper, D.J.W., Campbell, D.C., 2011. The Quaternary Lancaster Sound trough-mouth fan, NW Baffin Bay. *J. Quat. Sci.* 26, 511–522.
- Lifton, N., Sato, T., Dunai, T.J., 2014. Scaling *in situ* cosmogenic nuclide production rates using analytical approximations to atmospheric cosmic-ray fluxes. *Earth Planet. Sci. Lett.* 386, 149–160.
- Lin, Y., Hibbert, F.D., Whitehouse, P.L., Woodroffe, S.A., Purcell, A., Shennan, I., Bradley, S.L., 2021. A reconciled solution of Meltwater Pulse 1A sources using sea-level fingerprinting. *Nat. Commun.* 12, 2015.
- Loope, H.M., Antinao, J.L., Lowell, T.V., Curry, B.B., Monaghan, G.W., 2018a. Chronology of Laurentide Ice Sheet Fluctuations Surrounding the Last Glacial Maximum, Central Indiana, USA. *Geological Society of America 130th Annual Meeting*, Indianapolis, Indiana.

- Loope, H.M., Antinao, J.L., Monaghan, G.W., Autio, R.J., Curry, B.B., Grimley, D.A., Huot, S., Lowell, T.V., Nash, T.A., 2018b. At the edge of the Laurentide Ice Sheet: Stratigraphy and chronology of glacial deposits in central Indiana. In: Florea, L.J. (Ed.), Ancient Oceans, Orogenic Uplifts, and Glacial Ice: Geologic Crossroads in America's Heartland, vol. 51. Geological Society of America Field Guide, pp. 245–258.
- Lowdon, J.A., Robertson, I.M., Blake, W.J., 1971. Geol. Surv. Can Radiocarbon Dates XI. Radiocarbon 13, 255–324.
- Lowell, T.V., Larson, G.J., Hughes, J.D., Denton, G.H., 1999. Age verification of the Lake Gribbin forest bed and the Younger Dryas Advance of the Laurentide Ice Sheet. Can. J. Earth Sci. 36, 383–393.
- Lowell, T.V., Kelly, M.A., Howley, J.A., Fisher, T.G., Barnett, P.J., Schwartz, R., Zimmerman, S.R.H., Norris, N., Malone, A.G.O., 2021. Near-constant retreat rate of a terrestrial margin of the Laurentide Ice Sheet during the last deglaciation. Geology 49, 1511–1515.
- Lusardi, B.A., Jennings, C.E., Harris, K.L., 2011. Provenance of Des Moines lobe till records ice-stream catchment evolution during Laurentide deglaciation. Boreas 40, 585–597.
- MacLean, B., Blasco, S., Bennett, R., Lakeman, T., Hughes-Clarke, J., Kuus, P., Patton, E., 2015. New marine evidence for a Late Wisconsinan ice stream in Amundsen Gulf, Arctic Canada. Quat. Sci. Rev. 114, 149–166.
- MacLean, B., Blasco, S., Bennett, R., Lakeman, T., Pieńkowski, A.J., Furze, M.F.A., Hughes Clarke, J., Patton, E., 2017. Seafloor features delineate Late Wisconsinan ice stream configurations in eastern Parry Channel, Canadian Arctic Archipelago. Quat. Sci. Rev. 160, 67–84.
- Manabe, S., Broccoli, A.J., 1985. A Comparison of Climate Model Sensitivity with Data from the Last Glacial Maximum. J. Atmos. Sci. 42, 2643–2651.
- Mann, D.H., Petet, D.M., 1994. Extent and timing of the Last Glacial Maximum in Southwestern Alaska. Quat. Res. 42, 136–148.
- Marcott, S.A., Clark, P.U., Shakun, J.D., Brook, E.J., Davis, P.T., Caffee, M.W., 2019.  $^{10}\text{Be}$  age constraints on latest Pleistocene and Holocene cirque glaciation across the western United States. Clim. Atmos. Sci. 2, 5.
- Margold, M., Jansson, K.N., Kleman, J., Stroeve, A.P., 2011. Glacial meltwater landforms of central British Columbia. J. Maps 7, 486–506.
- Margold, M., Jansson, K.N., Kleman, J., Stroeve, A.P., Clague, J.J., 2013. Retreat pattern of the Cordilleran Ice Sheet in central British Columbia at the end of the last glaciation reconstructed from glacial meltwater landforms. Boreas 42, 830–847.
- Margold, M., Stroeve, A.P., Clague, J.J., Heyman, J., 2014. Timing of terminal Pleistocene deglaciation at high elevations in southern and central British Columbia constrained by  $^{10}\text{Be}$  exposure dating. Quat. Sci. Rev. 99, 193–202.
- Margold, M., Stokes, C.R., Clark, C.D., 2015a. Ice streams in the Laurentide Ice Sheet: Identification, characteristics and comparison to modern ice sheets. Earth Sci. Rev. 143, 117–146.
- Margold, M., Stokes, C.R., Clark, C.D., 2015b. Ice streams in the Laurentide Ice Sheet: a new mapping inventory. J. Maps 11, 380–395.
- Margold, M., Stokes, C.R., Clark, C.D., 2018. Reconciling records of ice streaming and ice margin retreat to produce a palaeogeographic reconstruction of the deglaciation of the Laurentide Ice Sheet. Quat. Sci. Rev. 189, 1–30.
- Margold, M., Gosse, J.C., Hidy, A.J., Woywitka, R.J., Young, J.M., Froese, D., 2019. Beryllium-10 dating of the Foothills Erratics Train in Alberta, Canada, indicates detachment of the Laurentide Ice Sheet from the Rocky Mountains at ~15 ka. Quat. Res. 92, 469–482.
- Margreth, A., Gosse, J.C., Dyke, A.S., 2016. Quantification of subaerial and episodic subglacial erosion rates on high latitude upland plateaus: Cumberland Peninsula, Baffin Island, Arctic Canada. Quat. Sci. Rev. 133, 108–129.
- Margreth, A., Gosse, J.C., Dyke, A.S., 2017. Wisconsinan and early Holocene glacial dynamics of Cumberland Peninsula, Baffin Island, Arctic Canada. Quat. Sci. Rev. 168, 79–100.
- Marrero, S.M., Phillips, F.M., Borchers, B., Lifton, N., Aumer, R., Balco, G., 2016. Cosmogenic nuclide systematics and the CRONUScalc program. Quat. Geochronol. 31, 160–187.
- Martin, J.E., Sawyer, J.F., Fahrenbach, M.D., Tomhave, D.W., Schulz, L.D., 2004. Geologic map of South Dakota. South Dakota Geological Survey. Scale, 1:500,000.
- Martinson, D.G., Pisias, N.G., Hays, J.D., Imbrie, J., Moore, T.C., Shackleton, N.J., 1987. Age Dating and the orbital theory of the Ice Ages: Development of a high-resolution 0 to 300,000-year chronostratigraphy. Quat. Res. 27, 1–29.
- Matero, I.S.O., Gregoire, L.J., Ivanovic, R.F., Tindall, J.C., Haywood, A.M., 2017. The 8.2 ka cooling event caused by Laurentide ice saddle collapse. Earth Planet. Sci. Lett. 473, 205–214.
- Mathewes, R.W., Clague, J.J., 2017. Paleoecology and ice limits of the early Fraser Glaciation (Marine Isotope Stage 2) on Haida Gwaii, British Columbia, Canada. Quat. Res. 88, 277–292.
- McCarthy, D.P., Luckman, B.H., 1993. Estimating Ecesis for Tree-Ring Dating of Moraines: A Comparative Study from the Canadian Cordillera. Arct. Alp. Res. 25, 63–68.
- McMartin, I., Henderson, P.J., 2004. Evidence from Keewatin (Central Nunavut) for paleo-ice divide migration. Géogr. Phys. Quaternaire 58, 163–186.
- McMartin, I., Campbell, J.E., Dredge, L.A., Robertson, L., 2012. Surficial Geology Map Compilation of the TGI-3 Flin Flon Project Area, Manitoba and Saskatchewan. Geol. Surv. Can Open File 7089.
- McMartin, I., Campbell, J.E., Dredge, L.A., 2013. Pre-Late Wisconsinan Shells in Rae Isthmus Ice Stream Tills: Implications for LIS Dynamics and Deglaciation of Northwestern Hudson Bay. CANQUA-CGRG biannual meeting, Edmonton, Alberta.
- McMartin, I., Campbell, J.E., Dredge, L.A., LeCheminant, A.N., McCurdy, M.W., Scromeda, N., 2015. Quaternary Geology and till Composition North of Wager Bay, Nunavut: Results from the GEM Wager Bay Surficial Geology Project. Geol. Surv. Can Open File 7748.
- McMartin, I., Godbout, P.M., Campbell, J.E., Tremblay, T., Behnia, P., 2020. A New Map of Glaciogenic Features and Glacial Landsystems in Central Mainland Nunavut, Canada. Boreas 50, 51–75.
- McMartin, I., Godbout, P.-M., Campbell, J.E., Tremblay, T., Behnia, P., 2021. A new map of glaciogenic features and glacial landsystems in central mainland Nunavut, Canada. Boreas 50, 51–75.
- McQuinn, M., 1996. Refined Late Wisconsin Chronostratigraphy of Indiana Using In-Situ Cosmogenic Radionuclides  $^{10}\text{Be}$  and  $^{26}\text{Al}$  [M.Sc Thesis. Purdue University, Indiana, United States.
- Menounos, B., Goehring, B.M., Osborn, G., Margold, M., Ward, B., Bond, J., Clarke, G.K.C., Clague, J.J., Lakeman, T., Koch, J., Caffee, M.W., Gosse, J., Stroeve, A.P., Seguinot, J., Heyman, J., 2017. Cordilleran Ice Sheet mass loss preceded climate reversals near the Pleistocene Termination. Science 358, 781–784.
- Mickelson, D.M., Attig, J.W., 2017. Laurentide Ice Sheet: ice-margin positions in Wisconsin. Wisconsin Geological and Natural History Survey Educational Series 56, 46.
- Miles, B.W.J., Jordan, J.R., Stokes, C.R., Jamieson, S.S.R., Gudmundsson, G.H., Jenkins, A., 2021. Recent acceleration of Denman Glacier (1972–2017), East Antarctica, driven by grounding line retreat and changes in ice tongue configuration. Cryosphere 15, 663–676.
- Mott, R.J., Stea, R.R., 1994. Late-glacial (Allerød/Younger Dryas) buried organic deposits, Nova Scotia, Canada: A contribution to the 'North Atlantic seaboard programme' of IGCP-253, 'Termination of the Pleistocene'. Quat. Sci. Rev. 12, 645–657.
- Mott, R.J., Grant, D.R., Stea, R., Occhietti, S., 1986. Late-glacial climatic oscillation in Atlantic Canada equivalent to the Allerød/younger Dryas event. Nature 323, 247–250.
- Mulligan, R.P.M., Bajc, A.F., Eyles, C.H., 2018. Drumlinized tunnel valleys in south-central Ontario. Quat. Sci. Rev. 197, 49–74.
- Munyikwa, K., Feathers, J.K., Rittenour, T.M., Shrimpton, H.K., 2011. Constraining the Late Wisconsinan retreat of the Laurentide ice sheet from western Canada using luminescence ages from postglacial aeolian dunes. Quat. Geochronol. 6, 407–422.
- Munyikwa, K., Rittenour, T.M., Feathers, J.K., 2017. Temporal constraints for the Late Wisconsinan deglaciation of western Canada using eolian dune luminescence chronologies from Alberta. Palaeogeogr. Palaeoclimatol. Palaeoecol. 470, 147–165.
- Murton, J.B., Frechen, M., Maddy, D., 2007. Luminescence dating of mid- to Late Wisconsinan aeolian sand as a constraint on the last advance of the Laurentide Ice Sheet across the Tuktoyaktuk Coastlands, western Arctic Canada. Can. J. Earth Sci. 44, 857–869.
- Murton, D.K., Bateman, M.D., Waller, R.I., Whiteman, C.A., 2015. Late Wisconsin Glaciation of Hadwen and Summer Islands, Tuktoyaktuk Coastlands, NWT, Canada. GEO Quebec: Challenges from North to South.
- Natural Earth, 2021. Glaciated Areas v.4.0.0 available: <https://www.naturalearthdata.com/downloads/10m-physical-vectors/10m-glaciated-areas/>. (Accessed 6 April 2021).
- Naughton, D., Harrington, C.R., Dalby, A., Rose, M., Dawson, J., 2003. Annotated Bibliography of Quaternary Vertebrates of Northern North America. University of Toronto Press.
- Nishiizumi, K., 2004. Preparation of  $^{26}\text{Al}$  AMS standards. Nucl. Instrum. Methods Phys. Res. Sect. B Beam Interact. Mater. Atoms 223–224, 388–392.
- Nishiizumi, K., Winterer, E.L., Kohl, C.P., Klein, J., Middleton, R., Lal, D., Arnold, J.R., 1989. Cosmic ray production rates of  $^{10}\text{Be}$  and  $^{26}\text{Al}$  in quartz from glacially polished rocks. J. Geophys. Res. Solid Earth 94, 17907–17915.
- Nixon, F.C., England, J.H., 2014. Expanded Late Wisconsinan ice cap and ice sheet margins in the western Queen Elizabeth Islands, Arctic Canada. Quat. Sci. Rev. 91, 146–164.
- Norris, S.L., Margold, M., Froese, D.G., 2017. Glacial landforms of northwest Saskatchewan. J. Maps 13, 600–607.
- Norris, S.L., Garcia-Castellanos, D., Jansen, J.D., Carling, P.A., Margold, M., Woywitka, R.J., Froese, D.G., 2021. Catastrophic drainage from the northwestern outlet of glacial Lake Agassiz during the Younger Dryas. Geophys. Res. Lett. 48, e2021GL093919.
- Norris, S.L., Tarasov, L., Monteath, A.J., Gosse, J., Hidy, A.J., Margold, M., Froese, D., 2022. Rapid retreat of the southwestern Laurentide Ice Sheet driven by Bølling-Allerød warming. Geology 50, 417–421.
- Ó Coifáigh, C., England, J., Zreda, M., 2000. Late Wisconsinan glaciation of southern Eureka Sound: evidence for extensive Innuitian ice in the Canadian High Arctic during the Last Glacial Maximum. Quat. Sci. Rev. 19, 1319–1341.
- O'Regan, M., Coxall, H., Hill, P., Hilton, R., Muschitiello, F., Swärd, H., 2018. Early Holocene sea level in the Canadian Beaufort Sea constrained by radiocarbon dates from a deep borehole in the Mackenzie Trough, Arctic Canada. Boreas 47, 1102–1117.
- Occhietti, S., 1980. Le Quaternaire de la région de Trois-Rivières-Shawinigan, Québec: contribution à la paléographie de la vallée moyenne du Saint-Laurent et corrélations stratigraphiques. Paléo-Québec 10, 227.
- Occhietti, S., Richard, P., 2003. Effet réservoir sur les âges  $^{14}\text{C}$  de la Mer de Champlain à la transition Pléistocène-Holocène : révision de la chronologie de la déglaciation au Québec méridional. Géogr. Phys. Quaternaire 57, 115–138.
- Occhietti, S., Parent, M., Lajeunesse, P., Robert, F., Govare, É., 2011. Late Pleistocene-Early Holocene decay of the Laurentide Ice Sheet in Québec-Labrador. In: van der Meer, J. (Ed.), Developments in Quaternary Science, pp. 601–630.
- Orlemans, J., 2005. Extracting a Climate Signal from 169 Glacier Records. Science 308, 675–677.

- Parent, M., Occhietti, S., 1999. Late Wisconsinan deglaciation and glacial lake development in the Appalachians of southeastern Québec. *Géogr. Phys. Quaternaire* 53, 117–135.
- Patterson, C.J., 1997a. Southern Laurentide ice lobes were created by ice streams: Des Moines Lobe in Minnesota, USA. *Sediment. Geol.* 111, 249–261.
- Patterson, C.J., 1997b. Surficial geology of southwestern Minnesota. In: Patterson, C.J. (Ed.), Contributions to the Quaternary Geology of Southwestern Minnesota: Minnesota Geological Survey Report of Investigations, vol. 47, p. 45.
- Paulen, R.C., 2001. Quaternary Geology of the Timmins Area, Northeastern Ontario [MSc Thesis]. University of Waterloo, p. 449.
- Pedersen, M.W., Ruter, A., Schweger, C., Friebe, H., Staff, R.A., Kjeldsen, K.K., Mendoza, M.L., Beaudoin, A.B., Zutter, C., Larsen, N.K., Potter, B.A., Nielsen, R., Rainville, R.A., Orlando, L., Meltzer, D.J., Kjaer, K.H., Willerslev, E., 2016. Postglacial viability and colonization in North America's ice-free corridor. *Nature* 537, 45–49.
- Peltier, W.R., Fairbanks, R.G., 2006. Global glacial ice volume and Last Glacial Maximum duration from an extended Barbados sea level record. *Quat. Sci. Rev.* 25, 3322–3337.
- Peltier, W.R., Argus, D.F., Drummond, R., 2015. Space geodesy constrains ice age terminal deglaciation: The global ICE-6G\_C (VM5a) model. *J. Geophys. Res. Solid Earth* 120, 450–487.
- Phillips, F.M., Leavy, B.D., Jannik, N.O., Elmore, D., Kubik, P.W., 1986. The accumulation of cosmogenic Chlorine-36 in rocks: a method for surface exposure dating. *Science* 231, 41–43.
- Pieńkowski, A.J., England, J.H., Furze, M.F.A., MacLean, B., Blasco, S., 2014. The late Quaternary environmental evolution of marine Arctic Canada: Barrow Strait to Lancaster Sound. *Quat. Sci. Rev.* 91, 184–203.
- Pieńkowski, A.J., Coulthard, R.D., Furze, M.F.A., 2022. Revised marine reservoir offset ( $\Delta R$ ) values for molluscs and marine mammals from Arctic North America. *Boreas*. <https://doi.org/10.1111/bor.12606>.
- Plug, L.J., Gosse, J.C., McIntosh, J.J., Bigley, R., 2007. Attenuation of cosmic ray flux in temperate forest. *J. Geophys. Res.: Earth Surf.* 112, F02022.
- Porter, S.C., Swanson, T.W., 1998. Radiocarbon age constraints on rates of advance and retreat of the Puget Lobe of the Cordilleran Ice Sheet during the last glaciation. *Quat. Res.* 50, 205–213.
- Potter, B.A., Baichtal, J.F., Beaudoin, A.B., Fehren-Schmitz, L., Haynes, C.V., Holliday, V.T., Holmes, C.E., Ives, J.W., Kelly, R.L., Llamas, B., Malhi, R.S., Miller, D.S., Reich, D., Reuther, J.D., Schiffels, S., Sturovell, T.A., 2018. Current evidence allows multiple models for the peopling of the Americas. *Sci. Adv.* 4, eaat5473.
- Prest, V.K., 1969. Retreat of Wisconsin and Recent Ice in North America. *Geol. Surv. Can. Map*, 1257A scale 1:5,000,000.
- Prest, V.K., Grant, D.R., Rampton, V.N., 1968. Glacial Map of Canada: Geol. Surv. Can. "A" Series Map 1253A, 1968, 1 sheet.
- Rampton, V.N., 1988. Quaternary Geology of the Tuktoyaktuk Coastlands, Northwest Territories. *Geol. Surv. Can. Map* 423, 98.
- Rasmussen, S.O., Bigler, M., Blockley, S.P., Blunier, T., Buchardt, S.L., Clausen, H.B., Cvijanovic, I., Dahl-Jensen, D., Johnsen, S.J., Fischer, H., Gkinis, V., Guillemin, M., Hoek, W.Z., Lowe, J.J., Pedro, J.B., Popp, T., Seierstad, I.K., Steffensen, J.P., Svensson, A.M., Valelonga, P., Vinther, B.M., Walker, M.J.C., Wheatley, J.J., Winstrup, M., 2014. A stratigraphic framework for abrupt climatic changes during the Last Glacial period based on three synchronized Greenland ice-core records: refining and extending the INTIMATE event stratigraphy. *Quat. Sci. Rev.* 106, 14–28.
- Reimer, P.J., 2021. Evolution of radiocarbon calibration. *Radiocarbon* 64, 523–539.
- Reimer, P.J., Austin, W.E.N., Bard, E., Bayliss, A., Blackwell, P.G., Bronk Ramsey, C., Butzin, M., Cheng, H., Edwards, R.L., Friedrich, M., Grootes, P.M., Guilderson, T.P., Hajdas, I., Heaton, T.J., Hogg, A.G., Hughen, K.A., Kromer, B., Manning, S.W., Muscheler, R., Palmer, J.G., Pearson, C., van der Plicht, J., Reimer, R.W., Richards, D.A., Scott, E.M., Southon, J.R., Turney, C.S.M., Wacker, L., Adolphi, F., Büntgen, U., Capino, M., Fahri, S.M., Fothmann-Schulz, A., Friedrich, R., Köhler, P., Kudsk, S., Miyake, F., Olsen, J., Reining, F., Sakamoto, M., Sookdeo, A., Talamo, S., 2020. The IntCal20 Northern Hemisphere radiocarbon age calibration curve (0–55 cal kBP). *Radiocarbon* 62, 725–757.
- Reyes, A.V., Carlson, A.E., Milne, G.A., Tarasov, L., Reimink, J.R., Caffee, M.W., 2022. Revised chronology of northwest Laurentide ice-sheet deglaciation from  $^{10}\text{Be}$  exposure ages on boulder erratics. *Quat. Sci. Rev.* 277, 107369.
- Rice, J.M., Ross, M., Paulen, R.C., Kelley, S.E., Briner, J.P., Neudorf, C.M., Lian, O.B., 2019. Refining the ice flow chronology and subglacial dynamics across the migrating Labrador Divide of the Laurentide Ice Sheet with age constraints on deglaciation. *J. Quat. Sci.* 34, 519–535.
- Richard, P., Labelle, C., 1989. Histoire postglaciaire de la végétation au lac du Diable, mont Albert, Gaspésie, Québec. *Géogr. Phys. Quaternaire* 43, 337–354.
- Richard, P.J.H., Occhietti, S., 2005.  $^{14}\text{C}$  chronology for ice retreat and inception of Champlain Sea in the St Lawrence Lowlands, Canada. *Quat. Res.* 63, 353–358.
- Ridge, J.C., Evenson, E.B., Sevon, W.D., 1992. A model of late Quaternary landscape development in the Delaware Valley, New Jersey and Pennsylvania. *Geomorphology* 4, 319–345.
- Ridge, J.C., Balco, G., Bayless, R.L., Beck, C.C., Carter, L.B., Dean, J.L., Voytek, E.B., Wei, J.H., 2012. The new North American Varve Chronology: A precise record of southeastern Laurentide Ice Sheet deglaciation and climate, 18.2–12.5 kyr BP, and correlations with Greenland ice core records. *Am. J. Sci.* 312, 685–722.
- Riedel, J.L., 2017. Deglaciation of the North Cascade Range, Washington and British Columbia, from the Last Glacial Maximum to the Holocene. *Cuadernos de Investigación Geográfica* 43, 467–496.
- Riedel, J.L., Clague, J.J., Ward, B.C., 2010. Timing and extent of early marine oxygen isotope stage 2 alpine glaciation in Skagit Valley, Washington. *Quat. Res.* 73, 313–323.
- Roger, J., Saint-Ange, F., Lajeunesse, P., Duchesne, M.J., St-Onge, G., 2013. Late Quaternary glacial history and meltwater discharges along the Northeastern Newfoundland Shelf. *Can. J. Earth Sci.* 50, 1178–1194.
- Ross, M., Campbell, J.E., Parent, M., Adams, R.S., 2009. Palaeo-ice streams and the subglacial landscape mosaic of the North American mid-continental prairies. *Boreas* 38, 421–439.
- Roy, M., Dell'oste, F., Veillette, J.J., de Vernal, A., Hélie, J.F., Parent, M., 2011. Insights on the events surrounding the final drainage of Lake Ojibway based on James Bay stratigraphic sequences. *Quat. Sci. Rev.* 30, 682–692.
- Roy, M., Veillette, J.J., Daubois, V., Ménard, M., 2015. Late-stage phases of glacial Lake Ojibway in the central Abitibi region, eastern Canada. *Geomorphology* 248, 14–23.
- Ruhe, R.V., 1952. Topographic discontinuities of the Des Moines Lobe. *Am. J. Sci.* 250, 46–56.
- Ruhe, R.V., 1969. Quaternary Landscapes in Iowa. Iowa State University Press, Ames, 537.
- Schaefgen, J.M., Denton, G.H., Kaplan, M., Putnam, A., Finkel, R.C., Barrell, D.J.A., Andersen, B.G., Schwartz, R., Mackintosh, A., Chinn, T., Schlüchter, C., 2009. High-Frequency Holocene glacier fluctuations in New Zealand differ from the Northern Signature. *Science* 324, 622–625.
- Schaetzl, R.J., Weisenborn, B.N., 2004. The Grayling Fingers region of Michigan: soils, sedimentology, stratigraphy and geomorphic development. *Geomorphology* 61, 251–274.
- Schaetzl, R.J., Lepper, K., Thomas, S.E., Grove, L., Treiber, E., Farmer, A., Fillmore, A., Lee, J., Dickerson, B., Alme, K., 2017. Kame deltas provide evidence for a new glacial lake and suggest early glacial retreat from central Lower Michigan, USA. *Geomorphology* 280, 167–178.
- Schildgen, T.F., Phillips, W.M., Purves, R.S., 2005. Simulation of snow shielding corrections for cosmogenic nuclide surface exposure studies. *Geomorphology* 64, 67–85.
- Schlee, J., 1973. Atlantic Continental Shelf and Slope of the United States - Sediment Texture of the Northeastern Part. United States Geological Survey Professional Paper 529L, p. 64.
- Schnitker, D., Belknap, D.F., Bacchus, T.S., Fries, J.K., Lusardi, B.A., Popek, D.M., Weddle, T.K., Retelle, M.J., 2001. Deglaciation of the Gulf of Maine. In: Weddle, T., Retelle, M. (Eds.), *Deglaciation History and Relative Sea-Level Changes, Northern New England and Adjacent Canada*. Geological Society of America.
- Seierstad, I.K., Abbott, P.M., Bigler, M., Blunier, T., Bourne, A.J., Brook, E., Buchardt, S.L., Buzert, C., Clausen, H.B., Cook, E., Dahl-Jensen, D., Davies, S.M., Guillemin, M., Johnsen, S.J., Pedersen, D.S., Popp, T.J., Rasmussen, S.O., Severinghaus, J.P., Svensson, A., Vinther, B.M., 2014. Consistently dated records from the Greenland GRIP, GISP2 and NGRIP ice cores for the past 104 ka reveal regional millennial-scale 818O gradients with possible Heinrich event imprint. *Quat. Sci. Rev.* 106, 29–46.
- Shaw, J., Piper, D.J.W., Fader, G.B.J., King, E.L., Todd, B.J., Bell, T., Batterson, M.J., Liverman, D.G.E., 2006. A conceptual model of the deglaciation of Atlantic Canada. *Quat. Sci. Rev.* 25, 2059–2081.
- Shaw, J., Barrie, J.V., Conway, K.W., Lintern, D.G., Kung, R., 2020. Glaciation of the northern British Columbia continental shelf: the geomorphic evidence derived from multibeam bathymetric data. *Boreas* 49, 17–37.
- Shephard, A., Ivins, E., Rignot, E., Smith, B., van den Broeke, M., Velicogna, I., Whitehouse, P., Briggs, K., Joughin, I., Krinner, G., Nowicki, S., Payne, T., Scambos, T., Schlegel, N., Agosta, C., Ahlstrom, A., Babonis, G., Barletta, V.R., Björk, A.A., Blazquez, A., Bonin, J., Colgan, W., Csatho, B., Cullather, R., Engdahl, M.E., Felikson, D., Fettweis, X., Forsberg, R., Hogg, A.E., Galley, H., Gardner, A., Gilbert, L., Gourmelen, N., Groh, A., Gunter, B., Hanna, E., Harig, C., Helm, V., Horvath, A., Horwath, M., Khan, S., Kjeldsen, K.K., Konrad, H., Langen, P.L., Lecavalier, B., Loomis, B., Luthcke, S., McMillan, M., Melini, D., Mernild, S., Mohajerani, Y., Moore, P., Mottram, R., Mouginot, J., Moyano, G., Muir, A., Nagler, T., Nield, G., Nilsson, J., Noël, B., Otosaka, I., Pattle, M.E., Peltier, W.R., Pie, N., Riethbroek, R., Rott, H., Sandberg Sørensen, L., Sasgen, I., Save, H., Scheuchl, B., Schrama, E., Schröder, L., Seo, K.-W., Simonsen, S.B., Slater, T., Spada, G., Sutterley, T., Talpe, M., Tarasov, L., van de Berg, W.J., van der Wal, W., van Wessem, M., Vishwakarma, B.D., Wiese, D., Wilton, D., Wagner, T., Wouters, B., Wuite, J., The Imbie Team, 2020. Mass balance of the Greenland Ice Sheet from 1992 to 2018. *Nature* 579, 233–239.
- Sinclair, G., Carlson, A.E., Mix, A.C., Lecavalier, B.S., Milne, G., Mathias, A., Buzert, C., DeConto, R., 2016. Diachronous retreat of the Greenland ice sheet during the last deglaciation. *Quat. Sci. Rev.* 145, 243–258.
- Slater, T., Lawrence, I.R., Otosaka, I.N., Shepherd, A., Gourmelen, N., Jakob, L., Tapete, P., Gilbert, L., Nienow, P., 2021. Earth's ice imbalance. *Cryosphere* 15, 233–246.
- Small, D., Clark, C.D., Chiverrell, R.C., Smedley, R.K., Bateman, M.D., Duller, G.A.T., Ely, J.C., Fabel, D., Medialdea, A., Moreton, S.G., 2017. Devising quality assurance procedures for assessment of legacy geochronological data relating to deglaciation of the last British-Irish Ice Sheet. *Earth Sci. Rev.* 164, 232–250.
- Small, D., Bentley, M.J., Jones, R.S., Pittard, M.L., Whitehouse, P.L., 2019. Antarctic ice sheet palaeo-thinning rates from vertical transects of cosmogenic exposure ages. *Quat. Sci. Rev.* 206, 65–80.
- Smith, D.G., 1992. Glacial Lake Mackenzie, Mackenzie Valley, Northwest Territories, Canada. *Can. J. Earth Sci.* 29, 1756–1766.
- Smith, I.R., 2000. Diamictitic sediments within high Arctic lake sediment cores: evidence for lake ice rafting along the lateral glacial margin. *Sedimentology* 47, 1157–1179.
- Spratt, R.M., Lisiecki, L.E., 2016. A Late Pleistocene sea level stack. *Clim. Past* 12, 1079–1092.
- Staiger, J.K.W., Gosse, J.C., Johnson, J.V., Fastook, J., Gray, J.T., Stockli, D.F., Stockli, L., Finkel, R., 2005. Quaternary relief generation by polythermal glacier ice. *Earth Surf. Process. Landforms* 30, 1145–1159.

- Staiger, J., Gosse, J., Toracinta, R., Oglesby, B., Fastook, J., Johnson, J.V., 2007. Atmospheric scaling of cosmogenic nuclide production: Climate effect. *J. Geophys. Res. Solid Earth* 112.
- Stalker, A.M., 1962. *Surficial Geology, Lethbridge (East Half)*, Alberta. Geol. Surv. Can Map, pp. 41–1962.
- Stanford, S.D., 1993. Late Wisconsinan glacial geology of the New Jersey Highlands. *Northeast. Geol.* 15, 210–223.
- Stanford, S.D., Stone, B.D., Ridge, J.C., Witte, R.W., Pardi, R.R., Reimer, G.E., 2020. Chronology of Laurentide glaciation in New Jersey and the New York City area, United States. *Quat. Res.* 99, 142–167.
- Stea, R.R., Mott, R.J., 2005. Younger Dryas glacial advance in the southern Gulf of St. Lawrence, Canada: analogue for ice inception? *Boreas* 34, 345–362.
- Stea, R.R., Finck, P.W., Wightman, D.M., 1986. Quaternary geology and till geochemistry of the western part of Cumberland county, Nova Scotia [Sheet 9]. *Geol. Surv. Can* 58, Paper 85-17.
- Stea, R.R., Seaman, A.A., Pronk, T., Parkhill, M.A., Allard, S., Utting, D., 2011. The Appalachian Glacier Complex in Maritime Canada. In: Ehlers, J., Gibbard, P.L., Hughes, P.D. (Eds.), *Developments in Quaternary Science*, vol. 15, pp. 631–659. Amsterdam.
- Stenni, B., Masson-Delmotte, V., Johnsen, S., Jouzel, J., Longinelli, A., Monnin, E., Röhlisberger, R., Selmo, E., 2001. An Oceanic Cold Reversal During the Last Deglaciation. *Science* 293, 2074–2077.
- Stoker, B.J., Margold, M., Gosse, J.C., Hidy, A.J., Monteath, A.J., Young, J.M., Gandy, N., Gregoire, L.J., Norris, S.L., Froese, D., 2022. The collapse of the Laurentide-Cordilleran ice saddle and early opening of the Mackenzie Valley, Northwest Territories, constrained by  $^{10}\text{Be}$  exposure dating. *Cryosphere* 16, 4865–4886.
- Stokes, C.R., Clark, C.D., Winsborrow, M.C.M., 2006. Subglacial bedform evidence for a major palaeo-ice stream and its retreat phases in Amundsen Gulf, Canadian Arctic Archipelago. *J. Quat. Sci.* 21, 399–412.
- Stokes, C.R., Clark, C.D., Storrar, R., 2009. Major changes in ice stream dynamics during deglaciation of the north-western margin of the Laurentide Ice Sheet. *Quat. Sci. Rev.* 28, 721–738.
- Stokes, C.R., Tarasov, L., Dyke, A.S., 2012. Dynamics of the North American Ice Sheet Complex during its inception and build-up to the Last Glacial Maximum. *Quat. Sci. Rev.* 50, 86–104.
- Stokes, C.R., Tarasov, L., Blomdin, R., Cronin, T.M., Fisher, T.G., Gyllencreutz, R., Hättestrånd, C., Heyman, J., Hindmarsh, R.C.A., Hughes, A.L.C., Jakobsson, M., Kirchner, N., Livingstone, S.J., Margold, M., Murton, J.B., Noormets, R., Peltier, W.R., Peteet, D.M., Piper, D.J.W., Preusser, F., Renssen, H., Roberts, D.H., Roche, D.M., Saint-Ange, F., Stroeve, A.P., Teller, J.T., 2015. On the reconstruction of palaeo-ice sheets: Recent advances and future challenges. *Quat. Sci. Rev.* 125, 15–49.
- Stone, B.D., Burns Jr., H.W., 1986. Pleistocene glacial and interglacial stratigraphy of New England, Long Island, and Adjacent Georges Bank and Gulf of Maine. *Quat. Sci. Rev.* 5, 39–52.
- Stone, J.O., Balco, G.A., Sugden, D.E., Caffee, M.W., Sass 3rd, L.C., Cowdery, S.G., Siddoway, C., 2003. Holocene deglaciation of Marie Byrd Land, West Antarctica. *Science* 299, 99–102.
- Storrar, R., Stokes, C.R., 2007. A Glacial Geomorphological Map of Victoria Island, Canadian Arctic. *J. Maps* 3, 191–210.
- Storrar, R.D., Stokes, C.R., Evans, D.J.A., 2013. A map of large Canadian eskers from Landsat satellite imagery. *J. Maps* 9, 456–473.
- Stravers, J.A., Miller, G.H., Kaufman, D.S., 1992. Late glacial ice margins and deglacial chronology for southeastern Baffin Island and Hudson Strait, eastern Canadian Arctic. *Can. J. Earth Sci.* 29, 1000–1017.
- Stroeve, A.P., Fabel, D., Codilean, A.T., Kleman, J., Clague, J.J., Miguens-Rodriguez, M., Xu, S., 2010. Investigating the glacial history of the northern sector of the Cordilleran Ice Sheet with cosmogenic  $^{10}\text{Be}$  concentrations in quartz. *Quat. Sci. Rev.* 29, 3630–3643.
- Stuiver, M., Reimer, P.J., 1993. Extended  $^{14}\text{C}$  data base and revised Calib 3.0  $^{14}\text{C}$  age calibration program. *Radiocarbon* 35, 215–230.
- Stuiver, M., Pearson, G.W., Braziunas, T.F., 1986. Radiocarbon age calibration of marine samples back to 9000 cal yr BP. *Radiocarbon* 28, 980–1021.
- Sutherland, J.L., Carrivick, J.L., Gandy, N., Shulmeister, J., Quincey, D.J., Cornford, S.L., 2020. Proglacial lakes control glacier geometry and behavior during recession. *Geophys. Res. Lett.* 47, e2020GL088865.
- Tarasov, L., Dyke, A.S., Neal, R.M., Peltier, W.R., 2012. A data-calibrated distribution of deglacial chronologies for the North American ice complex from glaciological modeling. *Earth Planet Sci. Lett.* 315–316, 30–40.
- Taylor, M.A., Hundy, I.L., Pak, D.K., 2014. Deglacial ocean warming and marine margin retreat of the Cordilleran Ice Sheet in the North Pacific Ocean. *Earth Planet Sci. Lett.* 403, 89–98.
- Teller, J.T., Leverington, D.W., Mann, J.D., 2002. Freshwater outbursts to the oceans from glacial Lake Agassiz and their role in climate change during the last deglaciation. *Quat. Sci. Rev.* 21, 879–887.
- Teller, J.T., Boyd, M., Yang, Z., Kor, P.S.G., Mokhtari Fard, A., 2005. Alternative routing of Lake Agassiz overflow during the Younger Dryas: new dates, paleotopography, and a re-evaluation. *Quat. Sci. Rev.* 24, 1890–1905.
- Teller, J.T., McGinn, R.A., Rajapara, H.M., Shukla, A.D., Singhvi, A.K., 2018. Optically stimulated luminescence ages from the Lake Agassiz basin in Manitoba. *Quat. Res.* 89, 478–493.
- Thackray, G.D., 2008. Varied climatic and topographic influences on Late Pleistocene mountain glaciation in the western United States. *J. Quat. Sci.* 23, 671–681.
- Thompson, W.B., Griggs, C.B., Miller, N.G., Nelson, R.E., Weddle, T.K., Kilian, T.M., 2011. Associated terrestrial and marine fossils in the late-glacial Presumpscot Formation, southern Maine, USA, and the marine reservoir effect on radiocarbon ages. *Quat. Res.* 75, 552–565.
- Thompson, W.B., Dorion, C.C., Ridge, J.C., Balco, G., Fowler, B.K., Svendsen, K.M., 2017. Deglaciation and late-glacial climate change in the White Mountains, New Hampshire, USA. *Quat. Res.* 87, 96–120.
- Todd, B.J., Valentine, P.C., Longva, O., Shaw, J., 2007. Glacial landforms on German Bank, Scotian Shelf: evidence for Late Wisconsinan ice-sheet dynamics and implications for the formation of De Geer moraines. *Boreas* 36, 148–169.
- Tremblay, T., Leblanc-Dumas, J., Allard, M., Ross, M., Johnson, C., 2013. Surficial Geology of Central Hall Peninsula, Baffin Island, Nunavut: Summary of the 2013 Field Season. *Summary of Activities 2013*, Canada-Nunavut Geoscience Office; Canada-Nunavut Geoscience Office, *Summary of Activities 2013*, pp. 109–120.
- Ullman, D.J., Carlson, A.E., LeGrande, A.N., Anslow, F.S., Moore, A.K., Caffee, M., Syverson, K.M., Licciardi, J.M., 2015. Southern Laurentide ice-sheet retreat synchronous with rising boreal summer insolation. *Geology* 43, 23–26.
- Ullman, D.J., Carlson, A.E., Hostetler, S.W., Clark, P.U., Cuzzone, J., Milne, G.A., Winsor, K., Caffee, M., 2016. Final Laurentide ice-sheet deglaciation and Holocene climate-sea level change. *Quat. Sci. Rev.* 152, 49–59.
- Utting, D.J., Atkinson, N., 2019. Proglacial lakes and the retreat pattern of the southwest Laurentide Ice Sheet across Alberta, Canada. *Quat. Sci. Rev.* 225, 106034.
- Veillette, J., 1988. Déglaciation et évolution des lacs proglaciaires post-Algonquin et Barlow au Témiscamingue, Québec et Ontario. *Géogr. Phys. Quaternaire* 42, 7–31.
- Veillette, J.J., 1994. Evolution and paleohydrology of glacial Lakes Barlow and Ojibway. *Quat. Sci. Rev.* 13, 945–971.
- Veillette, J.J., Dyke, A.S., Roy, M., 1999. Ice-flow evolution of the Labrador sector of the Laurentide Ice Sheet: a review, with new evidence from northern Quebec. *Quat. Sci. Rev.* 18, 993–1019.
- Veillette, J.J., Roy, M., Paulen, R.C., Ménard, M., St-Jacques, G., 2017. Uncovering the hidden part of a large ice stream of the Laurentide Ice Sheet, northern Ontario, Canada. *Quat. Sci. Rev.* 155, 136–158.
- Vickers, K.J., Ward, B.C., Utting, D.J., Telka, A.M., 2010. Deglacial reservoir age and implications, Foxe Peninsula, Baffin Island. *J. Quat. Sci.* 25, 1338–1346.
- Vincent, J.-S., Hardy, L., 1977. L'évolution et l'extension des lacs glaciaires Barlow et Ojibway en territoire québécois. *Géogr. Phys. Quaternaire* 31, 357–372.
- Wahrhaftig, C., 1958. Quaternary Geology of the Nenana River Valley and Adjacent Parts of the Alaska Range. U.S. Geological Survey Professional Paper, 293A, p. 118.
- Ward, B.C., Thomson, B., 2004. Late Pleistocene stratigraphy and chronology of lower Chehalis River valley, southwestern British Columbia: evidence for a restricted Coquitlam Stade. *Can. J. Earth Sci.* 41, 881–895.
- Waters, M.R., 2019. Late Pleistocene exploration and settlement of the Americas by modern humans. *Science* 365, eaat5447.
- Wayne, W.J., Thornbury, W.D., 1951. Glacial Geology of Wabash County, Indiana. Indiana Department of Conservation: Geological Survey Bulletin No. 5.
- Williams, L.D., 1978. Ice-sheet initiation and climatic influences of expanded snow cover in Arctic Canada. *Quat. Res.* 10, 141–149.
- Williams, L.D., 1979. An energy balance model of potential glacierization of Northern Canada. *Arct. Alp. Res.* 11, 443–456.
- Wisconsin Geological and Natural History Survey, 2011. Lexicon of Pleistocene Stratigraphic Units of Wisconsin. In: Syverson, K.M., Clayton, L., Attig, J.W., Mickelson, D.M. (Eds.), *Wisconsin Geological and Natural History Survey Technical Report 1*, p. 180.
- Wolfe, S., Huntley, D., Ollerhead, J., 2004. Relict Late Wisconsinan Dune Fields of the Northern Great Plains, Canada. *Géogr. Phys. Quaternaire* 58, 323–336.
- Wolfe, S.A., Paulen, R.C., Smith, I.R., Lamothe, M., 2007. Age and paleoenvironmental significance of Late Wisconsinan dune fields in the Mount Watt and Fontas River map areas, northern Alberta and British Columbia. *Geol. Surv. Canada Curr. Res.* 2007-B4, 10.
- Wolfe, S.A., Lian, O.B., Hugenholtz, C.H., Riches, J.R., 2016. Holocene eolian sand deposition linked to climatic variability, Northern Great Plains, Canada. *Holocene* 27, 579–593.
- Wright, H.E., Matsch, C.L., Cushing, E.J., 1973. The Superior and Des Moines Lobes. *Geological Society of America Memoir* 136, pp. 153–188.
- Yokoyama, Y., Lambeck, K., De Deckker, P., Johnston, P., Fifield, L.K., 2000. Timing of the Last Glacial Maximum from observed sea-level minima. *Nature* 406, 713–716.
- Young, R.R., Burns, J.A., Smith, D.G., Arnold, L.D., Rains, R.B., 1994. A single, late Wisconsin, Laurentide glaciation, Edmonton area and southwestern Alberta. *Geology* 22, 683–686.
- Young, N.E., Briner, J.P., Rood, D.H., Finkel, R.C., 2012. Glacier extent during the Younger Dryas and 8.2-ka event on Baffin Island, Arctic Canada. *Science* 337, 1330–1333.
- Young, N.E., Schaefer, J.M., Briner, J.P., Goehring, B.M., 2013. A  $^{10}\text{Be}$  production-rate calibration for the Arctic. *J. Quat. Sci.* 28, 515–526.
- Young, N.E., Schweinsberg, A.D., Briner, J.P., Schaefer, J.M., 2015. Glacier maxima in Baffin Bay during the Medieval Warm Period coeval with Norse settlement. *Sci. Adv.* 1, e1500806.
- Young, N.E., Briner, J.P., Miller, G.H., Lesnek, A.J., Crump, S.E., Thomas, E.K., Pendleton, S.L., Cuzzone, J., Lamp, J., Zimmerman, S., Caffee, M., Schaefer, J.M., 2020. Deglaciation of the Greenland and Laurentide ice sheets interrupted by glacier advance during abrupt coolings. *Quat. Sci. Rev.* 229, 106091.
- Young, N.E., Briner, J.P., Miller, G.H., Lesnek, A.J., Crump, S.E., Pendleton, S.L., Schwartz, R., Schaefer, J.M., 2021. Pulsebeat of early Holocene glaciation in Baffin Bay from high-resolution beryllium-10 moraine chronologies. *Quat. Sci. Rev.* 270, 107179.
- Zimmerman, S.G., Evenson, E.B., Gosse, J.C., Erskine, C.P., 1994. Extensive Boulder Erosion Resulting from a Range Fire on the Type-Pinedale Moraines, Fremont Lake, Wyoming. *Quat. Res.* 42, 255–265.

## Key references used to constrain NADI-1

- Ali, A.A., Blarquez, O., Girardin, M.P., Hély, C., Tinquaut, F., El Guellab, A., Valsecchi, V., Terrier, A., Bremond, L., Genries, A., Gauthier, S., Bergeron, Y., 2012. Control of the multimillennial wildfire size in boreal North America by spring climatic conditions. *Proc. Natl. Acad. Sci. USA* 109, 20966–20970.
- Allard, M., Seguin, M.K., 1985. La déglaciation d'une partie du versant hudsonien Québécois: bassins des rivières Nastapoca, Sheldrake et à l'Eau-Claire. *Géogr. Phys. Quaternaire* 34, 13–24.
- Allard, M., Tremblay, G., 1981. Observations sur le Quaternaire de l'extrémité orientale de la péninsule de Gaspé, Québec. *Géogr. Phys. Quaternaire* 35, 105–125.
- Alley, N.F., Young, G.K., 1978. Environmental significance of geomorphic processes in the northern Skeena Mountains. British Columb. Ministry Environ. Resour. Anal. Branch Bull. 3, 83.
- Anderson, R.C., 2005. Geomorphic History of the Rock River, South-Central Wisconsin, Northwestern Illinois. Ill. State Geol. Surv. Circ. 565.
- Anderson, R.K., Miller, G.H., Briner, J.P., Lifton, N.A., DeVogel, S.B., 2008. A millennial perspective on Arctic warming from  $^{14}\text{C}$  in quartz and plants emerging from beneath ice caps. *Geophys. Res. Lett.* 35.
- Anderson, T.W., Macpherson, J.B., 1994. Wisconsinan Late-glacial environmental change in Newfoundland: A regional review. *J. Quat. Sci.* 9, 171–178.
- Anderson, W.T., Mullins, H.T., Ito, E., 1997. Stable isotope record from Seneca Lake, New York: Evidence for a cold paleoclimate following the Younger Dryas. *Geology* 25, 135–138.
- Andrews, J., Kirby, M., Jennings, A., Barber, D., 1998. Late Quaternary stratigraphy, chronology, and depositional processes on the slope of S.E. Baffin Island, detrital carbonate and Heinrich events: Implications for onshore glacial history. *Géogr. Phys. Quaternaire* 52, 91–105.
- Andrews, J.T., 1966. Pattern of coastal uplift and deglaciation, West Baffin Island, N.W.T. *Geogr. Bull.* 8, 174–193.
- Andrews, J.T., 1976. Radiocarbon Date List III: Baffin Island, N.W.T. Canada. Institute of Arctic and Alpine Research Occasional Paper No. 21, p. 47.
- Andrews, J.T., Buckley, J.T., England, J.H., 1970. Late-Glacial Chronology and Glacio-Isostatic Recovery, Home Bay, East Baffin Island, Canada. *Geol. Soc. Am. Bull.* 81, 1123–1148.
- Andrews, J.T., Drapier, L., 1967. Radiocarbon dates obtained through the Geographical Branch field observations. *Geogr. Bull.* 9, 115–162.
- Andrews, J.T., Jennings, A., Cooper, T., Williams, K.M., Mienert, J., 1996. Late Quaternary sedimentation along a fjord to shelf (trough) transect, east Greenland (c. 68 degrees N). In: Andrews, J.T., Austin, W.E.N., Bergsten, H., Jennings, A.E. (Eds.), *Late Quaternary Palaeoceanography of the North Atlantic Margins*. Geological Society Special Publication no. 111, pp. 153–166.
- Andrews, J.T., Keigwin, L., Hall, F., Jennings, A.E., 1999. Abrupt deglaciation events and Holocene palaeoceanography from high-resolution cores, Cartwright Saddle, Labrador Shelf, Canada. *J. Quat. Sci.* 14, 383–397.
- Andrews, J.T., Miller, G.H., 1972. The Quaternary History of Northern Cumberland Peninsula, East Baffin Island, N. W. T. Part X: Radiocarbon Date List. *Arct. Alp. Res.* 4, 261–277.
- Anundsen, K., Abella, S., Leopold, E., Stuiver, M., Turner, S., 1994. Late-Glacial and Early Holocene Sea-Level Fluctuations in the Central Puget Lowland, Washington, Inferred from Lake Sediments. *Quat. Res.* 42, 149–161.
- Ashworth, A.C., Schwert, D.P., Watts, W.A., Wright, H.E., 1981. Plant and insect fossils at Norwood in south-central Minnesota: A record of late-glacial succession. *Quat. Res.* 16, 66–79.
- Atkinson, N., 2003. Late Wisconsinan glaciation of Amund and Ellef Ringnes islands, Nunavut: evidence for the configuration, dynamics, and deglacial chronology of the northwest sector of the Innuittian Ice Sheet. *Can. J. Earth Sci.* 40, 351–363.
- Atkinson, N., Utting, D.J., Pawley, S.M., 2014. Landform signature of the Laurentide and Cordilleran ice sheets across Alberta during the last glaciation. *Can. J. Earth Sci.* 51, 1067–1083.
- Attig, J.W., Clayton, L., Mickelson, D.M., 1985. Correlation of late Wisconsin glacial phases in the western Great Lakes area. *Geol. Soc. Am. Bull.* 96, 1585–1593.
- Attig, J.W., Hanson, P.R., Rawling, J.E., Young, A.R., Carson, E.C., 2011. Optical ages indicate the southwestern margin of the Green Bay Lobe in Wisconsin, USA, was at its maximum extent until about 18,500 years ago. *Geomorphology* 130, 384–390.
- Atwater, B.F., 1986. Pleistocene glacial-lake deposits of the Sanpoil River valley, Northeastern Washington. *United States Geol. Surv. Bull.* 1661, 39.
- Barnett, D.M., Forbes, D.L., 1972. Surficial Geology and Geomorphology of Melville Island. *Geol. Surv. Can. Pap.* 73-1A, pp. 189–192.
- Barnett, P.J., 1979. Glacial Lake Whittlesey: The probable ice frontal position in the eastern end of the Erie basin. *Can. J. Earth Sci.* 16, 568–574.
- Barnett, P.J., 1988a. Chapter 21 Quaternary Geology of Ontario, *Geology of Ontario*, pp. 1011–1088.
- Barnett, P.J., 1988b. History of the northwestern arm of the Champlain Sea. In: Gadd, N. R. (Ed.), *The Quaternary Developpement of the Champlain Sea Basin*. Geological Association of Canada Special Paper 35.
- Barrie, C.Q., Piper, D.J.W., 1982. Late Quaternary marine geology of Makkovik Bay, Labrador. *Geol. Surv. Can. Pap.* 37. Paper 81-17.
- Barrie, J.V., Collins, W.T., Segall, M.F., Lewis, C.F.M., 1987. Holocene development and sediment transport on the northeastern Grand Banks of Newfoundland. *Geol. Surv. Can Open File* 1396, 168.
- Barrie, J.V., Conway, K.W., 1999. Late Quaternary Glaciation and Postglacial Stratigraphy of the Northern Pacific Margin of Canada. *Quat. Res.* 51, 113–123.
- Batterson, M.J., Liverman, D.G.E., Kirby, G.E., 1993. Glacial Lake development and marine inundation, Deer Lake area, Newfoundland, Canada: Topographically controlled deglaciation of an interior Basin. *J. Quat. Sci.* 8, 327–337.
- Bauer, E.J., Retzler, A.J., Jirsa, M.A., Chandler, V.W., Pettus, M.C., Gowen, A.S., Hamilton, J.D., 2020. C-47, Geologic Atlas of Rock County, Minnesota. Minnesota Geological Survey. Retrieved from the University of Minnesota Digital Conservancy. <https://hdl.handle.net/11299/218637>.
- Bednarski, J., 1986. Late Quaternary glacial and sea-level events, Clements Markham Inlet, northern Ellesmere Island, Arctic Canada. *Can. J. Earth Sci.* 23, 1343–1355.
- Bednarski, J.M., 1995. Glacial advances and stratigraphy in Otto Fiord and adjacent areas, Ellesmere Island, Northwest Territories. *Can. J. Earth Sci.* 32, 52–64.
- Beierle, B., Smith, D.G., 1998. Severe drought in the early Holocene (10,000–6800 BP) interpreted from lake sediment cores, southwestern Alberta, Canada. *Palaeogeogr. Palaeoclimatol. Palaeoecol.* 140, 75–83.
- Bell, T., Batterson, M.J., Liverman, D.G., Shaw, J., 2003. A new late-glacial sea-level record for St. George's Bay, Newfoundland. *Can. J. Earth Sci.* 40, 1053–1070.
- Bell, T., Liverman, D.G.E., Batterson, M.J., Sheppard, K., 2001. Late Wisconsinan stratigraphy and chronology of southern St. George's Bay, Newfoundland: a reappraisal. *Can. J. Earth Sci.* 38, 851–869.
- Berger, G.W., Eyles, N., 1994. Thermoluminescence chronology of Toronto-area Quaternary sediments and implications for the extent of the midcontinent ice sheet (s). *Geology* 22, 31–34.
- Berry, J.C., Drummie, R.J., 1982. University of Waterloo Radiocarbon Dates I. *Radiocarbon* 24, 68–82.
- Bettis, E.A., Hoyer, B.E., 1986. Late Wisconsinan and Holocene landscape evolution and alluvial stratigraphy in the Saylorville Lake area, central Des Moines River Valley, Iowa. *Iowa Geological Survey Open File Report* 86-1, 71.
- Bettis III, E.A., Quade, D.J., Kemmis, T.J., 1996. Hogs, Bogs, & Logs: Quaternary deposits and environmental geology of the Des Moines Lobe. *Geol. Surv. Bureau: Guidebook Series No. 18* 171.
- Björck, S., 1985. Deglaciation chronology and revegetation in northwestern Ontario. *Can. J. Earth Sci.* 22, 850–871.
- Black, R.F., Rubin, M., 1968. Radiocarbon dates of Wisconsin. *Wisconsin Acad. Sci. Arts Lett.* 56, 99–115.
- Blais-Stevens, A., Sun, C., Fulton, R.J., 1999. Surficial geology, Virden, Manitoba-Saskatchewan. *Geol. Surv. Can. Map* 1922A, 1:125 000.
- Blake, W., 1956. Landforms and topography of the Lake Melville area, Labrador, Newfoundland. *Geogr. Bull.* 9, 75–100.
- Blake, W., 1966. End moraines and deglaciation chronology in northern Canada with special reference to southern Baffin Island. *Geol. Surv. Can. Paper* 66-26.
- Blake, W., 1982. *Geol. Surv. Can Radiocarbon Dates XXII*. *Geol. Surv. Can. Paper* 82-7, 22.
- Blake, W.J., 1983. *Geol. Surv. Can Radiocarbon Dates XXIII*. *Geol. Surv. Can* 34. Paper 83-7.
- Blake, W.J., 1987. *Geol. Surv. Can Radiocarbon Dates XXVI*. *Geol. Surv. Can* 60. Paper 86-7.
- Blake, W.J., 1988. *Geol. Surv. Can Radiocarbon Dates XXVII*. *Geol. Surv. Can* 100. Paper 87-7.
- Blake, W.J., 1992. Holocene emergence at Cape Herschel, east-central Ellesmere Island, Arctic Canada: implications for ice sheet configuration. *Can. J. Earth Sci.* 29, 1958–1980.
- Bleuer, N.K., 1974. Buried Till Ridges in the Fort Wayne Area, Indiana, and their Regional Significance. *Geol. Soc. Am. Bull.* 85, 917–920.
- Blewett, W.L., Rieck, R.L., 1987. Reinterpretation of a portion of the Munising moraine in northern Michigan. *Geol. Soc. Am. Bull.* 98, 169–175.
- Bobrowsky, P., 1989. Late Cenozoic Geology of the Northern Rocky Mountain Trench. *British Columbia [PhD thesis]* University of Alberta, Edmonton.
- Bobrowsky, P., Rutter, N.W., 1992. The Quaternary Geologic History of the Canadian Rocky Mountains. *Géogr. Phys. Quaternaire* 46, 5–50.
- Boissonneau, A.N., 1968. Glacial history of Northeastern Ontario II. The Timiskaming-Algoma area. *Can. J. Earth Sci.* 5, 97–109.
- Bonifay, D., Piper, D.J.W., 1988. Probable Late Wisconsinan ice margin on the upper continental slope off St. Pierre Bank, eastern Canada. *Can. J. Earth Sci.* 25, 853–865.
- Booth, D.B., Troost, K.G., Clague, J.J., Waitt, R.B., 2003. The Cordilleran Ice Sheet, Developments in Quaternary Sciences. Elsevier, pp. 17–43.
- Bouchard, M.A., 1980. Late Quaternary Geology of the Temiscamie Area, Central Quebec, Canada. *PhD thesis*. McGill University, Montreal, p. 284.
- Breckenridge, A., 2013. An analysis of the late glacial lake levels within the western Lake Superior basin based on digital elevation models. *Quat. Res.* 80, 383–395.
- Breckenridge, R.M., Phillips, W.M., 2010. New cosmogenic  $^{10}\text{Be}$  surface exposure ages for the Purcell Trench lobe of the Cordilleran ice sheet in Idaho. *Geol. Soc. Am. Abstracts with Programs* 42, 309.
- Briner, J.P., Bini, A.C., Anderson, R.S., 2009. Rapid early Holocene retreat of a Laurentide outlet glacier through an Arctic fjord. *Nat. Geosci.* 2, 496–499.
- Briner, J.P., Kauffman, D.S., 2008. Late Pleistocene mountain glaciation in Alaska: key chronologies. *J. Quat. Sci.* 23, 659–670.
- Briner, J.P., Overeem, I., Miller, G., Finkel, R., 2007. The deglaciation of Clyde Inlet, northeastern Baffin Island, Arctic Canada. *J. Quat. Sci.* 22, 223–232.
- Broecker, W.S., Kulp, J.L., 1957. Lamont Natural Radiocarbon Measurements IV. *Science* 126, 1324–1334.
- Brookes, I.A., 1974. Late-Wisconsin glaciation of southwestern Newfoundland (with special reference to the Stephenville map-area). *Geol. Surv. Can. Paper* 73-40.
- Brookes, I.A., 1977. Radiocarbon age of Robinson's Head moraine, west Newfoundland, and its significance for postglacial sea level changes. *Can. J. Earth Sci.* 14, 2121–2126.
- Broster, B.E., Dickinson, P.C., 2015. Late Wisconsinan and Holocene development of Grand Lake Meadows area and southern reaches of the Saint John River Valley, New Brunswick, Canada. *Atl. Geol.* 51, 206–220.

- Brown, K.J., Fitton, R.J., Schoups, G., Allen, G.B., Wahl, K.A., Hebda, R.J., 2006. Holocene precipitation in the coastal temperate rainforest complex of southern British Columbia, Canada. *Quat. Sci. Rev.* 25, 2762–2779.
- Bruegger, A., 2016. Refining the Span and Rates of Deposition of the Glenwood Phase of Lake Chicago. M.Sc thesis] University of Illinois at Urbana-Champaign, p. 61.
- Bruneau, D., Gray, J.T., 1997. Écoulements glaciaires et déglaciation hâtive (ca 11 ka BP ?) du nord-est de la péninsule d'Ungava, Québec, Canada. *Can. J. Earth Sci.* 34, 1089–1100.
- Brush, G.S., 1967. Pollen analysis of late-glacial sediments in Iowa. In: Cushing, E.J., Wright, D.K. (Eds.), *Quaternary Paleoecology*. Yale University Press, pp. 99–116.
- Burgis, W.A., 1970. The Imlay Outlet at Glacial Lake Maumee Imlay City. M.Sc thesis] University of Michigan, Michigan.
- Cadwell, D.H., 1989. Surficial geology map of New York (lower Hudson sheet): New York State. Museum Map and Chart Series 40 scale 1:250,000.
- Calhoun, R.H.H., 1906. Montana Lobe of the Keewatin Ice Sheet. United States Geological Survey Professional Paper 50, 62.
- Calkin, P.E., 1970. Strand lines and chronology of the glacial Great Lakes in northwestern New York. *Ohio J. Sci.* 70, 78–96.
- Calkin, P.E., Miller, K.E., 1977. Late Quaternary Environment and man in Western New York. *Ann. N. Y. Acad. Sci.* 288, 297–315.
- Carrara, P.E., 1995. A 12 000 year radiocarbon date of deglaciation from the Continental Divide of northwestern Montana. *Can. J. Earth Sci.* 32, 1303–1307.
- Carrara, P.E., Kiver, E.P., Stradling, D.F., 1996. The southern limit of Cordilleran ice in the Colville and Pend Oreille valleys of northeastern Washington during the Late Wisconsin glaciation. *Can. J. Earth Sci.* 33, 769–778.
- Carson, E.C., Hanson, P.R., Attig, J.W., Young, A.R., 2012. Numeric control on the late-glacial chronology of the southern Laurentide Ice Sheet derived from ice-proximal lacustrine deposits. *Quat. Res.* 78, 583–589.
- Chauvin, L., 1977. Géologie des dépôts meubles de la région de Joutel-Matagami. Ministère des Richesses naturelles, dossier 539, 106.
- Christiansen, E.A., 1971. Tills in Southern Saskatchewan, Canada. In: Goldthwait, R.P. (Ed.), *Till: a Symposium*. Ohio State University Press, Columbus, pp. 167–183.
- Christiansen, E.A., 1979. The Wisconsinan deglaciation, of southern Saskatchewan and adjacent areas. *Can. J. Earth Sci.* 16, 913–938.
- Clague, J., 1988. Quaternary Stratigraphy and History, Quesnel, British Columbia. *Géogr. Phys. Quaternaire* 42, 279–288.
- Clague, J.J., 1977. Quadra sand: a study of the Late Pleistocene geology and geomorphic history of coastal southwest British Columbia. *Geol. Surv. Can.* 24, Paper 77-17.
- Clague, J.J., 1980a. Late Quaternary geology and geochronology of British Columbia, Part 1: Radiocarbon dates. *Geol. Surv. Can.* 33, Paper 80-13.
- Clague, J.J., 1980b. Late Quaternary geology and geochronology of British Columbia. Part 2: summary and discussion of radiocarbon-dated Quaternary history. *Geol. Surv. Can.* 41, Paper 80-35.
- Clague, J.J., 1984. Quaternary Geology and Geomorphology, Smithers-Terrace-Prince Rupert Area, British Columbia. *Geol. Surv. Can. Memoir* 413, p. 82.
- Clague, J.J., 1987. Quaternary stratigraphy and history, Williams Lake, British Columbia. *Can. J. Earth Sci.* 24, 147–158.
- Clague, J.J., James, T.S., 2002. History and isostatic effects of the last ice sheet in southern British Columbia. *Quat. Sci. Rev.* 21, 71–87.
- Clague, J.J., Mathewes, R.W., Guibault, J.-P., Hutchinson, I., Ricketts, B.D., 1997. Pre-Younger Dryas resurgence of the southwestern margin of the Cordilleran ice sheet, British Columbia, Canada. *Boreas* 26, 261–278.
- Clague, J.J., Roberts, N.J., Miller, B., Menounos, B., Goehring, B., 2021. A huge flood in the Fraser River valley, British Columbia, near the Pleistocene Termination. *Geomorphology* 374, 107473.
- Clague, J.J., Saunders, I.R., Roberts, M.C., 1988. Ice-free conditions in southwestern British Columbia at 16000 years BP. *Can. J. Earth Sci.* 25, 938–941.
- Clark, D.H., Clague, J.J., 2021. Glaciers, Isostasy, and Eustasy in the Fraser Lowland: A New Interpretation of Late Pleistocene Glaciation across the International Boundary. Untangling the Quaternary Period—A Legacy of Stephen C. Porter, Richard B. Waitt, Glenn D. Thackray, Alan R. Gillespie. *Geological Society of America* 548.
- Clark, J., Carlson, A.E., Reyes, A.V., Carlson, E.C.B., Guillaume, L., Milne, G.A., Tarasov, L., Caffee, M., Wilcken, K., Rood, D.H., 2022. The age of the opening of the Ice-Free Corridor and implications for the peopling of the Americas. *Proc. Natl. Acad. Sci. USA* 119, e2118558119.
- Clark, J.A., Befus, K.M., Hooyer, T.S., Stewart, P.W., Shipman, T.D., Gregory, C.T., Zylstra, D.J., 2008. Numerical simulation of the paleohydrology of glacial Lake Oshkosh, eastern Wisconsin, USA. *Quat. Res.* 69, 117–129.
- Clark, P., 1985. A note on the glacial geology and postglacial emergence of the Lake Harbour region, Baffin Island, N.W.T. *Can. J. Earth Sci.* 22, 1864–1871.
- Clayton, L., 1966. Notes on Pleistocene stratigraphy of North Dakota. *North Dakota Geol. Surv. Rep. Invest.* 44, 26.
- Clayton, L., Attig, J.W., 1989. Glacial Lake Wisconsin. *Geological Society of America Memoir* 173, p. 80.
- Coleman, A.P., 1922. Physiography and glacial geology of Gaspe Peninsula, Quebec. *Geol. Surv. Can. Bull.* 34, 52.
- Coleman, D.D., 1973. Illinois State Geological Survey Radiocarbon Dates IV, vol. 15, pp. 75–85.
- Colman, S.M., Breckenridge, A., Zoet, L.K., Wattus, N.J., Johnson, T.C., 2020. Moraines and late-glacial stratigraphy in central Lake Superior. *Quat. Res.* 98, 19–35.
- Conley, G.G., 1986. Surficial Geology and Stratigraphy of the Killarney-Holmfield Area, Southwestern Manitoba [M.Sc. Thesis]. University of Manitoba, p. 186.
- Cooper, A.J., 1979. Quaternary geology of the Grand Bend–Parkhill area, southern Ontario. *Ontario Geol. Surv. Rep.* 188, 70.
- Cowan, W.R., 1975. Quaternary geology of the Woodstock area, southern Ontario. *Ontario Geol. Surv. Geol. Rep.* 119, 91.
- Craig, B.G., 1965. Notes on moraines and radiocarbon dates in northwestern Baffin Island, Melville Peninsula, and northeast District of Keewatin. *Geol. Surv. Can.* 7, Paper 65-20.
- Crandell, D.R., 1963. *Surficial Geology and Geomorphology of the Lake Tapps Quadrangle*. United States Geological Survey Professional Paper 388-A, Washington, p. 84.
- Crowl, G.H., 1980. Woodfordian age of the Wisconsin glacial border in northeastern Pennsylvania. *Geology* 8, 51–55.
- Crump, S.E., Miller, G.H., Power, M., Septúlveda, J., Dildar, N., Coglan, M., Bunce, M., 2019. Arctic shrub colonization lagged peak postglacial warmth: Molecular evidence in lake sediment from Arctic Canada. *Global Change Biol.* 25, 4244–4256.
- Crump, S.E., Young, N.E., Miller, G.H., Pendleton, S.L., Tulenko, J.P., Anderson, R.S., Briner, J.P., 2020. Glacier expansion on Baffin Island during early Holocene cold reversals. *Quat. Sci. Rev.* 241, 106419.
- Cumming, E.H., Aksu, A.E., Mudie, P.J., 1992. Late Quaternary glacial and sedimentary history of Bonavista Bay, northeast Newfoundland. *Can. J. Earth Sci.* 29, 222–235.
- Cwynar, L.C., 1988. Late Quaternary vegetation history of Kettlehole Pond, southwestern Yukon. *Can. J. For. Res.* 18, 1270–1279.
- Dadswell, M.J., 1974. Distribution, ecology, and postglacial dispersal of certain crustaceans and fishes in eastern North America. *Natl. Mus. Can., Publ. Zool.* 11, 110.
- Daigneault, R.-A., Occhietti, S., 2006. Les moraines du massif Algonquin, Ontario, au début du Dryas récent, et corrélation avec la Moraine de Saint-Narcisse. *Géogr. Phys. Quaternaire* 60, 103–118.
- Daigneault, R.A., 2008. *Géologie du Quaternaire du nord de la péninsule d'Ungava, Québec*. Commission géologique du Canada, Bulletin no 533, 116.
- David, P.P., Lebusi, J., 1985. Glacial maximum and deglaciation of western Gaspé, Québec, Canada. In: Borns, H.W., Lasalle, P., Thompson, W.B. (Eds.), *Late Pleistocene History of Northern New England and Adjacent Quebec*. Geological Society of America, Special paper 197, pp. 85–109.
- Davis, P., 1999. Cirques of the Presidential Range, New Hampshire, and surrounding alpine areas in the northeastern United States. *Géogr. Phys. Quaternaire* 53, 25–45.
- Davis, R.B., Bradstreet, T.E., Stuckenrath, R., Borns, H.W., 1975. Vegetation and associated environments during the past 14,000 years near Moulton Pond, Maine. *Quat. Res.* 5, 435–465.
- deVries, H., Dreimanis, A., 1960. Finite Radiocarbon Dates of the Port Talbot Interstadial Deposits in Southern Ontario. *Science* 131, 1738–1739.
- Dieffenbacher-Krall, A.C., Borns, H.W., Nurse, A.M., Langley, G.E.C., Birkel, S., Cwynar, L.C., Doner, L.A., Dorion, C.C., Fastook, J., Jr, G.L.J., Sayles, C., 2016. Younger Dryas Paleoenvironments and Ice Dynamics in Northern Maine: A Multi-Proxy, Case History. *Northeast. Nat.* 23, 67–87.
- Dieffenbacher-Krall, A.C., Nurse, A.M., 2005. Late-Glacial and Holocene Record of Lake Levels of Mathews Pond and Whitehead Lake, Northern Maine, USA. *J. Paleolimnol.* 34, 283–309.
- Dionne, J.-C., 1977. La mer de Goldthwait au Québec. *Géogr. Phys. Quaternaire* 31, 61–80.
- Dionne, J.-C., Coll, D., 1995. Le niveau marin relatif dans la région de Matane (Québec), de la déglaciation à nos jours. *Géogr. Phys. Quaternaire* 49, 363–380.
- Dionne, J.-C., Occhietti, S., 1996. Aperçu du Quaternaire à l'embouchure du Saguenay. Québec. *Géographie physique et Quaternaire* 50, 5–34.
- Dredge, L.A., 2004. Surficial geology, Lake Gillian, central Baffin Island, Nunavut. *Geol. Surv. Can. Map* 2076A, scale 1:250 000.
- Dredge, L.A., Cowan, W.R., 1989. Quaternary geology of the southwestern Canadian Shield. In: Fulton, R.J. (Ed.), *Quaternary Geology of Canada and Greenland*. *Geol. Surv. Can.*, pp. 214–249.
- Dredge, L.A., Ward, B.C., Kerr, D.E., 1995. *Surficial Geology Aylmer Lake, District of Mackenzie, Northwest Territories*. *Geol. Surv. Can. Map* 1867A, scale 1:125 000.
- Dredge, L.A., Ward, B.C., Kerr, D.E., 1998. Surficial geology, Kikerk Lake, District of Mackenzie, Northwest Territories. *Geol. Surv. Can. Map* 1909A scale 1:125 000.
- Driver, J.C., Handly, M., Fladmark, K.R., Nelson, D.E., Sullivan, G.M., Preston, R., 1996. Stratigraphy, Radiocarbon Dating, and Culture History of Charlie Lake Cave, British Columbia. *Arcic* 49, 265–277.
- Dubé-Loubert, H., Roy, M., Schaefer, J.M., Clark, P.U., 2018. 10Be dating of former glacial Lake Naskaupi (Québec-Labrador) and timing of its discharges during the last deglaciation. *Quat. Sci. Rev.* 191, 31–40.
- Dubé-Loubert, H., Roy, M., Veillette, J.J., Brouard, E., Schaefer, J.M., Wittmann, H., 2021. The role of glacial dynamics in the development of ice divides and the Horseshoe Intersection Zone of the northeastern Labrador Sector of the Laurentide Ice Sheet. *Geomorphology* 387, 107777.
- Dubois, J.-M.M., Dionne, J.-C., Borns Jr., H.W., LaSalle, P., Thompson, W.B., 1985. The Québec North Shore Moraine System: A major feature of Late Wisconsin deglaciation, Late Pleistocene History of Northeastern New England and Adjacent Quebec. *Geol. Soc. Am. Special Paper* 197, p. 125-133.
- Dubois, J.-M.M., Occhietti, S., Pichet, P., Page, P., Jacob, C., Bigras, P., 1988. Université du Québec à Montréal GEOTOP Radiocarbon Dates I. Radiocarbon 30, 355–365.
- Dubois Verret, M., 2015. Géomorphologie quaternaire de l'Outaouais (Québec): écoulements glaciaires et paléogéographie de la déglaciation [M. Sc thesis]. Université du Québec à Montréal, p. 159.
- Duckworth, P.B., 1979. The late depositional history of the western end of the Oak Ridges Moraine, Ontario. *Can. J. Earth Sci.* 16, 1094–1107.
- Duk-Rodkin, A., Barendregt, R.W., Tarnocai, C., Phillips, F.M., 1996. Late Tertiary to late Quaternary record in the Mackenzie Mountains, Northwest Territories, Canada: stratigraphy, paleosols, paleomagnetism, and chlorine - 36. *Can. J. Earth Sci.* 33, 875–895.
- Dyck, W., Fyles, J.G., 1963. *Geol. Surv. Can Radiocarbon Dates II. Radiocarbon* 5, 39–55.

- Dyck, W., Fyles, J.G., 1964. Geol. Surv. Can Radiocarbon Dates III. Radiocarbon 6, 167–181.
- Dyck, W., Fyles, J.G., Blake, W., 1965a. Geol. Surv. Can Radiocarbon Dates IV. Radiocarbon 7, 24–46.
- Dyck, W., Fyles, J.G., Blake, W.J., 1965b. Geol. Surv. Can Radiocarbon Dates IV. Geol. Surv. Can. Pap. 65–4, 23.
- Dyck, W., Lowdon, J.A., Fyles, J.G., Blake, W., 1966. Geol. Surv. Can Radiocarbon Dates V. Radiocarbon 8, 96–127.
- Dyke, A.S., 1979. Glacial and Sea-Level History of Southwestern Cumberland Peninsula, Baffin Island, N.W.T., Canada. Arct. Alp. Res. 11, 179–202.
- Dyke, A.S., 1984. Quaternary geology of Boothia Peninsula and northern District of Keewatin, central Canadian Arctic. Geol. Surv. Can. Map 407, 26.
- Dyke, A.S., 1998. Holocene levelling of Devon Island, Arctic Canada: implications for ice sheet geometry and crustal response. Can. J. Earth Sci. 35, 885–904.
- Dyke, A.S., Hooper, J.M.G., 2001. Deglaciation of Northwest Baffin Island. Geol. Surv. Can. Map 1999A.
- Dyke, A.S., Morris, T.F., Green, D.E.C., 1991. Postglacial tectonic and sea level history of the central Canadian Arctic. Geol. Surv. Can. Bull. 397, 56.
- Dyke, A.S., St-Onge, D.A., Savelle, J.M., 2003. Deglaciation of southwestern Victoria Island and adjacent Arctic mainland, Nunavut–Northwest Territories. Geol. Surv. Can. Map 2027A scale 1:500,000.
- Eamer, J.B.R., Shugar, D.H., Walker, I.J., Lian, O.B., Neudorf, C.M., Telka, A.M., 2017. A glacial readvance during retreat of the Cordilleran Ice Sheet, British Columbia central coast. Quat. Res. 87, 468–481.
- Easterbrook, D., 1992. Advance and Retreat of Cordilleran Ice Sheets in Washington, U.S. A. Géogr. Phys. Quaternaire 46, 51–68.
- El-Guellaab, A., Asselin, H., Gauthier, S., Bergeron, Y., Ali, A.A., 2015. Holocene variations of wildfire occurrence as a guide for sustainable management of the northeastern Canadian boreal forest. Forest Ecosyst. 2, 15.
- Elmore, C.R., Gulick, S.P.S., Willem, B., Powell, R., 2013. Seismic stratigraphic evidence for glacial expanse during glacial maxima in the Yakutat Bay Region, Gulf of Alaska. G-cubed 14, 1294–1311.
- Elson, J.A., 1956. Surficial Geology of the Tiger Hills Region, Manitoba, Canada. Ph.D. thesis. Yale University, p. 471.
- England, J., 1976. Late Quaternary Glaciation of the Eastern Queen Elizabeth Islands, N.W.T., Canada: Alternative Models. Quat. Res. 6, 185–202.
- England, J., 1990. The late Quaternary history of Greely Fiord and its tributaries, west-central Ellesmere Island. Can. J. Earth Sci. 27, 255–270.
- England, J., 1997. Unusual rates and patterns of Holocene emergence, Ellesmere Island, Arctic Canada. J. Geol. Soc. 154, 781–792.
- England, J., 1999. Coalescent Greenland and Innuitian ice during the Last Glacial Maximum: revising the Quaternary of the Canadian High Arctic. Quat. Sci. Rev. 18, 421–456.
- England, J., Smith, I.R., Evans, D.J.A., 2000. The last glaciation of east-central Ellesmere Island, Nunavut: ice dynamics, deglacial chronology, and sea level change. Can. J. Earth Sci. 37, 1355–1371.
- England, J.H., Lakeman, T.R., Lemmen, D.S., Bednarzki, J.M., Stewart, T.G., Evans, D.J. A., 2008. A millennial-scale record of Arctic Ocean sea ice variability and the demise of the Ellesmere Island ice shelves. Geophys. Res. Lett. 35, L19502.
- Engstrom, D.R., Hansen, B.C.S., 1985. Postglacial vegetational change and soil development in southeastern Labrador as inferred from pollen and chemical stratigraphy. Can. J. Bot. 63, 543–561.
- Evans, D.J.A., 1990. The last glaciation and relative sea level history of Northwest Ellesmere Island, Canadian high arctic. J. Quat. Sci. 5, 67–82.
- Falconer, G., Ives, J.D., Loken, O.H., Andrews, J.T., 1965. Major end moraines in eastern and central Arctic Canada. Can. Geog. Branch. Geogr. Bull. 137–153.
- Fisher, T.G., Horton, J., Lepper, K., Loope, H., 2019. Aeolian activity during Late Glacial time, with an example from Mongo, Indiana, USA. Can. J. Earth Sci. 56, 175–182.
- Fisher, T.G., Waterson, N., Lowell, T.V., Hajdas, I., 2009. Deglaciational ages and meltwater routing in the Fort McMurray region, northeastern Alberta and northwestern Saskatchewan, Canada. Quat. Sci. Rev. 28, 1608–1624.
- Fortier, D., Allard, M., 2004. Late Holocene syn genetic ice-wedge polygons development, Bylot Island, Canadian Arctic Archipelago. Can. J. Earth Sci. 41, 997–1012.
- Franzi, D.A., Ridge, J.C., Pair, D.L., Desimone, D., Rayburn, J.A., Barclay, D.J., 2016. Post-valley heads deglaciation of the Adirondack Mountains and adjacent lowlands. Adirondack J. Environ. Stud. 21, 119–146.
- Fréchette, B., de Vernal, A., 2009. Relationship between Holocene climate variations over southern Greenland and eastern Baffin Island and synoptic circulation pattern. Clim. Past 5, 347–359.
- Friels, P.A., Clague, J.J., 2002. Younger Dryas readvance in Squamish river valley, southern Coast mountains, British Columbia. Quat. Sci. Rev. 21, 1925–1933.
- Fuller, M.L., 1914. The Geology of Long Island. U. S. Geological Survey Professional Paper. 82, New York, p. 231.
- Fullerton, D.S., 1980. Preliminary Correlation of Post-Erie Interstadial Events: (16,000–10,000 Radiocarbon Years before Present), Central and Eastern Great Lakes Region, and Hudson, Champlain, and St. Lawrence Lowlands, United States and Canada. United States Geological Survey Professional Paper. 1089, p. 52.
- Fulton, R., 1991. A Conceptual Model for Growth and Decay of the Cordilleran Ice Sheet. Géogr. Phys. Quaternaire 45, 281–286.
- Fulton, R.J., Hodgson, D.A., 1979. Wisconsin Glacial Retreat, Southern Labrador. Geol. Surv. Can. pp. 17–21. Paper 79-ic.
- Gajewski, K., Payette, S., Ritchie, J.C., 1993. Holocene Vegetation History at the Boreal Forest-Shrub-Tundra Transition in North-Western Quebec. J. Ecol. 81, 433–443.
- Genies, A., Finsinger, W., Asnong, H., Bergeron, Y., Carcaillet, C., Garneau, M., Hély, C., Ali, A.A., 2012. Local versus regional processes: can soil characteristics overcome climate and fire regimes by modifying vegetation trajectories? J. Quat. Sci. 27, 745–756.
- Gipp, M.R., Piper, D.J.W., 1989. Chronology of Late Wisconsinan glaciation, Emerald Basin, Scotian Shelf. Can. J. Earth Sci. 26, 333–335.
- Glover, K.C., Lowell, T.V., Wiles, G.C., Pair, D., Applegate, P., Hajdas, I., 2011. Deglaciation, basin formation and post-glacial climate change from a regional network of sediment core sites in Ohio and eastern Indiana. Quat. Res. 76, 401–410.
- Godbout, P.-M., Roy, M., Veillette, J.J., Schaefer, J.M., 2017. Cosmogenic 10Be dating of raised shorelines constrains the timing of lake levels in the eastern Lake Agassiz-Ojibway basin. Quat. Res. 88, 265–276.
- Goldthwait, J.S., 1907. The abandoned shoreline of eastern Wisconsin. Wisconsin Geol. Surv. Bull. 17, 134.
- Goldthwait, R.P., 1958. Wisconsin age forests in western Ohio I. Age and glacial events. Ohio J. Sci. 58, 209–219.
- Goldthwait, R.P., White, G.W., Forsyth, J.L., 1961. Glacial Map of Ohio. United States Geological Survey Map, pp. 1–316.
- Gorokhovich, Y., Nelson, M., Eaton, T., Wolk-Stanley, J., Sen, G., 2018. Geochronology and geomorphology of the Jones Point glacial landform in Lower Hudson Valley (New York): Insight into deglaciation processes since the Last Glacial Maximum. Geomorphology 321, 87–102.
- Gratton, D., Gwyn, Q.H.J., M Dubois, J.M., 1984. Les paléoenvironnements sédimentaires au Wisconsinien moyen et supérieur, île d'Anticosti, golfe du Saint-Laurent, Québec. Géogr. Phys. Quaternaire 38, 229–242.
- Gray, J.T., Hétu, B., 1981. L'évolution morphologique du secteur nord de la Gaspésie suite à la déglaciation dans les zones d'altération et le problème des limites glaciaires. AMQUA-CANQUA booklet, p. 167.
- Hansel, A.K., Mickelson, D.M., 1988. A Reevaluation of the Timing and Causes of High Lake Phases in the Lake Michigan Basin. Quat. Res. 29, 113–128.
- Hansel, A.K., Mickelson, D.M., Schneider, A.F., Larsen, C.E., 1985. Late Wisconsinan and Holocene History of the Lake Michigan Basin. Geological Association of Canada, Special Paper. 30, pp. 39–53.
- Hanson, M.A., 2003. Late Quaternary Glaciation, Relative Sea-Level History and Recent Coastal Submergence of Northeast Melville Island. Nunavut [M.Sc thesis] University of Alberta, Edmonton, Canada, p. 108.
- Haugerud, R.A., 2021. Deglaciation of the Puget Lowland, Washington, Untangling the Quaternary Period—A Legacy of Stephen C. Porter, Richard B. Wait, Glenn D. Thackray, Alan R. Gillespie. Geological Society of America Special Paper 548.
- Hebda, C.F.G., McLaren, D., Mackie, Q., Fedje, D., Pedersen, M.W., Willerslev, E., Brown, K.J., Hebda, R.J., 2022. Late Pleistocene palaeoenvironments and a possible glacial refugium on northern Vancouver Island, Canada: Evidence for the viability of early human settlement on the northwest coast of North America. Quat. Sci. Rev. 279, 107388.
- Hebda, R.J., Burns, J.A., Geertsema, M., Jull, A.J.T., 2008. AMS-dated late Pleistocene taiga vole (Rodentia: *Microtus xanthognathus*) from northeast British Columbia, Canada: a cautionary lesson in chronology This article is one of a selection of papers published in this Special Issue on the theme Geology of northeastern British Columbia and northwestern Alberta: diamonds, shallow gas, gravel, and glaciers. Can. J. Earth Sci. 45, 611–618.
- Hein, F., Mudie, P., 1991. Glaciol-Marine Sedimentation, Canadian Polar Margin, North of Axel Heiberg Island. Géogr. Phys. Quaternaire 45, 213–227.
- Heinrichs, M.L., Antos, J.A., Hebda, R.J., Allen, G.B., 2002. *Abies lasiocarpa* (Hook.) Nutt. in the late-glacial and early-Holocene vegetation of British Columbia, Canada, and adjacent regions in Washington, USA. Rev. Palaeobot. Palynol. 120, 107–122.
- Henderson, E.P., 1974. Surficial geology: Avalon Peninsula, Newfoundland. Geol. Surv. Can. Map 1320A scale 1:250,000.
- Heusser, C.J., 1973. Environmental sequence following the Fraser advance of the Juan de Fuca lobe, Washington. Quat. Res. 3, 284–306.
- Hickman, M., Schweger, C.E., 1996. The Late Quaternary palaeoenvironmental history of a presently deep freshwater lake in east-central Alberta, Canada and paleoclimate implications. Palaeogeogr. Palaeoclimatol. Palaeoecol. 123, 161–178.
- Hill, P.R., Mudie, P.J., Moran, K., Blasco, S.M., 1985. A sea-level curve for the Canadian Beaufort Shelf. Can. J. Earth Sci. 22, 1383–1393.
- Hillaire-Marcel, C., 1976. La déglaciation et le relèvement isostatique sur la côte est de la baie d'Hudson. Cahiers de géographie de Québec 20, 185–220.
- Hillaire-Marcel, C., Occhietti, S., Vincent, J.-S., 1981. Sakami moraine, Quebec: A 500-km-long moraine without climatic control. Geology 9, 210–214.
- Hobbs, H.C., Aronow, S., Patterson, C.J., 1990. Surficial Geology of Dakota County, Minnesota. County Atlas Series Atlas C-6, Plate 3 of 9. University of Minnesota, Minnesota Geological Survey.
- Hodgson, D., Haselton, G., 1974. Reconnaissance glacial geology, northeastern Baffin Island. Geol. Surv. Can. Pap. 74-20, 10 p.
- Hodgson, D.A., 1981. Surficial Geology, Lougheed Island, Northwest Arctic Archipelago. Geol. Surv. Can. Paper 81-1C, pp. 27–34.
- Hodgson, D.A., 1985. The last glaciation of west-central Ellesmere Island, Arctic Archipelago, Canada. Can. J. Earth Sci. 22, 347–368.
- Hodgson, D.A., Vincent, J.-S., 1984. Surficial Geology, Central Melville Island, District of Franklin, Northwest Territories. Geol. Surv. Can. "A" Series Map 1583A.
- Hooke, R.L., Hanson, P.R., 2017. Late- and Post-glacial history of the East Branch of the Penobscot River, Maine, USA. Atl. Geol. 53, 285–300.
- Hooyer, T.S., 2007. Late Glacial History of East Central Wisconsin. Wisconsin Geological and Natural History Survey Open-File, p. 95. Report 2007-01.
- Houde-Poirier, M., 2014. Écoulements glaciaires au Wisconsinien supérieur, déglaciation et variations du niveau marin relatif dans la région de Gaspé, Québec [M.Sc thesis] Montréal (Québec, Canada). Université du Québec à Montréal, p. 174.

- Hughes, O.L., 1972. Surficial geology of northern Yukon Territory and northwestern District of Mackenzie, Northwest Territories (Report and Map 1319A). Geol. Surv. Can 11. Paper 69-36.
- Hyvärinen, H., 1985. Holocene pollen stratigraphy of Baird Inlet, east-central Ellesmere Island, Arctic Canada. *Boreas* 14, 19–32.
- Jackson, L., Ward, B., Duk-Rodkin, A., Hughes, O., 1991. The Last Cordilleran Ice Sheet in Southern Yukon Territory. *Géogr. Phys. Quaternaire* 45, 341–354.
- Jackson, R., Carlson, A.E., Hillaire-Marcel, C., Wacker, L., Vogt, C., Kucera, M., 2017. Asynchronous instability of the North American-Arctic and Greenland ice sheets during the last deglaciation. *Quat. Sci. Rev.* 164, 140–153.
- Jacobs, J.D., Mode, W.N., Dowdeswell, E.K., 1985. Contemporary Pollen Deposition and the Distribution of *Betula glandulosa* at the Limit of Low Arctic Tundra in Southern Baffin Island, N.W.T., Canada. *Arct. Alp. Res.* 17, 279–287.
- Jelgersma, S., 1962. A late-glacial pollen diagram from Madelia, south-central Minnesota. *Am. J. Sci.* 260, 522–529.
- Jennings, A., 1993. The Quaternary History of Cumberland Sound, Southeastern Baffin Island: The Marine Evidence. *Géogr. Phys. Quaternaire* 47, 21–42.
- Jennings, A., Andrews, J., Pearce, C., Wilson, L., Ólfasdóttir, S., 2015. Detrital carbonate peaks on the Labrador shelf, a 13–7ka template for freshwater forcing from the Hudson Strait outlet of the Laurentide Ice Sheet into the subpolar gyre. *Quat. Sci. Rev.* 107, 62–80.
- Jennings, A.E., Andrews, J.T., Ó Cofaigh, C., St-Onge, G., Belt, S., Cabedo-Sanz, P., Pearce, C., Hillaire-Marcel, C., Calvin Campbell, D., 2018. Baffin Bay paleoenvironments in the LGM and HS1: Resolving the ice-shelf question. *Mar. Geol.* 402, 5–16.
- Jennings, A.E., Manley, W.F., Maclean, B., Andrews, J.T., 1998. Marine evidence for the last glacial advance across eastern Hudson Strait, eastern Canadian Arctic. *J. Quat. Sci.* 13, 501–514.
- Jennings, A.E., Tedesco, K.A., Andrews, J.T., Kirby, M.E., 1996. Shelf erosion and glacial ice proximity in the Labrador Sea during and after Heinrich events (H-3 or 4 to H-0) as shown by foraminifera. *Geol. Soc. London, Special Publications* 111, 29–49.
- Jennings, C.E., Knaeble, A.R., Meyer, G.N., Lusardi, B.A., Bovee, T.L., Curry, B., Murphy, M., V S, Wright, H.E., 2011. A glacial record spanning the Pleistocene in southern Minnesota. In: Miller, J.D., Hudak, G.J., Wittkop, C., McLaughlin, P.I. (Eds.), Archean to Anthropocene: Field Guides to the Geology of the Mid-continent of North America, vol. 24. GSA Field Guide, pp. 351–378.
- Johnson, M.D., Addis, K.L., Ferber, L.R., Hemstad, C.B., Meyer, G.N., Komai, L.T., 1999. Glacial Lake Lind, Wisconsin and Minnesota. *Geological Society of America Bulletin*, 111, pp. 1371–1386.
- Johnson, M.D., Mooers, H.D., 1998. Ice-margin positions of the Superior lobe during late Wisconsinan deglaciation. Jr. In: Patterson, C.J., Wright, H.E. (Eds.), Contributions to Quaternary Studies in Minnesota: Minnesota Geological Survey Report of Investigations, vol. 49, pp. 7–14.
- Johnson, W.H., Glass, H.D., Gross, D.L., Moran, S.R., 1971. Glacial drift of the Shelbyville Moraine at Shelbyville, Illinois. *Illinois Geol. Surv. Circular* 459, 22.
- Josenhans, H.W., Zevenhuizen, J., 1990. Dynamics of the Laurentide Ice Sheet in Hudson Bay, Canada. *Mar. Geol.* 92, 1–26.
- Karrow, P.F., 1974. Till stratigraphy in parts of Southwestern Ontario. *Geol. Soc. Am. Bull.* 85, 761–768.
- Karrow, P.F., 1987a. Glacial and glaciolacustrine events in northwestern Lake Huron, Michigan and Ontario. *Geol. Soc. Am. Bull.* 98, 113–120.
- Karrow, P.F., 1987b. Quaternary geology of the Hamilton-Cambridge area, southern Ontario, Ontario. *Geol. Surv. Rep.* No 255, 94.
- Karrow, P.F., 1988. Catfish Creek Till: An important glacial deposit in southwestern Ontario. In: 41st Canadian Geotechnical Conference Preprints, pp. 186–192.
- Kaufman, D.S., Williams, K.M., 1992. Radiocarbon Date List VII: Baffin Island, N.W.T. Institute of Arctic and Alpine Research Occasional, Canada. Paper No. 48.
- Kaye, C.A., 1964. Illinoian and Early Wisconsinan Moraines of Martha's Vineyard. US Geological Survey Professional Paper 501-C, Massachusetts. C140–C143.
- Kaye, C.A., 1972. Preliminary Surficial Map of Martha's Vineyard, Nomans Land, and Parts of Naushon and Pasque Islands, Massachusetts. US Geological Survey Open-File Report, pp. 72–205.
- Kelly, M.A., Fisher, T.G., Lowell, T.V., Barnett, P.J., Schwartz, R., 2016. 10Be ages of flood deposits west of Lake Nipigon, Ontario: evidence for eastward meltwater drainage during the early Holocene Epoch. *Can. J. Earth Sci.* 53, 321–330.
- Kerr, D.E., 1996. Late Quaternary sea level history in the Paulatuk to Bathurst Inlet area, Northwest Territories. *Can. J. Earth Sci.* 33, 389–403.
- Kerr, P.J., Tassier-Surine, S.A., Kilgore, S.M., Bettis III, E.A., Dorale, J.A., Cramer, B.D., 2021. Timing, provenance, and implications of two MIS 3 advances of the Laurentide Ice Sheet into the Upper Mississippi River Basin, USA. *Quat. Sci. Rev.* 261, 106926.
- King, C.A.M., 1969. Glacial Geomorphology and Chronology of Henry Kater Peninsula, East Baffin Island, N.W.T. *Arct. Alp. Res.* 1, 195–212.
- King, C.A.M., Buckley, J.T., 1967. The chronology of deglaciation around Ege Bay and Lake Gillian, Baffin Island, N.W.T. *Geogr. Bull.* 9, 20–32.
- King, G., 1985. A Standard Method for Evaluating Radiocarbon Dates of Local Deglaciation: Application to the Deglaciation History of Southern Labrador and Adjacent Québec. *Géogr. Phys. Quaternaire* 39, 163–182.
- King, G.A., 1987. Deglaciation and Vegetational History of Western Labrador and Adjacent Quebec [PhD Thesis. University of Minnesota, Minneapolis, Minnesota, p. 266].
- Klassen, R.A., 1993. Quaternary Geology and Glacial History of Bylot Island, Northwest Territories, vol. 429. *Geol. Surv. Can Memoir*.
- Klassen, R.A., Paradis, S., Bolduc, A.M., Thompson, R.D., 1992. Glacial landforms and deposits, Labrador, Newfoundland and eastern Québec. *Geol. Surv. Can. Map 1814A*, 1:1,000,000 scale.
- Klassen, R.W., 1967. Surficial Geology, Waterhen-Grand Rapids Area, West of Principal Meridian, Manitoba. *Geol. Surv. Can.* p. 440. Preliminary Map 13-1966 and Paper 66-36, 1:253.
- Klassen, R.W., 1972. Wisconsin Events and the Assiniboine and Qu'Appelle Valleys of Manitoba and Saskatchewan. *Can. J. Earth Sci.* 9, 544–560.
- Klassen, R.W., 1983. Lake Agassiz and the Late Glacial History of Northern Manitoba, vol. 26. Geological Association of Canada, Special Paper, pp. 97–115.
- Klassen, R.W., 1986. Surficial geology of north-central Manitoba. *Geol. Surv. Can. Map 419*, 57.
- Klassen, R.W., 1987. The Tertiary-Pleistocene stratigraphy of the Liard Plain, southeastern Yukon. *Geol. Surv. Can. Paper* 86-17, 16 p.
- Klassen, R.W., 1994. Late Wisconsinan and Holocene history of southwestern Saskatchewan. *Can. J. Earth Sci.* 31, 1822–1837.
- Knaeble, A.R., 2006. Landforms, stratigraphy, and lithologic characteristics of glacial deposits in central Minnesota. Prepared for the 50th Midwest Friends of the Pleistocene Field Conference, June 4–6, 2004. Minn. Geol. Surv. Guidebook 22, 44.
- Koch, J., Osborn, G.D., Clague, J.J., 2007. Pre-'Little Ice Age' glacier fluctuations in Garibaldi Provincial Park, Coast Mountains, British Columbia, Canada. *Holocene* 17, 1069–1078.
- Kovanen, D.J., Easterbrook, D.J., 2001. Late Pleistocene, post-Vashon, Alpine Glaciation of the Nooksack Drainage, North Cascades, Washington. *Geological Society of America Bulletin* 113, pp. 274–288.
- Kovanen, D.J., Easterbrook, D.J., 2002a. Paleodeviations of radiocarbon marine reservoir values for the northeast Pacific. *Geology* 30, 243–246.
- Kovanen, D.J., Easterbrook, D.J., 2002b. Timing and Extent of Allerød and Younger Dryas Age (ca. 12,500–10,000 14C yr B.P.) Oscillations of the Cordilleran Ice Sheet in the Fraser Lowland, Western North America. *Quat. Res.* 57, 208–224.
- Krzyszkowski, D., Karrow, P.F., 2001. Wisconsinan Inter-Lobal Stratigraphy in Three Quarries Near Woodstock, Ontario. *Géogr. Phys. Quaternaire* 55, 3.
- Kulig, J.J., 1996. The glaciation of the Cypress Hills of Alberta and Saskatchewan and its regional implications. *Quat. Int.* 32, 53–77.
- Labelle, C., Richard, P., 1981. Végétation tardiglaciaire et postglaciaire au sud-est du parc des Laurentides, Québec. *Géogr. Phys. Quaternaire* 35, 345–359.
- Lacelle, D., Lauriol, B., Clark, I.D., 2007. Origin, age, and paleoenvironmental significance of carbonate precipitates from a granitic environment, Akshayuk Pass, southern Baffin Island, Canada. *Can. J. Earth Sci.* 44, 61–79.
- LaFarge-England, C., Vitt, D.H., England, J., 1991. Holocene Soligenous Fens on a High Arctic Fault Block, Northern Ellesmere Island (82°N), N.W.T., Canada. *Arct. Alp. Res.* 23, 80–98.
- Lajeunesse, P., Allard, M., 2003. The Nastapoka drift belt, eastern Hudson Bay: implications of a stillstand of the Quebec Labrador ice margin in the Tyrrell Sea at 8 ka BP. *Can. J. Earth Sci.* 40, 65–76.
- Lajeunesse, P., St-Onge, G., 2008. The subglacial origin of the Lake Agassiz–Ojibway final outburst flood. *Nat. Geosci.* 1, 184–188.
- Lakeman, T.R., Pieńkowski, A.J., Nixon, F.C., Furze, M.F.A., Blasco, S., Andrews, J.T., King, E.L., 2018. Collapse of a marine-based ice stream during the early Younger Dryas chronozone, western Canadian Arctic. *Geology* 46, 211–214.
- Lamb, H.F., 1980. Late Quaternary Vegetational History of Southeastern Labrador. *Arct. Alp. Res.* 12, 117–135.
- Lamoureux, S.F., England, J.H., 2000. Late Wisconsinan Glaciation of the Central Sector of the Canadian High Arctic. *Quat. Res.* 54, 182–188.
- Landmesser, C.W., Johnson, T.C., Wold, R.J., 1982. Seismic Reflection Study of Recessional Moraines beneath Lake Superior and Their Relationship to Regional Deglaciation. *Quat. Res.* 17, 173–190.
- Larsen, P., 1996. In-Situ Production Rates of Cosmogenic 10Be and 26Al over the Past 21,500 Years Determined from the Terminal Moraine of the Laurentide Ice Sheet. North-Central New Jersey [MSc thesis] University of Vermont, Burlington.
- Larson, G.J., 2011. Chapter 37-Ice-Margin Fluctuations at the End of the Wisconsin Episode, Michigan, USA. In: Ehlers, J., Gibbard, P.L., Hughes, P.D. (Eds.), Developments in Quaternary Sciences. Elsevier, pp. 489–497.
- Lauriol, B., 1982. Géomorphologie quaternaire du sud de l'Ungava. *Paléo-Québec* 15, 224–224.
- Lavoie, M., Pellerin, S., Larocque, M., 2013. Examining the role of alloogenous and autogenous factors in the long-term dynamics of a temperate headwater peatland (southern Québec, Canada). *Palaeogeogr. Palaeoclimatol. Palaeoecol.* 386, 336–348.
- Lavoie, M., Richard, P.J., 2000. The role of climate on the developmental history of Frontenac Peatland, southern Quebec. *Can. J. Bot.* 78, 668–684.
- Lemmen, D.S., 1989. The last glaciation of Marvin Peninsula, northern Ellesmere Island, High Arctic, Canada. *Can. J. Earth Sci.* 26, 2578–2590.
- Leopold, E.B., Nickmann, R., Hedges, J.I., Ertel, J.R., 1982. Pollen and Lignin Records of Late Quaternary Vegetation, Lake Washington. *Science* 218, 1305–1307.
- Lepper, K., Fisher, T.G., Hajdas, I., Lowell, T.V., 2007. Ages for the Big Stone Moraine and the oldest beaches of glacial Lake Agassiz: Implications for deglaciation chronology. *Geology* 35.
- Lepper, K., Gorz, K.L., Fisher, T.G., Lowell, T.V., 2011. Age determinations for glacial Lake Agassiz shorelines west of Fargo, North Dakota, USA. *Can. J. Earth Sci.* 48, 1199–1207.
- Lesnek, A.J., Briner, J.P., Baichtal, J.F., Lyles, A.S., 2020. New constraints on the last deglaciation of the Cordilleran Ice Sheet in coastal Southeast Alaska. *Quat. Res.* 96, 140–160.
- Leverett, F., Taylor, F.B., 1915. The Pleistocene of Indiana and Michigan and the History of the Great Lakes: US Government Printing Office. United States Geological Survey Monograph 53.
- Leverington, D.W., Mann, J.D., Teller, J.T., 2000. Changes in the Bathymetry and Volume of Glacial Lake Agassiz Between 11,000 and 9300 14C yr B.P. *Quat. Res.* 54, 174–181.

- Lewis, C.F.M., Todd, B.J., Anderson, T.W., King, J.W., Matile, G.L.D., Rodrigues, C.G., Thorleifson, L.H., 2011. Evolution of late glacial Lake Agassiz as shown by its offshore sedimentary record beneath northern Lake Winnipeg, Manitoba, Canada. *Abstracts with Programs Geological Society of America* 43, 348, No. 5.
- Leydet, D.J., Carlson, A.E., Teller, J.T., Breckenridge, A., Barth, A.M., Ullman, D.J., Sinclair, G., Milne, G.A., Cuzzone, J.K., Caffee, M.W., 2018. Opening of glacial Lake Agassiz's eastern outlets by the start of the Younger Dryas cold period. *Geology* 46, 155–158.
- Little, E.C., 2006. *Surficial Geology, Ellice Hills (North), Nunavut*. Geol. Surv. Can Open File 5016.
- Liux, X., Fisher, T.G., Lepper, K., Lowell, T.V., 2014. Geochemical characteristics of glacial Lake Agassiz sediments and new ages for the Moorhead Phase at Fargo, North Dakota, USA. *Can. J. Earth Sci.* 51, 850–861.
- Liverman, D., Batterson, M., Bell, T., Marich, N.A., Putt, M., 2006. Digital Elevation Models from Shuttle Radar Topography Mission Data – New Insights into the Quaternary History of Newfoundland. *Current Research (2006) Newfoundland and Labrador Department of Natural Resources Geological Survey. Report 06-1*.
- Liverman, D.G.E., 1994. Relative sea-level history and isostatic rebound in Newfoundland, Canada. *Boreas* 23, 217–230.
- Loope, H.M., Antinao, J.L., Lowell, T.V., Curry, B.B., Monaghan, G.W., 2018. Chronology of Laurentide Ice Sheet Fluctuations Surrounding the Last Glacial Maximum, Central Indiana, USA. *Geological Society of America 130th Annual Meeting, Indianapolis, Indiana*.
- Loope, H.M., Loope, W.L., Goble, R.J., Fisher, T.G., Jol, H.M., Seong, J.C., 2010. Early Holocene dune activity linked with final destruction of Glacial Lake Minong, eastern Upper Michigan, USA. *Quat. Res.* 74, 73–81.
- Loope, W.L., Loope, H.M., Goble, R.J., Fisher, T.G., Lytle, D.E., Legg, R.J., Wysocki, D.A., Hanson, P.R., Young, A.R., 2012. Drought drove forest decline and dune building in eastern upper Michigan, USA, as the upper Great Lakes became closed basins. *Geology* 40, 315–318.
- Lowdon, J.A., Blake, W., 1968. *Geol. Surv. Can Radiocarbon Dates VII*. Radiocarbon 10, 207–245.
- Lowdon, J.A., Blake, W., 1973. *Geol. Surv. Can Radiocarbon Dates XIII*. Geol. Surv. Can 61. Paper 70-7.
- Lowdon, J.A., Blake, W.J., 1970. *Geol. Surv. Can Radiocarbon Dates IX*. Radiocarbon 12, 46–86.
- Lowdon, J.A., Blake, W.J., 1975. *Geol. Surv. Can Radiocarbon Dates XV*. Geol. Surv. Can 32. Paper 75-7.
- Lowdon, J.A., Blake, W.J., 1978. *Geol. Surv. Can Radiocarbon Dates XVIII*. Geol. Surv. Can 20. Paper 78-7.
- Lowdon, J.A., Blake, W.J., 1980. *Geol. Surv. Can Radiocarbon Dates XX*. Geol. Surv. Can. Lowdon, J.A., Blake, W.J., 1981. *Geol. Surv. Can Radiocarbon Dates XXI*. Geol. Surv. Can. Paper 81-7, 22 p.
- Lowdon, J.A., Fyles, J.G., Blake, W.J., 1967. *Geol. Surv. Can Radiocarbon Dates VI*. Radiocarbon 9, 156–197.
- Lowell, T., Watsoner, N., Fisher, T., Loope, H., Glover, K., Comer, G., Hajdas, I., Denton, G., Schaefer, J., Rinterknecht, V., Broecker, W., Teller, J., 2005. Testing the Lake Agassiz meltwater trigger for the Younger Dryas. *Eos, Trans. Am. Geophys. Union* 86, 365–372.
- Lowell, T.V., Fisher, T.G., Hajdas, I., Glover, K., Loope, H., Henry, T., 2009. Radiocarbon deglaciation chronology of the Thunder Bay, Ontario area and implications for ice sheet retreat patterns. *Quat. Sci. Rev.* 28, 1597–1607.
- Luehmann, M.D., Schaetzl, R.J., Miller, B.A., Biggsy, M.E., 2013. Thin, pedoturbated, and locally sourced loess in the western Upper Peninsula of Michigan. *Aeolian Res.* 8, 85–100.
- Lundstrom, S., 2013. Aspects of the latest Pleistocene glacial geologic record of the James lobe of eastern South Dakota. *Geol. Soc. Am. Abstracts with Programs* 45, 413.
- Mackay, J.R., Mathews, W.H., 1973. Geomorphology and Quaternary History of the Mackenzie River Valley near Fort Good Hope, N.W.T., Canada. *Can. J. Earth Sci.* 10, 26–41.
- MacPherson, J.B., 1996. Delayed Deglaciation by Downwasting of the Northeast Avalon Peninsula, Newfoundland: An Application of the Early Postglacial Pollen Record. *Géogr. Phys. Quaternaire* 50, 201–220.
- Maher, L.J., Mickelson, D.M., 1996. Palynological and Radiocarbon Evidence for Deglaciation Events in the Green Bay Lobe, Wisconsin. *Quat. Res.* 46, 251–259.
- Maher, L.J., Miller, N.G., Baker, R.G., Curry, B.B., Mickelson, D.M., 1998. Paleobiology of the Sand Beneath the Valders Diamicton at Valders, Wisconsin. *Quat. Res.* 49, 208–221.
- Manley, W.F., 1996. Late-glacial flow patterns, deglaciation, and postglacial emergence of the south-central Baffin Island and the north-central coast of Hudson Strait, eastern Canadian Arctic. *Can. J. Earth Sci.* 33, 1499–1510.
- Manley, W.F., Jennings, A.E., 1996. Radiocarbon Date List VII: Eastern Canadian Arctic, Labrador, Northern Quebec, East Greenland Shelf, Iceland Shelf, and Antarctica, Occasional Paper No. 50. University of Colorado, Institute of Arctic and Alpine Research, p. 163.
- Manley, W.F., Miller, G.H., 2001. Glacial-geological record on southern Baffin Island reflecting late glacial ice-sheet dynamics in the eastern Hudson Strait region. *Geol. Surv. Can. Bull.* 566, 19–30.
- Marcoux, N., Richard, P.J.H., 1995. Végétation et fluctuations climatiques postglaciaires sur la côte septentrionale gaspésienne. Québec. *Can. J. Earth Sci.* 32, 79–96.
- Matile, G.L.D., Keller, G.R., 2004. Shaded Relief Topography of Manitoba. Manitoba Industry Economic Development and Mines. Manitoba Geological Survey. Geoscientific map 2004-4, 1:1 000 000.
- Matsch, C.L., Schneider, A.F., 1986. Stratigraphy and correlation of the glacial deposits of the glacial lobe complex in Minnesota and Northwestern Wisconsin. *Quat. Sci. Rev.* 5, 59–64.
- Matthews, B., 1967. Late Quaternary Land Emergence in Northern Ungava, Quebec. *Arctic* 20, 176–202.
- Mayle, F.E., Cwynar, L.C., 1995. A review of multi-proxy data for the younger dryas in Atlantic Canada. *Quat. Sci. Rev.* 14, 813–821.
- Mayle, F.E., Levesque, A.J., Cwynar, L.C., 1993a. Accelerator-Mass-Spectrometer Ages for the Younger Dryas Event in Atlantic Canada. *Quat. Res.* 39, 355–360.
- Mayle, F.E., Levesque, A.J., Cwynar, L.C., 1993b. Alnus as an indicator taxon of the Younger Dryas cooling in eastern North America. *Quat. Sci. Rev.* 12, 295–305.
- McCallum, K.J., Wittenberg, J., 1968. University of Saskatchewan radiocarbon dates V. Radiocarbon 10, 365–378.
- McHenry, M., Dunlop, P., 2016. The subglacial imprint of the last Newfoundland Ice Sheet. *Canada. J. Maps* 12, 462–483.
- McLaren, P., Barnett, D.M., 1978. Holocene Emergence of the South and East Coasts of Melville Island, Queen Elizabeth Islands, Northwest Territories, Canada. *Arctic* 31, 415–427.
- McMartin, I., 1994. Ice Flow Events in the Cormorant Lake-Wekusko Lake Area, Northern Manitoba. *Geol. Surv. Can.* pp. 175–182. Current Research no. 1994-C.
- McNeely, R., 1989. *Geol. Surv. Can Radiocarbon Dates XXVIII*. Geol. Surv. Can 93. Paper 88-7.
- McNeely, R., 2002. *Geol. Surv. Can Radiocarbon Dates XXXIII*. Geol. Surv. Can Current Research 2001, pp. 1–51.
- McNeely, R., 2006. *Geol. Surv. Can Radiocarbon Dates XXXV*. Geol. Surv. Can Paper 2006-G, p. 156.
- McNeely, R., Atkinson, D.E., 1995. *Geol. Surv. Can Radiocarbon Dates XXXII*. Geol. Surv. Can Paper 1995-G, p. 92.
- McNeely, R., Brennan, J., 2005. *Geol. Surv. Can revised shell dates*. Geol. Surv. Can Open File 5019, 530.
- McNeely, R., Jorgensen, P.K., 1993. *Geol. Surv. Can Radiocarbon Dates XXXI*. Geol. Surv. Can 85. Paper 91-7.
- McNeely, R., McCuaig, S., 1991. *Geol. Surv. Can Radiocarbon Dates XXIX*. Geol. Surv. Can 134. Paper 89-7.
- Menounos, B., Osborn, G., Clague, J.J., Luckman, B.H., 2009. Latest Pleistocene and Holocene glacier fluctuations in western Canada. *Quat. Sci. Rev.* 28, 2049–2074.
- Miller, G.H., 1979. Radiocarbon Date List IV: Baffin Island, N.W.T., Canada. Institute of Arctic and Alpine Research Occasional Paper No., p. 61, 29.
- Miller, G.H., 1980. Late Foxe Glaciation of Southern Baffin Island, N.W.T., Canada. *Geological Society of America Bulletin*, pp. 399–405, 91.
- Miller, G.H., Andrews, J.T., Short, S.K., 1977. The last interglacial-glacial cycle, Clyde foreland, Baffin Island, N.W.T.: stratigraphy, biostratigraphy, and chronology. *Can. J. Earth Sci.* 14, 2824–2857.
- Miller, G.H., Wolfe, A.P., Briner, J.P., Sauer, P.E., Nesje, A., 2005. Holocene glaciation and climate evolution of Baffin Island, Arctic Canada. *Quat. Sci. Rev.* 24, 1703–1721.
- Miller, G.H., Wolfe, A.P., Steig, E.J., Sauer, P.E., Kaplan, M.R., Briner, J.P., 2002. The Goldilocks dilemma: big ice, little ice, or "just-right" ice in the Eastern Canadian Arctic. *Quat. Sci. Rev.* 21, 33–48.
- Monaghan, G.W., Larson, G.J., Gephart, G.D., 1986. Late Wisconsinan drift stratigraphy of the Lake Michigan Lobe in southwestern Michigan. *Geol. Soc. Am. Bull.* 97, 329–334.
- Montelli, A., Gulick, S.P.S., Worthington, L.L., Mix, A., Davies-Walczak, M., Zellers, S.D., Jaeger, J.M., 2017. Late Quaternary glacial dynamics and sedimentation variability in the Bering Trough, Gulf of Alaska. *Geology* 45, 251–254.
- Moors, H.D., Lehr, J.D., 1997. Terrestrial record of Laurentide Ice Sheet reorganization during Heinrich events. *Geology* 25, 987–990.
- Moore, J.J., Hughen, K.A., Miller, G.H., Overpeck, J.T., 2001. Little Ice Age recorded in summer temperature reconstruction from varved sediments of Donard Lake, Baffin Island, Canada. *J. Paleolimnol.* 25, 503–517.
- Moorman, B.J., 1998. The Development and Preservation of Tabular Massive Ground Ice in Permafrost Regions [PhD Thesis]. Carleton University, Ottawa, Canada, p. 308.
- Mott, R., 1973. Palynological studies in central Saskatchewan - pollen stratigraphy from lake sediment sequences. *Geol. Surv. Can* 18. Paper 72-49.
- Mott, R., 1977. Late-Pleistocene and Holocene palynology in southeastern Québec. *Géogr. Phys. Quaternaire* 31, 139–149.
- Mott, R.J., Stea, R.R., 1993. Late-glacial (Allerød/Younger Dryas) buried organic deposits, Nova Scotia, Canada: A contribution to the 'North Atlantic seaboard programme' of IGCP-253, 'Termination of the Pleistocene'. *Quat. Sci. Rev.* 12, 645–657.
- Muhs, D.R., Bettis III, E.A., Roberts, H.M., Harlan, S.S., Paces, J.B., Reynolds, R.L., 2013. Chronology and provenance of last-glacial (Peoria) loess in western Iowa and paleoclimatic implications. *Quat. Res.* 80, 468–481.
- Muhs, D.R., Bettis III, E.A., Skipp, G.L., 2018. Geochemistry and mineralogy of late Quaternary loess in the upper Mississippi River valley, USA: Provenance and correlation with Laurentide Ice Sheet history. *Quat. Sci. Rev.* 187, 235–269.
- Muller, E.H., Calkin, P.E., 1993. Timing of Pleistocene glacial events in New York State. *Can. J. Earth Sci.* 30, 1829–1845.
- Murton, J.B., 2009. Stratigraphy and palaeoenvironments of Richards Island and the eastern Beaufort Continental Shelf during the last glacial-interglacial cycle. *Permafrost. Periglac. Process.* 20, 107–125.
- Murton, J.B., Bateman, M.D., Dallimore, S.R., Teller, J.T., Yang, Z., 2010. Identification of Younger Dryas outburst flood path from Lake Agassiz to the Arctic Ocean. *Nature* 464, 740–743.
- Murton, J.B., Bateman, M.D., Telka, A.M., Waller, R., Whiteman, C., Kuzmina, S., 2017. Early to mid Wisconsin Fluvial Deposits and Palaeoenvironment of the Kidluit

- Formation, Tuktoyaktuk Coastlands, Western Arctic Canada. *Permafrost and Glaciation*. 28, 523–533.
- Narancic, B., Pienitz, R., Chapligin, B., Meyer, H., Francus, P., Guilbault, J.-P., 2016. Postglacial environmental succession of Nettilling Lake (Baffin Island, Canadian Arctic) inferred from biogeochemical and microfossil proxies. *Quat. Sci. Rev.* 147, 391–405.
- Nelson, A.R., 1982. Aminostratigraphy of Quaternary marine and glaciomarine sediments, Qivitu Peninsula, Baffin Island. *Can. J. Earth Sci.* 19, 945–961.
- Nielsen, E., 1980. Quaternary Geology and Gravel Resources of the Island Lake-Red Sucker Lake Area. Manitoba Energy and Mines Mineral Resources Division, p. 24. Geological Report GR80-3.
- Nielsen, E., 1988. Surficial Geology of the Swan River Area. Manitoba Energy and Mines Geological Services, p. 58. Geological report GR80-7.
- Nixon, F.C., England, J.H., Lajeunesse, P., Hanson, M.A., 2014. Deciphering patterns of postglacial sea level at the junction of the Laurentide and Innuitian Ice Sheets, western Canadian High Arctic. *Quat. Sci. Rev.* 91, 165–183.
- Nutz, A., Ghienne, J.-F., Schuster, M., Dietrich, P., Roquin, C., Hay, M.B., Bouchette, F., Cousineau, P.A., 2015. Forced regressive deposits of a deglaciation sequence: Example from the Late Quaternary succession in the Lake Saint-Jean basin (Québec, Canada). *Sedimentology* 62, 1573–1610.
- Packalen, M.S., Finkelstein, S.A., McLaughlin, J.W., 2014. Carbon storage and potential methane production in the Hudson Bay Lowlands since mid-Holocene peat initiation. *Nat. Commun.* 5, 4078.
- Pair, D.L., Rodrigues, C.G., 1993. Late Quaternary Deglaciation of the Southwestern St. Lawrence Lowland, New York and Ontario. *Geological Society of America Bulletin* 105, pp. 1151–1164.
- Patterson, C.J., 1994. Tunnel-valley fans of the St. Croix moraine, east-central Minnesota, U.S.A. In P W W, Croot, D.G. (Eds.), *Formation and Deformation of Glacial Deposits*, Rotterdam, pp. 69–87.
- Patterson, C.J., Knaebel, A.R., D R S, Berg, J.A., 1999a. Quaternary Stratigraphy, Plate 2 of Patterson, C.J., Project Manager, Regional Hydrogeologic Assessment: Quaternary Geology—Upper Minnesota River Basin: Minnesota Geological Survey Regional Hydrogeologic Assessment Series RHA-4 (Part A).
- Patterson, C.J., Knaebel, A.R., Gran, S.E., Philipp, S.J., 1999b. Surficial Geology, Plate 1 of Patterson, C.J., Project Manager, Regional Hydrogeologic Assessment: Quaternary Geology—Upper Minnesota River Basin: Minnesota Geological Survey Regional Hydrogeologic Assessment Series RHA-4, Part A scale 1:200,000.
- Patterson, C.J., Wright, H.E.J., 1998. RI-49 Contributions to Quaternary Studies in Minnesota. Retrieved from the University of Minnesota Digital Conservancy. <https://hdl.handle.net/11299/60828>.
- Peterson, W.L., 1986. Late Wisconsinan Glacial History of Northeastern Wisconsin and Western Upper Michigan. *United States Geol. Surv. Bull.* 1652, 14.
- Pigati, J.S., Rech, J.A., Nekola, J.C., 2010. Radiocarbon dating of small terrestrial gastropod shells in North America. *Quat. Geochronol.* 5, 519–532.
- Pilote, L.-M., Garneau, M., Van Bellen, S., Lamotte, M., 2018. Multiproxy analysis of inception and development of the Lac-à-la-Tortue peatland complex, St Lawrence Lowlands, eastern Canada. *Boreas* 47, 1084–1101.
- Piper, D.J., Fehr, S.D., 1991. Radiocarbon Chronology of Late Quaternary Sections on the Inner and Middle Scotian Shelf, South of Nova Scotia. *Geol. Surv. Can.* pp. 321–325. Paper 91-1E.
- Plouffe, A., 2000. Quaternary geology of the Fort Fraser and Manson River map areas, central British Columbia. *Geol. Surv. Can. Bull.* 554, 62.
- Porreca, C., Briner, J.P., Kozlowski, A., 2018. Laurentide ice sheet meltwater routing along the Iro-Mohawk River, eastern New York, USA. *Geomorphology* 303, 155–161.
- Prest, V.K., 1963. Red Lake - Lansdowne House Area, Northwestern Ontario. *Geol. Surv. Can. Paper* 63-6.
- Prest, V.K., 1968. Nomenclature of moraines and ice-flow features as applied to the glacial map of Canada. *Geol. Surv. Can* 32, Paper 67-57.
- Prest, V.K., 1973. Surficial Deposits of Prince Edward Island. *Geol. Surv. Can. Map*, p. 1366A.
- Prichonnet, G., 1995. Géologie glaciaire et géochronologie postglaciaire dans la région limittropic de la Gaspésie et du Bas-Saint-Laurent, Québec. Commission géologique du Canada Bulletin 488, 69.
- Prior, J.C., 1991. Landforms of Iowa. University of Iowa Press, Iowa City.
- Pritchard, K.L., 2006. Relationships and Patterns of Channel Formation during Deglaciation of the Miami Lobe, Near Piqua Ohio. M.Sc thesis] University of Cincinnati, Ohio, p. 102.
- Proudfoot, D.N., St Croix, L., 1987. Quaternary Mapping in the Bellburns (12 1/5 and 6) Map Area. Current Research Report 87-1. Newfoundland Department of Mines and Energy, pp. 11–21.
- Quinn, M.J., Goldthwait, R.P., 1979. Glacial Geology of Champaign County, Ohio. Ohio Department of Natural Resources Report of Investigations No. 111, p. 17.
- Rampton, V.N., Gauthier, R.C., Thibault, J., Seaman, A.A., 1984. Quaternary Geology of New Brunswick. *Geol. Surv. Can Memoir* 416, p. 77.
- Rappold, M., 1993. Ice flow and glacial transport in Lower St. Lawrence, Québec. *Geol. Surv. Can Paper* 90-19, p. 28.
- Reasoner, M.A., Osborn, G., Rutter, N.W., 1994. Age of the Crowfoot advance in the Canadian Rocky Mountains: A glacial event coeval with the Younger Dryas oscillation. *Geology* 22, 439–442.
- Rech, J.A., Nekola, J.C., Pigati, J.S., 2012. Radiocarbon ages of terrestrial gastropods extend duration of ice-free conditions at the Two Creeks forest bed, Wisconsin, USA. *Quat. Res.* 77.
- Rémillard, A.M., St-Onge, G., Bernatchez, P., Hétu, B., Buylaert, J.-P., Murray, A.S., Vigneault, B., 2016. Chronology and stratigraphy of the Magdalen Islands archipelago from the last glaciation to the early Holocene: new insights into the glacial and sea-level history of eastern Canada. *Boreas* 45, 604–628.
- Richard, P., Larouche, A., Bouchard, M., 1982. Âge de la déglaciation finale et histoire postglaciaire de la végétation dans la partie centrale du Nouveau-Québec. *Géogr. Phys. Quaternaire* 36, 63–90.
- Richard, P., Veillette, J., Larouche, A., Hétu, B., Gray, J., Gangloff, P., 1997. Chronologie de la déglaciation en Gaspésie : nouvelles données et implications. *Géogr. Phys. Quaternaire* 51, 163–184.
- Ridge, P., 2000. Surficial Geologic Map of the Claremont South 7.5-minute Quadrangle and Springfield 7.5-minute Quadrangle, Vermont-New Hampshire. Concord, New Hampshire Geological Survey Maps: Geo-129-024000-SMOF/Geo-130-024000-SMOF [scale 1:24,000].
- Riedel, J.L., Telka, A., Bunn, A., Clague, J.J., 2021. Reconstruction of climate and ecology of Skagit Valley, Washington, from 27.7 to 19.8 ka based on plant and beetle macrofossils. *Quat. Res.* 1–19.
- Ritchie, J.C., 1977. The Modern and Late Quaternary Vegetation of the Campbell-Dolomite Uplands, near Inuvik, N.W.T., Canada. *Ecol. Monogr.* 47, 401–423.
- Rittenour, T.M., Cotter, J.F.P., Arends, H.E., 2015. Application of single-grain OSL dating to ice-proximal deposits, glacial Lake Benson, west-central Minnesota, USA. *Quat. Geochronol.* 30, 306–313.
- Rodrigues, C.G., Ceman, J.A., Vilks, G., 1993. Late Quaternary paleoceanography of deep and intermediate water masses off Gaspé Peninsula, Gulf of St. Lawrence: foraminiferal evidence. *Can. J. Earth Sci.* 30, 1390–1403.
- Rubin, M., Suess, H.E., 1955. U.S. Geological Survey Radiocarbon Dates II. *Science* 121, 481–488.
- Ruhe, 1983. Depositional environment of late Wisconsin loess in the midcontinental United States. In: Porter, W.a. (Ed.), *Late-Quaternary Environments of the United States, the Late Pleistocene*. University of Minnesota Press, Minneapolis.
- Rutherford, A.A., Wittenberg, J., Gordon, B.C., 1984. University of Saskatchewan Radiocarbon Dates X. *Radiocarbon* 26, 241–292.
- Ryder, J., Fulton, R., Clague, J., 1991. The Cordilleran Ice Sheet and the Glacial Geomorphology of Southern and Central British Columbia. *Géogr. Phys. Quaternaire* 45, 365–377.
- Rydningen, T.A., Vorren, T.O., Laberg, J.S., Kolstad, V., 2013. The marine-based NW Fennoscandian ice sheet: glacial and deglacial dynamics as reconstructed from submarine landforms. *Quat. Sci. Rev.* 68, 126–141.
- Saarnisto, M., 1974. The Deglaciation History of the Lake Superior Region and its Climatic Implications. *Quat. Res.* 4, 316–339.
- Savelle, J.M., Dyke, A.S., 2014. Paleoeskimo Occupation History of Foxe Basin, Arctic Canada: Implications for the Core Area Model and Dorset Origins. *Am. Antiq.* 79, 249–276.
- Savioie, L., Richard, P., 1979. Paléophytogéographie de l'épisode de Saint-Narcisse dans la région de Sainte-Agathe, Québec. *Géogr. Phys. Quaternaire* 33, 175–188.
- Schnitker, D., Belknap, D.F., Bacchus, T.S., Friez, J.K., Lusardi, B.A., Popok, D.M., 2001. Deglaciation of the Gulf of Maine. In: Weddle, T.K., Retelle, M.J. (Eds.), *Deglaciation History and Relative Sea-Level Changes, Northern New England and Adjacent Canada*: Geological Society of America Special Paper 351, pp. 9–34.
- Schreiner, B.T., 1984. Quaternary Geology of the Precambrian Shield, Saskatchewan. Saskatchewan Energy and Mines Report 221, 106.
- Seaman, A.A., 1989. Glacial striae trends in New Brunswick: a compilation. New Brunswick Department of Natural Resources and Energy. Min. Energy Div. Open File Rep. 89–34, 136.
- Seaman, A.A., 2006. A new interpretation of Late Glacial history of central New Brunswick: The Gaspereau Ice Center as a Younger Dryas ice cap. In: Martin, G.L. (Ed.), *Geological Investigations in New Brunswick for 2005*, vol. 3. New Brunswick Department of Natural Resources, Mineral Resources Report 2006–, p. 36.
- Seaman, A.A., McCoy, S.M., 2008. Multiple Wisconsinan till in the Sisson Brook exploration trench of Geodex Minerals Ltd., York County, west-central New Brunswick. In: Martin, G.L. (Ed.), *Geological Investigations in New Brunswick for 2005*. New Brunswick Department of Natural Resources. Mineral Resources Report 2008–1.
- Senici, D., Chen, H.Y.H., Bergeron, Y., Ali, A.A., 2015. The effects of forest fuel connectivity on spatiotemporal dynamics of Holocene fire regimes in the central boreal forest of North America. *J. Quat. Sci.* 30, 365–375.
- Setterholm, D.R., 1995. Quaternary Geology-Southwestern Minnesota [Part A]. Minnesota Geological Survey. Minnesota Geological Survey Regional Hydrogeologic Assessment Series RHA-2, Part A, Scale, 1:200,000. Retrieved from the University of Minnesota Digital Conservancy. <https://hdl.handle.net/11299/59763>.
- Sevon, W.D., Braun, D.D., 2000. Glacial deposits of Pennsylvania, Map 59. In: Commonwealth of Pennsylvania Department of Conservation and Natural Resources Bureau of Topographic and Geologic Survey.
- Shapiro, B., Drummond, A.J., Rambaut, A., Wilson, M.C., Matheus, P.E., Sher, A.V., Pybus, O.G., Gilbert, M.T.P., Barnes, I., Binladen, J., Willerslev, E., Hansen, A.J., Baryshnikov, G.F., Burns, J.A., Davydov, S., Driver, J.C., Froese, D.G., Harrington, C. R., Keddie, G., Kosintsev, P., Kunz, M.L., Martin, L.D., Stephenson, R.O., Storer, J., Tedford, R., Zimov, S., Cooper, A., 2004. Rise and Fall of the Beringian Steppe Bison. *Science* 306, 1561–1564.
- Sharpe, D.R., Russell, H.A.J., 2016. A revised depositional setting for Halton sediments in the Oak Ridges Moraine area, Ontario. *Can. J. Earth Sci.* 53, 281–303.
- Sharpe, D.R., Russell, H.A.J., 2019. Converging ice streams: an unreasonable hypothesis for deposition of the Oak Ridges Moraine, southern Ontario. *Can. J. Earth Sci.* 57, 781–800.
- Shaw, J., Grant, D.R., Guilbault, J.-P., Anderson, T.W., Parrott, D.R., 2000. Submarine and onshore end moraines in southern Newfoundland: implications for the history of late Wisconsinan ice retreat. *Boreas* 29, 295–314.
- Shaw, J., Longva, O., 2017. Glacial geomorphology of the Northeast Newfoundland Shelf: ice-stream switching and widespread glaciectonics. *Boreas* 46, 622–641.

- Shaw, J., Stacey, C.D., Wu, Y., Lintern, D.G., 2017. Anatomy of the Kitimat fiord system, British Columbia. *Geomorphology* 293, 108–129.
- Short, S.K., 1981. Radiocarbon date list I: Labrador and northern Quebec, Canada. Inst. Arctic and Alpine Res. Occasional Paper No 36, 33.
- Simard, J., Occhietti, S., Robert, F., 2003. Retrait de l'inlandsis sur les Laurentides au début de l'Holocène : transect de 600 km entre le Saint-Maurice et le Témiscamingue (Québec). *Géogr. Phys. Quaternaire* 57, 189–204.
- Smith, D.G., Fisher, T.G., 1993. Glacial Lake Agassiz: The northwestern outlet and paleoflood. *Geology* 21.
- Smith, I.R., 1999. Late Quaternary glacial history of Lake Hazen Basin and eastern Hazen Plateau, northern Ellesmere Island, Nunavut, Canada. *Can. J. Earth Sci.* 36, 1547–1565.
- Sookhan, S., Eyles, N., Arbelaez-Moreno, L., 2018. Converging ice streams: a new paradigm for reconstructions of the Laurentide Ice Sheet in southern Ontario and deposition of the Oak Ridges Moraine. *Can. J. Earth Sci.* 55, 373–396.
- Spear, R.W., Cwynar, L.C., 1997. Late Quaternary Vegetation History of White Pass, Northern British Columbia, Canada. *Arct. Alp. Res.* 29, 45–52.
- Spooner, I.S., 1998. Changes in lake-sediment stratigraphy associated with late glacial climate change: examples from western Nova Scotia. *Atl. Geol.* 34, 229–240.
- Spooner, I.S., MacDonald, I., Beierle, B., Jull, A.J.T., 2005. A multi-proxy lithostratigraphic record of Late Glacial and Holocene climate variability from Piper Lake, Nova Scotia. *Can. J. Earth Sci.* 42, 2039–2049.
- St-Onge, D.A., McMartin, I., 1995. Quaternary geology of the Inman River area, Northwest Territories. *Geol. Surv. Can. Bull.* 446, 59.
- Stalker, A.M., 1956. The erratics train foothills of Alberta. *Geol. Surv. Can. Bull.* 37, 28.
- Stanley, V.L., Marshall, K.J., 2015. Evidence of Active Permafrost in Minnesota Following the Wisconsin Glaciation [abstract] North-Central Section - 49th Annual Meeting (19–20 May 2015). Geological Society of America Abstracts with Programs 47, p. 80.
- Stea, R.R., 2011. Geology and Palaeoenvironmental Reconstruction of the Debert-Belmont Site. In: Bernard, T., Rosenmeier, L., Farrell, S.L. (Eds.), *Ta'n Wetapeksi'k: Understanding from where We Come. Eastern Woodland Print Communications for the Confederacy of Mainland Mi'kmaq*, p. 21.
- Stea, R.R., Conley, H., Brown, Y., 1992. Surficial Geology of the Province of Nova Scotia. Nova Scotia Department of Natural Resources Map 92–1. Scale 1:500,000.
- Stea, R.R., Mott, R.J., 1989. Deglaciation environments and evidence for glaciers of Younger Dryas age in Nova Scotia, Canada. *Boreas* 18, 169–187.
- Stea, R.R., Mott, R.J., 1998. Deglaciation of Nova Scotia: Stratigraphy and chronology of lake sediment cores and buried organic sections. *Géogr. Phys. Quaternaire* 52, 3–21.
- Stea, R.R., Piper, D.J.W., Fader, G.B.J., Boyd, R., 1998. Wisconsinan glacial and sea-level history of Maritime Canada and the adjacent continental shelf: A correlation of land and sea events. *GSA Bulletin* 110, 821–845.
- Stea, R.R., Pullan, S.E., Feetham, M., 2003. Mesozoic-Cenozoic Stratigraphy of the Lowlands of Southwest Cape Breton Island (NTS 11F/11, 11F/14). Minerals and Energy Branch, Report of Activities 2002. Nova Scotia Department of Natural Resources, pp. 103–126. Report ME 2003-1.
- Steig, E.J., Wolfe, A.P., Miller, G.H., 1998. Wisconsinan refugia and the glacial history of eastern Baffin Island, Arctic Canada: Coupled evidence from cosmogenic isotopes and lake sediments. *Geology* 26, 835–838.
- Stone, B.D., Stanford, S.D., Witte, R.W., 2002. Surficial geologic map of northern New Jersey: U. S. Geological Survey Miscellaneous Investigations Series. Map I-2540-C. scale, 1:100,000.
- Stravers, J.A., Syvitski, J.P.M., 1991. Land-Sea Correlations and Evolution of the Cambridge Fiord Marine Basin during the Last Deglaciation of Northern Baffin Island. *Quat. Res.* 35, 72–90.
- Stroeven, A.P., Fabel, D., Margold, M., Clague, J.J., Xu, S., 2014. Investigating absolute chronologies of glacial advances in the NW sector of the Cordilleran Ice Sheet with terrestrial in situ cosmogenic nuclides. *Quat. Sci. Rev.* 92, 429–443.
- Stuiver, M., Burns Jr., H.W., 1975. Late Quaternary Marine Invasion in Maine: Its Chronology and Associated Crustal Movement. *Geol. Soc. Am. Bull.* 86, 99–104.
- Suess, H.E., 1954. U. S. Geological Survey Radiocarbon Dates I. *Science* 120, 467–473.
- Sun, C., 1993. Quaternary Geology and Stratigraphy of the Assiniboine Fan Delta Area, Southwestern Manitoba [M.Sc. Thesis]. University of Manitoba, p. 180.
- Sun, C.S., Teller, J.T., 1997. Reconstruction of glacial Lake Hind in southwestern Manitoba, Canada. *J. Paleolimnol.* 17, 9–21.
- Swartz, J.M., Gulick, S.P.S., Goff, J.A., 2015. Gulf of Alaska continental slope morphology: Evidence for recent trough mouth fan formation. *G-cubed* 16, 165–177.
- Sverson, K.M., Colgan, P.M., 2011. The Quaternary of Wisconsin, pp. 537–552.
- Taylor, F.B., 1913. The moraine systems of southwestern Ontario. *Trans. Roy. Can. Inst.* 10, 57–79.
- Teller, J., Boyd, M., LeCompte, M., Kennett, J., West, A., Telka, A., Diaz, A., Adedeji, V., Batchelor, D., Mooney, C., Garcia, R., 2020. A multi-proxy study of changing environmental conditions in a Younger Dryas sequence in southwestern Manitoba, Canada, and evidence for an extraterrestrial event. *Quat. Res.* 93, 60–87.
- Terasmae, J., 1980. Some problems of late Wisconsin history and geochronology in southeastern Ontario. *Can. J. Earth Sci.* 17, 361–381.
- Terasmae, J., Matthews, H.L., 1980. Late Wisconsin white spruce (*Picea glauca* (Moench) Voss) at Brampton, Ontario. *Can. J. Earth Sci.* 17, 1087–1095.
- Thomas, E.K., Szymanski, J., Briner, J.P., 2010. Holocene alpine glaciation inferred from lacustrine sediments on northeastern Baffin Island, Arctic Canada. *J. Quat. Sci.* 25, 146–161.
- Thomas, R.L., Kemp, A.L., Lewis, C.F., 1973. The surficial sediments of Lake Huron. *Can. J. Earth Sci.* 10, 226–271.
- Thompson, W., 1999. History of research on glaciation in the White Mountains, New Hampshire (U.S.A.). *Géogr. Phys. Quaternaire* 53, 7–24.
- Todd, B.J., Fader, G.B.J., Courtney, R.C., Pickrill, R.A., 1999. Quaternary geology and surficial sediment processes, Browns Bank, Scotian Shelf, based on multibeam bathymetry. *Mar. Geol.* 162, 165–214.
- Todd, B.J., Shaw, J., 2012. Laurentide Ice Sheet dynamics in the Bay of Fundy, Canada, revealed through multibeam sonar mapping of glacial landsystems. *Quat. Sci. Rev.* 58, 83–103.
- Totten, S.M., 1976. The "up-in-the-air" late Pleistocene beaver pond near Lodi, Medina County, northern Ohio. *Geol. Soc. Am. abstracts with programs* 8 (4), 514.
- Tripanas, E.K., Piper, D.J.W., 2008. Glaciogenic Debris-Flow Deposits of Orphan Basin, Offshore Eastern Canada: Sedimentological and Rheological Properties, Origin, and Relationship to Meltwater Discharge. *J. Sediment. Res.* 78, 724–744.
- Tucker, C.M., 1974. A Series of Raised Pleistocene Deltas; Halls Bay, Newfoundland. *Atl. Geol.* 10, 1–7.
- Tulenko, J.P., Briner, J.P., Young, N.E., Schaefer, J.M., 2022. The last deglaciation of Alaska and a new benchmark 10Be moraine chronology from the western Alaska Range. *Quat. Sci. Rev.* 287, 107549.
- Utting, D.J., Gosse, J.C., Kelley, S.E., Vickers, K.J., Ward, B.C., Trommelen, M.S., 2016. Advance, deglacial and sea-level chronology for Foxe Peninsula, Baffin Island, Nunavut. *Boreas* 45, 439–454.
- Veillette, J., Cloutier, M., 1993. Géologie des formations en surface, Gaspésie, Québec. Coordinates: N480000 N492000 W0640000 W0681500.
- Vincent, J.-S., 1982. The Quaternary History of Banks Island, N.W.T., Canada. *Géogr. Phys. Quaternaire* 36, 209.
- Vincent, J.S., Hardy, L.E., 1979. The Evolution of Glacial Lakes Barlow and Ojibway. Quebec and Ontario.
- Walters, K.A., 2013. Laurentide Ice Sheet Retreat during the Younger Dryas: Central Upper Peninsula of Michigan. M.Sc thesis] University of Cincinnati, USA, p. 78.
- Walton, A., Trautman, M.A., Friend, J.P., 1961. Isotopes, Inc. Radiocarbon Measurements I. *Radiocarbon* 3, 47–59.
- Ward, B.C., Wilson, M.C., Nagorsen, D.W., Nelson, D.E., Driver, J.C., Wigen, R.J., 2003. Port Eliza cave: North American West Coast interstadial environment and implications for human migrations. *Quat. Sci. Rev.* 22, 1383–1388.
- Waters, M.R., Stafford Jr., T.W., Kooyman, B., Hills, L.V., 2015. Late Pleistocene horse and camel hunting at the southern margin of the ice-free corridor: reassessing the age of Wally's Beach, Canada. *Proc. Natl. Acad. Sci. USA* 112, 4263–4267.
- Wayne, W.J., 1965. The Crawfordsville and Knightstown Moraines in Indiana. *Indiana Geol. Surv. Rep. Progress* 28, 15.
- Welsted, J., Young, H.R., 1980. Geology and origin of the Brandon Hills, southwest Manitoba. *Can. J. Earth Sci.* 17, 942–951.
- Westgate, J.A., 1968. Surficial Geology of the Foremost Cypress Hills Area, Alberta. Research Council of Alberta Bulletin 22, p. 122.
- White, G.W., 1968. Age and correlation of Pleistocene deposits at Garfield Heights (Cleveland), Ohio. *Geol. Soc. Am. Bull.* 79, 749–752.
- White, G.W., 1984. Glacial Geology of Summit County, Ohio. State of Ohio Department of Natural Resources Division of Geological Survey: Report of Investigations No. 123.
- White, G.W., Totten, S.M., 1979. Glacial Geology of Ashtabula County, Ohio. Ohio Department of Natural Resources Report of Investigations No. 112, p. 48.
- White, G.W., Totten, S.M., Gross, D.L., 1969. Pleistocene Stratigraphy of Northwestern Pennsylvania. Commonwealth of Pennsylvania General Geological Report G55, p. 108.
- Williams, J.J., McLauchlan, K.K., Mueller, J.R., Mellicant, E.M., Myrbo, A.E., Lascu, I., 2015. Ecosystem development following deglaciation: A new sedimentary record from Devils Lake, Wisconsin, USA. *Quat. Sci. Rev.* 125, 131–143.
- Willman, H.B., Frye, J.C., 1970. Pleistocene Stratigraphy of Illinois. Ill State Geol. Surv. Bull. 94, 204.
- Winn, C.E., 1977. Vegetational History and Geochronology of Several Sites in Southwestern Ontario with Discussion on Mastodon Extinction in Southern Ontario [M.Sc Thesis]. Brock University, St. Catharines, Ontario, p. 374.
- Wolfe, A.P., Butler, D.L., 1994. Late-glacial and early Holocene environments at Pine Hill Pond, Newfoundland, Canada: evidence from pollen and diatoms. *Boreas* 23, 53–65.
- Wood, J.R., Forman, S.L., Everton, D., Pierson, J., Gomez, J., 2010. Lacustrine sediments in Porter Cave, Central Indiana, USA and possible relation to Laurentide ice sheet marginal positions in the middle and late Wisconsinan. *Palaeogeogr. Palaeoclimatol. Palaeoecol.* 298, 421–431.
- Woywitka, R.J., 2019. Geoarchaeology of the Mineable Oil Sands Region, Canada [Ph.D. thesis]. University of Alberta, Northeastern Alberta, p. 111.
- Wright, H.E., 1976. Ice Retreat and Revegetation in the Western Great Lakes Area. Dowden, Hutchinson and Ross, Pennsylvania.
- Wright Jr., H.E., 1972. Quaternary history of Minnesota. In: Sims, P.K., Morey, G.B. (Eds.), *Geology of Minnesota: A Centennial Volume*. Minnesota Geological Survey, Minneapolis, Minnesota, pp. 515–578.
- Wright, H.E., Ruhe, R.V., 1965. Glaciation of Minnesota and Iowa. In: Wright, H.E., Frey, D.G. (Eds.), *The Quaternary of the United States*. Princeton University Press, Princeton, New Jersey, pp. 29–41.
- Young, N.E., Briner, J.P., Kaufman, D.S., 2009. Late Pleistocene and Holocene glaciation of the Fish Lake valley, northeastern Alaska Range, Alaska. *J. Quat. Sci.* 24, 677–689.
- Young, N.E., Briner, J.P., Miller, G.H., Lesnek, A.J., Crump, S.E., Pendleton, S.L., Schwartz, R., Schaefer, J.M., 2021a. Pulsebeat of early Holocene glaciation in Baffin Bay from high-resolution beryllium-10 moraine chronologies. *Quat. Sci. Rev.* 270, 107179.
- Young, R.A., Gordon, L.M., Owen, L.A., Huot, S., Zerfas, T.D., 2021b. Evidence for a late glacial advance near the beginning of the Younger Dryas in western New York State: An event postdating the record for local Laurentide ice sheet recession. *Geosphere* 17, 271–305.